UNIVERSITY OF OKLAHOMA

GRADUATE COLLEGE

TONB DEPENDENT TRANSPORT PROCESSES THROUGH *E. COLI* FEPA

A DISSERTATION

SUBMITTED TO THE GRADUATE FACULTY

in partial fulfillment of the requirements for the

degree of

Doctor of Philosophy

BY

WALLACE ANTON KASERER
Norman, Oklahoma
2007

UMI Number: 3294672

UMI Microform 3294672

ProQuest Information and Learning Company
300 North Zeeb Road
P.O. Box 1346
Ann Arbor, MI 48106-1346

TONB DEPENDENT PROCESSES
THROUGH *E. COLI* FEPA

A DISSERTATION APPROVED FOR THE
DEPARTMENT OF CHEMISTRY AND BIOCHEMISTRY

BY

_____
Dr. Phillip E. Klebba

_____
Dr. Paul Cook

_____
Dr. Ann H. West

_____
Dr. Roger Harrison

_____
Dr. Ivan Yip

Acknowledgements

My journey into science would have never happened if it were not for my major professor Dr. Phillip E. Klebba. His infinite patience, guidance and support have enabled me to pursue my dream of becoming a scientist. I also need to thank Dr. Sally Newton who has always been there for me, helping from day to day in the lab. Without her I would not know the secrets of molecular cloning. Her tough attitude and detail oriented mind has helped to pull the cloning work in this thesis together. I would also like to thank the members of my graduate committee, Drs. Ann West, Roger Harrison, Ivan Yip, and Bruce Roe for their constructive criticism and their helpful discussion. I also must thank Dr. Paul Cook for his encouragement, criticism and his gracious substitution for Dr. Roe on my committee at the last minute.

I also must thank my wife Alla, for her support and dependability during this incredible journey, without her nurturing support I would not have made it. Next I would like to thank my parents for always being there, supporting and encouraging me in this endeavor. I also need to thank my cousins Jeanie and Wes, for their support, picking me up for the first time from the Tulsa airport, helping me buy my first car and sending me off to Norman to start my Ph.D. Next I would like to thank my cousin Jack McFarland, who was my first role model as a scientist. His demonstration of the power of a scientific mind encouraged me to begin my study of science during my college career.

Next I would like to thank Dr. Danny Scott, for not only his friendship but also his guidance during my first years as a graduate student in biochemistry. I also must thank Paul Warfel, the first friend I made here in Norman and the catalyst for me taking the GRE and getting into graduate school. Another great friend during this journey was Dr. Rajasekaran Annamalai, a man that was always there for discussions on research or life. I would also like to thank all the other members of the Klebba lab that have come and gone during the time I have been here, this experience would not have been as enjoyable without them.

Table of Contents

List of Tables

List of Figures

Abstract

Gram negative bacteria use elaborate transport systems to acquire nutrients from their environment. One type of system is the ligand gated porin (LGP) transport system. All LGP's are TonB dependent and require energy in the form of proton motive force (PMF) to transport their substrates. LGP's are β-barrels with globular N-domains that reside in the barrel blocking the passage of molecules. Therefore in order for transport to occur the N-domain must change in conformation. This change in conformation is dependent on TonB, PMF and the presence of Ferric Enterobactin (FeEnt).

One of *E. coli's* LGP transport systems is the FepA system. The FepA system is used for the acquisition of iron. Located in the outer membrane of E. coli it binds and transports ferric enterobactin (FeEnt) a siderophore. In order for transport to occur through FepA the globular N-domain needs to either leave the barrel completely or structurally change inside the barrel to allow for transport through the barrel. To study the transport mechanism of FepA, the susceptibility of 25 cysteine mutants at different locations in FepA to alkylation by fluorecein maleimide (FM) was studied in live cells. The reactivity of those cysteine residues changed in response to the addition of FeEnt. This reactivity was also dependent on the presence or absence of TonB and energy. Of particular note is the reactivity of a residue located deep inside the barrel and the dependence of this labeling on the presence of TonB and energy. Also demonstrated is the functional complementation between the N-terminus and C-

terminal barrel expressed separately. The data collected offer support for the ball-and-chain theory for LGP transport.

H8 is a bacteriophage that was recently discovered to be FepA dependent for its infection of *E. coli* and the binding of H8 to *E. coli* is inhibited (50% inhibition concentration, 98 nM) by FeEnt the native siderophore of FepA. H8 did not require the other ferric catecholate receptors (Fui, Cir, or Iron) for infection. H8 has morphology and genomic structure of similarity to bacteriophage T5, a member of the family *Siphoviridae*. The DNA sequence of H8 showed that H8 has a 104.4 kb genome with a total of 143 open reading frames (ORFS). Of the 143 ORFS 120 of them are homologous to ORFS found in T5.

The tail protein of H8 that binds to FepA was compared to the tail proteins of the other bacteriophage T5 and BF23 that are also in the *Siphovirida* family. Relative to these other tail proteins H8's tail protein contains acidic and aromatic residues that are unique to it and are probably involved in the binding of the phage to FepA. Other than these residues this protein is similar to T5's tail protein suggesting a similar pore-forming mechanism through the cell envelope. Of further interest is a region on the H8 tail forming protein that contains a TonB box sequence. This suggests a link between this sequence and TonB dependent processes.

TonB is a 239 residue protein anchored in the inner membrane, spanning into the periplasm of *E. coli*. It is required by all LGP's for their transport of siderophores and their susceptibility to group B bacteriocins and certain bacteriophage. The

mechanism by which TonB accomplishes this is not yet understood. Several fusion proteins were constructed consisting of the green fluorescent protein (GFP) from *Aequaria victoria* either attached to the C-terminus or the N-terminus of TonB. All of the fusion proteins when expressed in *E. coli* were active with respect to the transport of FeEnt and the susceptibility to colicin B and D.

One of the previously proposed mechanisms of TonB is called the "shuttle hypothesis" which states that TonB shuttles from the inner membrane to the outer membrane. The data presented here demonstrates that TonB does not need to leave the inner membrane to accomplish its function, thereby presenting evidence against this hypothesis.

Chapter 1

1. Introduction

1.1Gram Negative Bacteria

Over a century ago Christian Gram invented a method to distinguish between two groups of bacteria. These are of course the Gram negative and the Gram positive bacteria. The Gram stain involves staining the bacteria with crystal violet and then counter staining with safranine. Crystal violet stains peptidoglycan and safranine acts as a counterstain. As a result Gram-positive bacteria appear purple due to the crystal violet and Gram-negative bacteria appear pink due to the safranine. It is believed that Gram-positive bacteria retain the violet dye because they contain no outer membrane and also have more peptidoglycan.

Peptidoglycan, also known as murein from the Latin *murus* meaning wall is attached to the outside of the cytoplasmic membrane in Gram-positive bacteria and attached to the inner leaflet of the outer membrane in Gram-negative bacteria. Peptidoglycan forms a scaffold for bacterial structure and strength giving the bacteria their shape and protecting them from osmotic stress. Peptidoglycan consists of alternating chains of β1-4 linked N-acetylmuramic acid (NAM) and N-acetlyglucosamine (NAG) linked to a D-amino acid containing tetrapeptide through NAM via an amide bond. The overall structure of the cell envelope in Gram-negative bacteria is an outer membrane followed by a periplasmic space with an inner or

cytoplasmic membrane. The peptidoglycan layer in Gram negative bacteria resides on the inner leaflet of the outer membrane.

One of the ways mammals protect themselves from bacteria is by secreting lysozyme, an enzyme that cleaves the β1-4 linkage between NAG and NAM. This enzyme is present in body secretions such as tears and mucus. Gram positive bacteria are especially susceptible to lysis by this enzyme because their outer layer is exposed peptidoglycan which can easily come into contact with lysozyme in the surrounding solution. Gram negative bacteria on the other hand are much less susceptible to lysozyme, because of an additional layer of defense in the form of an outer membrane (OM). The OM is important to enteric bacteria that reside in the intestinal tract of animals, protecting them from antibiotics, bile salts, and other degradative agents (77). The OM gives Gram negative bacteria a high level of resistance to antibiotics, making the pathogenic varieties that much more dangerous (94).

1.2 The Outer Membrane

The OM is an asymmetric bilayer. The lipid composition of the OM consists of exclusively lippopolysacharide (LPS) on the outer leaflet, and 70%-80% phosphatidylethanolamine, phosphatidylglycerol and cardiolipin on the inner periplasmic leaflet. The existence of an asymmetric bilayer was once thought to be thermodynamically impossible, and the idea that the outer membrane of Gram-negative bacteria was such a bilayer took years of experimental data to prove.

Labeling of amino groups found on phosphatidylethanolamine (PE) by a labeling molecule that was impermeable to the OM was not shown to cross-link to any PE (50).

It is now known that LPS is the only lipid on the outer leaflet of the OM. LPS is composed of lipid A, which in *E. coli* K-12 consists of a glucosamine disaccharide β-1',6 linked backbone that is acylated on the 2, 3, 2', and 3' carbons with (R)-3-hydroxymyristic acid. The 1 and 4' carbons are phosphorylated, giving the backbone sugars their charge on either side of the molecule. Lipid A is followed by a core domain made up of multiple 3-deoxy-D-manno-oct-2-ulosonic acid (KDO) molecules which make up its inner end, followed by phosphorylated heptose residues, which are then followed by hexose residues. The Lipid A and core LPS domains are followed by the O antigen, a long polysaccharide. *E. coli* K-12 cannot produce this O-antigen, however, making it less virulent (108). LPS makes the OM a permeability barrier. It is strongly hydrophilic, which is important in evading phagocytosis and hydrophobic antibiotics. LPS has a net negative charge, and therefore a tendency to bind divalent metal cations, such as Mg^{2+} and Ca^{2+}. The binding of divalent cations to LPS creates a tight impenetrable layer around Gram negative bacteria.

Septic shock brought from infection by Gram-negative bacteria results in roughly 20,000 deaths in the United States per year (84). These deaths are linked to the biological effects of LPS (endotoxin), a structure not actively secreted by the bacteria, but rather released upon their lysis. LPS induces the synthesis and release of TNF (tumor necrosis factor) and other cytokines that lead to shock. LPS is known as a

superantigen for its ability to cause such a strong response by the immune system. It is also LPS that is the main target for the immune system of mammalian hosts when they recognize bacteria, prompting effective clearance of infection by these organisms. This type of sepsis, in which LPS is the causative agent, is called endotoxemia; the condition in which bacteria cross into the blood is called bacteremia. Lipid A is the component of LPS responsible for the toxicity of LPS (111).

1.3 Porins

The OM is composed of 50% protein by mass; these proteins are of several different types. Most notable among these are the general porins, specific porins and ligand gated porins (LGPs). The general structure of the porins is a ß-barrel, as opposed to the α-helices that are found in cytoplasmic membrane proteins. Also of note is OmpA a ß-barrel protein involved in conjugation, bacteriophage and colicin reception, virulence and pathogenicty, it is also believed to be responsible for some structural stability in the OM (27, 37, 118, 119).

Since the OM forms such a great barrier to molecules entering the cell, it is important that the bacteria have a way to transport the molecules necessary for their survival. These molecules are transported by porins, which form β-barrel structures with hydrophobic residues on the exterior surface and hydrophilic residues on the interior surface. This causes the barrels to form a hydrophilic channel in the OM allowing for the transport of hydrophilic molecules through the OM barrier.

1.4 General porins

General porins are made up of open water-filled pores in the outer membrane. The crystal structures of these porins show that the polypeptides fold into 16-stranded β-structures which form transmembrane amphiphilic barrels (27, 58, 119). Further, this folding pattern occurs in many different general porins, even in the absence of sequence homology. It has been noted that this structural similarity without sequence homology could be a type of camouflage for the extra cellular area of the protein to prevent detection by antibodies or phage (101). The β-strands are connected by loops, some of which are quite large, reaching out into the extracellular space and creating more external surface area for the reception of solutes.

Of particular interest is the L3 loop in these porins, as it actually folds inside the channel, squeezing the barrel's diameter to 7x11Å and giving an exclusion limit of 600Da (78). In all general porins this key loop connects β-strands five and six. Negative charges on this loop bind to positive charges inside the barrel, decreasing pore size (117). This loop is not involved with the basic barrel structure, as can be seen by shortening or deleting L3 (62).

PhoE is produced under phosphate starvation and differs from the other general porins in that it contains a positively charged area next to its pore entrance. Basic residues cover the pore lining along the symmetry axis bound to each other via van-der-Waals interactions. This positively charged region is responsible for PhoE's greater selectivity for its negatively charged, substrates phosphate and polyphosphate. (57). By changing lysine to glutamine through mutagenesis the selectivity of PhoE

was changed from anion channel to cation channel (8). These barrels form trimers (72) and this formation of trimers increases the solute collection area by a factor of ten (54).

All of these porins transport via passive diffusion according to Ficks first law which states that the rate of diffusion is proportional to the concentration of solute. This also makes these porins behave as ohmic conductors in that they show a linear relationship between voltage and current (9). OmpF and PhoE have different voltage sensitivities as demonstrated by the opposing effects seen when arginine residues are mutated to cysteines in the constriction site (98, 112)

1.5 Specific porins

Specific porins are 18-stranded β-barrels that also form trimers. In contrast to general porins specific porins have more loops, and they are larger in size, suggesting that the loops play a role in transport. They exhibit substrate specificity, and are part of multi-protein systems, with a periplasmic binding protein, and an inner membrane (IM) ABC transporter. They are different from the general porins in that they bind their substrates; however they bind their substrates with low affinity, distinguishing them from the ligand gates porins. They follow Michaelis-Menten kinetics (76).

The best studied is maltoporin (LamB), which is responsible for the transport of polysaccharides, such as maltodextrin, an α-1-4 linked polyglucose. LamB takes its name from the fact that it was first discovered as a receptor for bacteriophage λ (93). LamB discriminates between substrates based on size and conformation (64). The β-

strands of the barrel are connected by loops, three of the loops cross over the center of pore (L4, L6 and L9). It has also been shown that L9 may contain an initial binding site for maltodextrin (53, 55). There is also a set of six aromatic residues that lay along one side of the channel and form a path of hydrophobicity known as the "greasy slide" (102) leading through the channel from the surface to the periplasmic side. This greasy slide functions as a guide to sugar molecules as they pass through the channel via hydrophobic interactions. The alteration of residues along the pore opening, Arg8 and Tyr118, have an effect on the binding of the substrate maltodextrin to LamB. As sugar molecules pass through LamB they lose their water shell which is replaced by ionic side chains as the sugar enters the pore. Sugars bound to the pore block ion conductance through LamB (10, 29). It has been proposed that maltose binds in two stages to LamB, first to a binding site on L9 and then on to the greasy slide. The evidence for this biphasic binding is supported by the fact that the K_d for LamB is 11mM and the K_m is 5μM (54).

1.6 Active Transport

Active transport is the uptake and accumulation of a substrate against a concentration gradient, without chemical modification of the substrate. Some active transport systems are sensitive to osmotic shock because their substrate binding proteins are released from the cells by osmotic shock. Active transport systems for the uptake of arabinose, galactose and histidine by Gram negative bacteria are well known and studied. These systems consist of a membrane component and a periplasmic

component. The lactose transporter in *E. coli* is another example of an active transporter. Lactose is smaller then 600Da and therefore freely diffuses past the outer membrane of Gram negative bacteria. It only requires an inner membrane transport protein that is a secondary transporter because it utilizes a preexisting ion gradient as the energy source for substrate accumulation.

1.7 Regulation of FepA expression

The *lac* operon regulates genes responsible for lactose transport, controlled through the *lac* promoter. Iron transport systems fall into a similar category, because they are regulated by Iron availability. However unlike the *lac* operon these fur regulated operons are repressed in the presence of their substrate.

Primary active transport uses ATP directly for transport. The best example of this kind of transporter is the ABC-transport systems. Secondary active transport uses ion gradients produced by electron transport or ATP hydrolysis as the energy source. These secondary active transporters were discovered when protonophoric uncouplers were seen to inhibit transport. It has been hypothesized ligand gated porins (LGP's) use this secondary active transport.

1.8 Ligand Gated Porins

Unlike general and specific Porins, Ligand Gated Porins (LGPs) have not been shown to form trimers. They are composed of 22-stranded anti-parallel β-sheets, that form β-barrels with the β-sheets oriented in a 45˚ angle in relation to the OM. These porins are different from the other porins in that their N-Domain, the ~150 residues on

the N-terminus of the polypeptide chain, folds into their barrels in a globular fashion, forming a plug that closes the barrel. These porins are active transporters, requiring both energy possibly in the form of proton motive force (PMF), and a set of three proteins, TonB, ExbB and ExbD, located in the IM. Like the specific porins the LGPs are also a part of a multi-protein transport system with a periplasmic binding protein and an IM ABC transport system. Examples of LGPs include FepA, FhuA and FecA.

The unique N-domain of these LGPs has a conserved set of β-strands with two loops connecting them. The first 17 residues contain a region of homology between all of the LGP's called the TonB box. The TonB box is hypothesized to bind to TonB and be responsible for the connection between the LGP's and TonB. The N-domain is also large enough to fit in the β-barrel of the LGP's and constrict their pores. In all, the outer membrane LGPs recognize two catecholate, one carboxylate, one corrinoid and three hydroxamate siderophores.

1.8.1 FepA

FepA, a well studied example of a LGP, was originally called *fep* for ferric enterobactin permease (28). However, after it was discovered that the product of the *fepA* gene resides in the OM, the permease was dropped, since this term is used to describe IM transport proteins, and the term porin was used instead to describe FepA's association with the OM. FepA is better called Ferric Enterobactin Porin A. FepA contains a 22-stranded β-barrel, with a globular domain made up of 150 N-terminal residues. The β-strands are connected to each other via loops that stick out into the

extra cellular space. FepA specifically and actively transports ferric enterobactin (FeEnt) against its concentration gradient. It has been shown that FeEnt binds to FepA by a biphasic binding mechanism, first associating with the loops and then the center of the barrel (75, 81). FepA binds its substrate FeEnt with high affinity with a K_d in the subnanomolar range and a dissociation half life of the FepA-FeEnt complex is over 1min (74). Therefore, FeEnt stays bound to FepA for a relatively long time, long enough to initiate its transport reaction, which takes about 20 seconds to complete (52).

There are a series of ion-pairs between the N-domain and the β-barrel of FepA. The minimum distance for ionic bonding to occur is 3.5Å. A specific example of ion-pairing is the ionic bonding between K147 and K148 on the N-domain bonding to acidic E248 and E250 on the β-barrel. If the H^+ concentration were to increase, to produce a pH of 4, these bonds would break, and the ion-pairing would be eliminated. This would in turn release the N-domain from the β-barrel, allowing FepA to change conformation.

Figure 1 Crystal structure of FepA. (15)**.** The outer membrane is represented by the two horizontal lines, this region was determined via hydrophobic regions. The extracellular space is located at the top of the figure and the periplasmic space is located at the bottom of the picture.

1.9 Iron:

Iron (Fe) along with nickel are the final elements produced in stellar nuclear synthesis. This means that they are the most abundant metals found in the core of planets. Fe is found in more biological systems than any other metal. Fe adheres non-specifically to biomolecules such as proteins, nucleic acids and membranes. It is found inside metalloproteins where it is stable, due to the fact that in free form or when exposed at the surface of a protein, it can form free radicals. Most living organisms require Fe^{2+}, the ferrous ion of Iron. This is usually found in the heme prosthetic groups found in such proteins as hemoglobin and cytochromes. Enzymes such as aconitase are involved in many biochemical processes contain iron-sulfur clusters. Fe is also found in such enzymes as ribonucleotide reductase, which is in part responsible for the synthesis of deoxyribonucleotides, the precursors of DNA. The exception to this requirement is the lactic acid bacteria in that they flourish in dairy products, which contain very little Fe. To get around this, these bacteria have developed a vitamin B_{12} system to replace the ribonucleotide reductase system found in most bacteria for DNA synthesis.

1.10 Iron Uptake in Gram-negative Bacteria

Most bacteria require an external Fe concentration of 10^{-8}M for growth. In anaerobic conditions a large amount of Fe exists in the environment in the ferrous form, but in the aerobic conditions where *E. coli* sometime lives, the concentration of

free Fe is much lower, at around 10^{-18}M. In water and aerobic conditions Fe is in this low concentration due to the formation of iron hydroxide polymers.

Bacteria face another barrier to iron acquisition in one of their major environments, the intestines of the animals they use as hosts. Animals use a variety of strategies to sequester iron and keep it from the bacteria. The major strategy is the use of iron binding proteins such as transferrin and lactoferrin.

As a result of their need for Iron and its often unavailability, aerobic and facultative anaerobic bacteria possess multiple systems for the acquisition of Iron. These systems can be separated into two major categories, nonspecific and specific. As long as free Fe is present in large amounts the nonspecific system works effectively; but when the Fe concentration drops to low levels the more specific systems are required. These more specific systems require carrier molecules know as siderophores.

1.11 Siderophores

Bacteria have evolved unique systems to acquire iron from the environments they reside in. By developing molecules that bind iron at a higher affinity than mammalian proteins bacteria are able to steal iron away from their hosts. These molecules, called siderophores (from the Greek iron carrier) are molecules with very high affinities for iron. Siderophores fall into three categories, catecholate, hydroxymate or a combination of both catecholate and hydroxymate. When these bi-dentate ligands bind Fe^{3+}, they form a hexacoordinate, octahedral complex with high

spin and kinetic instability. Aposiderophores are synthesized and then excreted into the bacteria's environment where they complex Fe^{3+}, in some cases removing it from host systems. Bacteria then bind ferric siderophores and transport them into their cells.

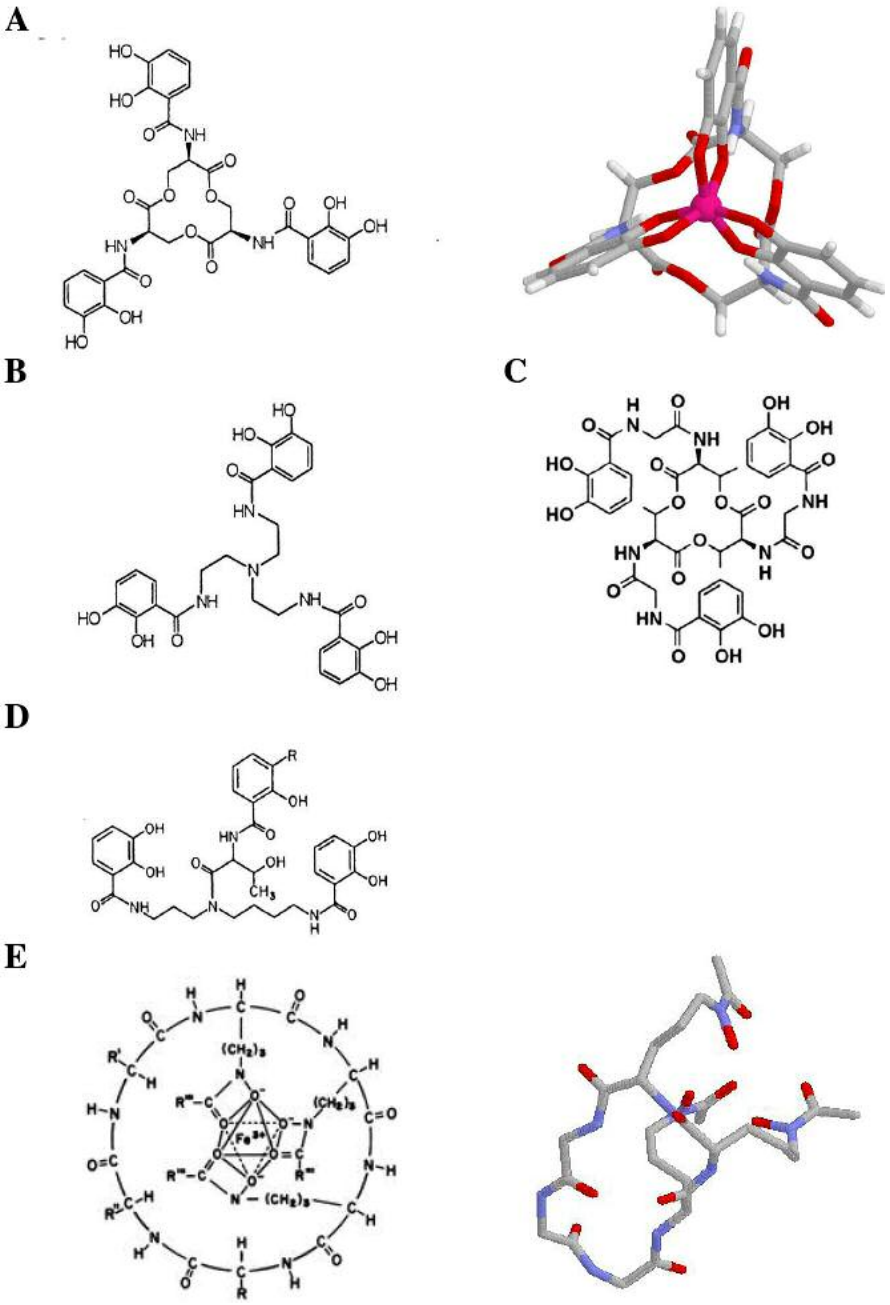

Figure 2 Catecholate and hydroxamate siderophores. A. Enterobactin, B. Trencam C. Corynebactin, D. Agrobactin, E. Ferrichrome (Neilands 1952, (86) (79, 80) van der Helm 1980, Rodgers 1987, Karpishin 1992, Budzikiewicz 1997). The crystal structures of vanadium enterobactin and apoferrichrome are shown to the right of the enterobactin and ferrichromerespectively.

1.12 Colicins

Colicins are proteins secreted by certain strains of *E. coli* to kill other strains of *E. coli*. Named colicin, by the discoverers Gratia and Fredericq in 1946, when they demonstrated that these were protein molecules with a certain specificity and activity spectra (38). These toxins were later redefined as bacteriocins in order to denote them as proteins produced by one bacterial species for the purpose of killing other related bacteria species (48). The nomenclature of the bacteriocins is given by the name of the bacteria that produces them followed by the suffix –cin. Bacteriocins are of relatively high molecular mass with molecular weights ranging from 20 to 80 kDa (21).

In order to avoid the lethality of the colicins that they secrete bacteria produce immunity proteins that protect them from the action of the toxin. The structure of a colicin is made up of three domains, the binding domain, the translocation domain and the killing domain. The killing domain can have many different biochemical actions. The binding domain of colicins is specific to unique sites on the cell surface, usually some kind of nutrient transport system created by porins. Colicin binding is highly specific, suggesting that these proteins mimic the nutrients their receptors are used for. Their binding domains often have anti-parallel β-sheet structure; this is seen in the X-ray structures of colicin N, and colicin Ia, and colicin B, in the context of an overall structure that is predominately α-helical.

The killing domains of colicins may achieve lethality by several different methods. For example colicin E1 inhibits all macromolecular synthesis, colicins E2 break down DNA, colicin E3 stops protein synthesis and colicin M degrades

peptidoglycan and colicins Ia and B form pores that collapse the proton gradient, across the IM (18).

Regarding translocation across the OM, two groups of colicins (group A and group B). Group A colicins are dependent on the Tol system, whereas group B colicins are dependent on the TonB system. Both groups target specific proteins on the surface of *E. coli* as their receptor binding sites.

1.13 Bacteriophage

Bacteriophages are viruses that infect bacteria. Bacteriophages, like all viruses, are metabolically inert and incorporate themselves into the biochemistry of their hosts. The structure of bacteriophages consists of the genome of the virus encapsulated in either a protein or lipoprotein coat known as a capsid. They can use proteins, lipopolysacharides, teichoic acids or flagella to bind on the surface of the host cell. After adsorption they inject their DNA into the cytoplasm of the cell. Once the phage DNA is inside the cell, host machinery will replicate it or incorporate the phage DNA into the host genome.

Greater than 95% of all phage that have been described in the literature up to this point are from the order Caudovirales. Caudovirales are the tailed phages and consist of 50% double stranded DNA and 50% protein by mass. There are three main families in Caudovirales, the *Siphoviridae* which contain long tail morphologies, the *Myoviridae* that have double layered contractile tails and the *Podoviridae* that have short tails.

The genomes of bacteriophage can range in size from only a few thousand base pairs to 480,000 base pairs which is the genome size of phage G. Their DNA consists of three phases pre-early, early and late. It is in the late phase that is involved in the construction of the virus particle itself.

1.14 Ligands of FepA

1.14.1 Ferric Enterobactin

With a K_a of 10^{54}, enterobactin (Ent), has the highest affinity for iron of any other iron binding compound known on this planet. Ent contains three catecholate rings that complex Fe^{3+} in a C_3 symmetric structure. When the Fe^{3+} is bound to enterobactin, forming FeEnt, the molecule contains a net negative charge (-3). This net negative charge and the aromatic catecholate groups are believed responsible for the association between FepA and FeEnt.

1.14.2 Colicin B and D

Colicin B is a group B colicin that requires both FepA (90) and the TonB ExbB, ExbD system. It has a molecular weight of 55kDa and its crystal structure (47) showed that it has a barbell shape (Figure 3). Colicin B kills the cell it recognizes by forming a pore in the cytoplasmic membrane, diffusing the proton gradient of the cell. At least three steps are required for the entry of colicin into the cell. Step one is the binding of the colicin to FepA. This initial binding step does not require energy or TonB. The second step is the translocation of the colicin (at least the killing domain) across the periplasmic space; this second step requires both energy and the TonB,

ExBB, ExbD system. The last step is the delivery of the killing domain to the cytoplasmic membrane.

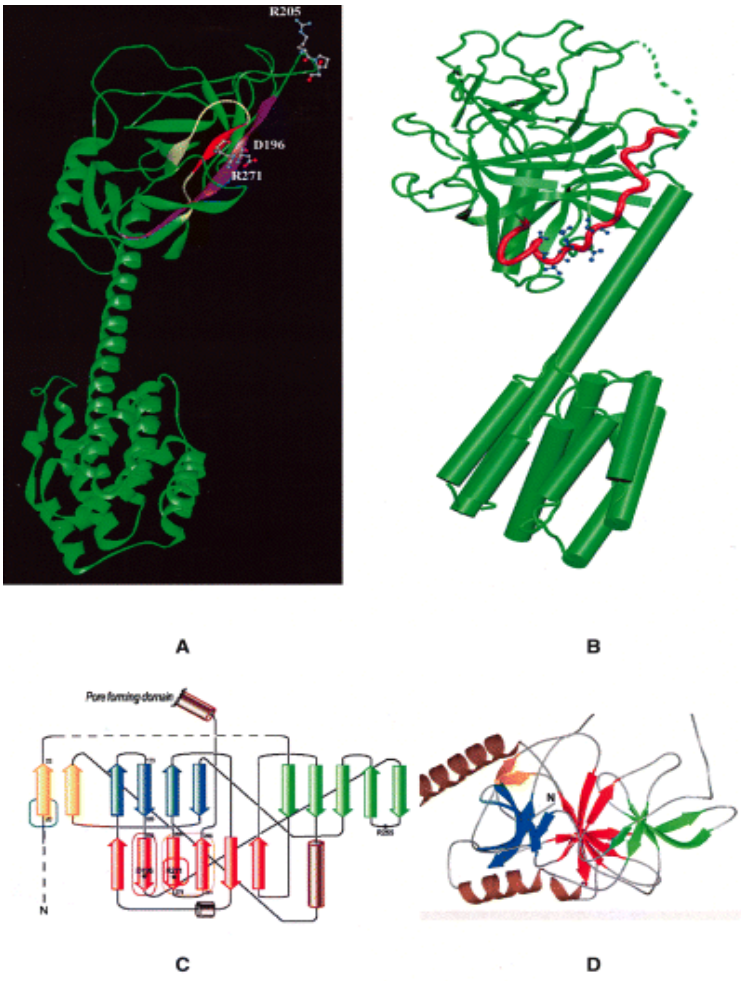

Figure 3 Structure of Colicin B.

A. Ribbon diagram of colicin B. Amino acids 262–282 (yellow) were shown to have sequence similarity to antiparallel β-strands in the receptor-binding domain of colicin Ia (amino acids 298–312). B. TonB box. Amino acids, 11–28 (red), and the amino acids corresponding to the TonB box, ^{17}DTMVV^{21} (blue).

C. N-terminal domain of colicin B. The TonB box (blue) and regions of similarity to T1 (violet), T2 (red), colicin Ia (yellow) TonB boxes.
D. N-terminal domain of colicin B with the distribution of the secondary structural elements shown in figure (C). (47)

Colicin D is a 75kDa protein and forms a heteromeric complex with the cognate immunity protein (ImmD). Colicin D also requires FepA and the TonB/ExbB-D system. The N-terminal 313 amino acids of both colicin B and D are required for the initial binding of the molecule to FepA. These N-terminal regions found in colicin B and D are 96% identical to each other suggesting similar binding strategies (96). However colicin D has a completely different mechanism for its killing activity. Unlike colicin B, colicin D's C-terminus has a catalytic activity that cleaves the anti-codon loop of tRNAs that encode arginine.

1.14.3 H8

H8 is a bacteriophage that was originally discovered in 1975, and until recently very little was known about this phage. H8 requires FepA for infection as well as the TonB/ExbB-D system. Although H8 was discovered over thirty years ago it was only recently shown that its dependence on FepA and the TonB/ExbB-D for infection was discovered (92).

1.15 TonB

TonB is a 239 amino acid protein found in *E. coli*. Originally TonB was discovered through the isolation of colonies resistant to T1 phage (1). Later the *tonB* colonies originally discovered to be resistant to T1 infection were also shown to be resistant to Φ80 phage infection (66) and also group B colicins (39). These mutants were also found to be defective in all high affinity active transport systems for Fe (14, 36, 41, 91) as well as defective in the active transport of vitamin B-12 (5). It is the

energy dependent step of the transport of B-12 that *tonB* affects (6) as well as the irreversible binding step of phage's T1 and Φ80 (40). Interestingly spheroplasts (*E. coli* cells that have been stripped of their outer membranes) of *tonB* mutants were shown to transport ferrichrome (116). Since the *tonB* mutants did not effect transport through the inner membrane as demonstrated by these experiments the *tonB* gene was therefore linked to outer membrane transport and binding processes.

Since TonB was shown to be responsible for OM transport processes it was first hypothesized to reside in the periplasm where it could freely connect with the OM. However TonB was later reported to reside in the inner membrane based on sarkosyl extraction (85).

A recent study of the conserved 90 amino acid C-terminal domain of TonB in the Entrez Database showed that there are 263 different TonB proteins known currently in Gram Negative bacteria (24). Some bacteria even require more then one TonB. Other bacteria that contain the *tonB* gene do not require TonB.

All of the Ligand Gated Porins of the outer membrane require a TonB. It has long been hypothesized that TonB functions as an energy transducer since the outer membrane lacks a known source of energy and LGPs require both energy and TonB. So the question arises, how does TonB transduce this energy. One hypothesis is that TonB actually leaves the inner membrane where it resides and travels across the periplasm to the outer membrane LGPs. After interacting with the LGPs, it returns to the inner membrane where it is recharged. ExbB and ExbD are two inner membrane

proteins that are believed to be responsible for the recharging of the TonB complex. There is also evidence that TonB physically interacts with the LGPs, specifically through a region on the N-terminus called the TonB box. The interaction between TonB and the LGPs has been shown through various cross-linking methods. Of note are several processes that do not require TonB, for example the penetration of T5 in FhuA, E-colicins in BtuB and cloacin in DF13 through IutA. However, uptake of all metals requires both TonB and energy.

1.15.1 Structure of TonB

Nine of the TonB proteins contain a 290 residue N-terminal extension which is homologous to MecR1. This region is predicted to have three additional transmembrane α-helices. Connecting the N-terminal transmembrane segment to the C-terminus is the periplasmic linker region. This linker region varies considerably in both length and proline content. The length of this region ranges from 22 to 283 amino acids, which could indicate that this region is not necessarily a requirement for all TonB proteins. The C-terminal domain is the most conserved in all families. However, in a region between the second α-helix and the third β-sheet exists an area of variability between TonBs from different bacteria. There is also another region of variability on the fourth β-strand as well.

Several TonB proteins contained two C-terminal domains in series. TonB has a 12 residue cytoplasmic domain (95) The hydropathy profile of the N-terminus is similar to that of penicillin binding protein 5 (PBP5). PBP5 is different from TonB in

that it is anchored in the IM by its C-terminus followed by the transmembrane region from residue 12 to 32. Residues 33-150 form a linker region. This linker region has a proline rich area (31) and a flexible region (82). The linker region is followed by the C-terminal domain (22, 56, 82).

1.15.2 The TonB Box

Recent studies of TonB have presented evidence for TonB existing as a monomer using NMR (82) as opposed to a dimer as previously shown using X-Ray crystallography (22). The main difference in these two studies was in the length of the TonB C-terminus that was used. In the earlier study residues 154-239 were used whereas in the more recent study residues 103-239 were used. The more recent study presented data indicating the following differences: first that residues 165-170 form a β-sheet in the old structure whereas these residues form an α-helix in the NMR structure; also that β_3 is buried in the X-ray structure but some of these residues (222-225) are exposed in the new. Another difference is that in β_2 the dihedral angles for 197-199 can turn back to helix2 in the new monomer structure.

This recent study also used NMR to present data indicating an interaction between TonB and the TonB box of FhuA, FepA, and BtuB. This data was collected by titrating the TonB box from FhuA into the TonB C-terminus. As the concentration of TonB box polypeptide increased there was a shift in the chemical environment of several residues located in the C-terminus of TonB. This data indicates that there is an interaction between the C-terminus of TonB and the TonB box of Ligand Gated Porins

(LGPs). Isotherm titration calorimetry gave a K_D of this interaction to be 36±7μM which is a fairly weak interaction.

1.15.3 Comparison between TonB and the Flagella Motor

Flagella are filaments that extend out of bacteria and propel bacteria towards a gradient of nutrients. Flagella consist of three main regions: the actual filament, the rotor, a motor that rotates the rotor, and a ring that holds them together. The rotor is composed of three proteins, FliG, FliM, and FliN. These three proteins form a FliG/M/N complex that is bound at its base by a ring termed the MS-ring. FliG/M/N has been implicated in motor rotation through mutational analysis and is termed the switch as it is believed to be responsible for the change in direction of flagellar rotation. The rotation of the flagellar motor between clockwise (CW) and counterclockwise (CCW) motion is reversible and dependent on chemotaxis.

The flagellum is rotated at its base by a motor that is driven by a transmembrane gradient of protons or Na+ ions. MotA and MotB form the rotational motor and MotA/MotB complexes that independently pump protons across the cytoplasmic membrane. MotA and MotB are integral membrane proteins that form the stator of the flagellar motor. MotA has four transmembrane segments while MotB has only one transmembrane segment. MotB also has a large domain in the periplasm that contains a peptidoglycan-binding motif that is believed to anchor the complex to the cell wall. The stoichiometry of the MotA/B complex is 4/2.

MotA and ExbB share sequence similarity and both use a proton gradient to perform their functions. ExbB has only three transmembrane segments as oppose to four in MotA. However, the three transmembrane segments in ExbB share homology in sequence and topology to those in MotA. TonB has one transmembrane segment which would make up for the one missing in ExbB. ExbB shares a conserved proline residue (Pro141) with MotA (Pro173). ExbB forms a complex with another protein, ExbD, like MotA. MotB which is homologous to ExbD has a single transmembrane segment just like MotB. ExbD like MotB has a very critical Asp residue (Asp25 in ExbD and Asp32 in MotB). Finally the MotA/B complex and the ExbB/D complex contain multiple copies of each protein.

1.16 GFP

Green Fluorescent Protein (GFP), isolated from *Aequoria victoria*, is a protein used as a fluorescent marker for a large range of applications. It has been shown to be active in both C-terminal and N-terminal fusions in organisms ranging from bacteria up through to mammals. GFP is non-invasive and can be used as a cell lineage tracer, reporter or tool to measure protein-protein interactions.

GFP is a 238aa polypeptide that forms an eleven stranded ß-barrel. The diameter of the barrel is 30Å and the length is 40Å. Small caps on the ends of the cylinders are formed by α-helix which then enter into the barrel and form a stabilizing pole that holds the fluorophore in the center of the barrel. There are no clefts that could be used to access the fluorophore by diffusible elements. It has been shown to

form dimers in solution at low ionic strengths, (<100mM) this causes a change in the excitation spectra energy transfer of GFP. GFP is highly resistant to denaturation by heat below 90°C, pH between 4 and 12 and to other denaturing agents. Once denatured it folds back to its original conformation. The environment around the fluorophore contains both apolar and polar as well as charged residues. Phe46 and Phe64 function to protect the fluorophore from Trp63.

1.16.1 Fluorescent Spectrum of GFP.

GFP has two excitation peaks in the UV spectrum with one major peak at 395nm and a minor peak at 475nm. The extinction coefficient at 395nm is 30,000 M^{-1} cm^{-1} and at 475nm it is 7,000 M^{-1} cm^{-1}. GFP emits in the green spectrum at 509nm. By increasing the pH, GFP is excited more at 475nm and has a decreased excitation at 395nm.

The fluorophore of GFP is made up of Ser65-Tyr66-Gly67 tripeptide. This sequence is autocatalytically modified to form a 4-(p-hydroxybenzylidene)-imidazolidin-5-one or a p-hydroxybenzylidene-imidazolidone structure. The autocatalytic process requires no co-factors or enzymatic components and is as follows. The reaction is initiated by a rapid cyclization between Ser65 and Gly67 to form the imidazolin-5-one intermediate, which is followed by a much slower rate-limiting oxygenation step in which Tyr66 is oxygenated by O_2 over a period of hours. Gly67 is required in the formation of the fluorophore. The reaction is thermo sensitive and decreases in yield below 30°C. Hydrogen bonding between His148 and Tyr66 and

Gln94 and Arg96 is believed to stabilize the fluorophore. The above mentioned His and Gln act also to stabilize and delocalize the charge on the fluorophore produced by the benzyl oxygen of tyrosine and the carbonyl oxygen of the imidazolidone ring.

Several mutants of GFP have been made that alter the fluorescence of the protein, for example a red-shifted mutant that absorbs at 490nm and emits more light at 509nm. A blue variant of GFP BFP is produced when Tyr66 is changed to His which causes an excitation maximum at 383nm and an emission at 448nm. There are Red and Yellow variants as well as a "Timer" GFP that changes from green to red over time. (109). Removal of more than 7 amino acids from the C-terminus or removal of the N-terminal residues past the methionine leads to total loss of fluorescence.

Fluorescence emission involves the excitation of an electron to a higher energy state. As the electron returns from its excited state back to its ground state it emits a photon of energy. All molecules absorb light and therefore there electrons transfer to higher energy levels. However, only fluorescent or phosphorescent molecules release energy through the emission of a photon. There are actually many ways by which a fluorescent molecule can release its excited state energy to return to its ground state. As is the case with non-fluorescent molecules, the energy can be released via vibrational and rotational energy which is dissipated as heat. Fluorescent and phosphorescent molecules have two other ways by which they can release their excited state energies. The first and most recognized way is through the emission of a

photon. This phenomenon is called fluorescence in fluorescent molecules and phosphorescence in phosphorescent molecules.

Another way fluorescent and phosphorescent molecules can give off the energy of their excited states is through quenching. Quenching occurs when the fluorescent molecule collides with another molecule and in so doing gives a part of its energy to the colliding molecule. If the fluorescent molecule emits its photon more quickly than the quenching molecules can take it away then the molecule still fluoresces. However, if the colliding molecules remove the energy of the fluorescent molecule rapidly before it can emit its photon, then the molecule does not fluoresce and is quenched. The more collisions a molecule experiences, the more rapidly it is quenched. GFP has a huge advantage to the quenching problem. Its fluor is enclosed in a very sturdy all encasing cover, an eleven stranded ß-barrel with plugs on both sides. This enclosure of the GFP fluor prevents it from being quenched through the rapid contact of colliding molecules. This means that GFP is ideal for fluorescent studies since its fluorescence quality is well protected.

1.17 Significance

The natural environment of *E. coli* is the intestines of animals. In this environment they actively sequester Fe from their host. The sequestering of Fe from their host specifically in man has been demonstrated to be a part of the pathogenesis of this organism as well as other Gram negative bacteria. This gives a direct link between Fe acquisition and infectious disease that revolves around the ability of these

pathogenic organisms to bind and transport Fe. In the absence of Fe bacteria growth is inhibited leading to the conclusion that a disruption in the ability of the bacteria to acquire Fe in their host may lead to a reduction in virulence. The ability of bacteria to acquire Fe is through a series of transport proteins. The understanding of these Fe transport proteins and the system of proteins they require has the potential of leading to insights in ways to prevent Gram-negative pathogenesis in humans.

1.18 Research Focus

The focus of this research is centered on FepA and the mechanism by which FepA performs its function as well as the role of TonB in this system. There are currently two major models for the mechanism of FepA transport; the transient pore model and the ball and chain model. The question is, does the globular N-domain of FepA leave the barrel of or does it shift in its conformation?

The bacteriophage H8 was discovered in 1975 by Rabsh, recently it was observed in our lab that this bacteriophage is specific for FepA and requires FepA for infection of the host. Bacteriophage are known to use proteins in the OM of gram-negative bacteria for infection. Of interest with this new phage is: Does it compete with FeEnt for binding sites on FepA? Is the infection of *E. coli* by H8 TonB dependent like colicin B and FeEnt? How similar is H8 to other bacteriophage that use OM proteins?

TonB is a protein required by all LGP's in the OM. It has been extensively studied but as of yet the mechanism by which it performs its function is unknown. One

of the major questions of its function is whether or not it leaves the inner membrane in order to perform its function in LGP transport.

Chapter 2

2.1 Materials and Methods

2.1.1 Bacterial Strains

The strains used in all of the studies are derived from *E. coli* K-12. AN102 was used in the purification of enterobactin, OKN3 was used for phenotypic studies of FepA its derivatives, OKN1 was used for studies relating to the relevance of TonB and OKN13 was used to look at the relevance of both FepA and TonB in conjunction. (Table 2)

Strain	Genotype	Reference
AN102		Cox 1970
BN1071	*F- thi entA pro trp rpsL*	Klebba 1982
OKN1	BN1071 *tonB*	Ma 2007
OKN3	BN1071 *fepA*	Ma 2007
OKN13	BN1071 *tonB fepA*	Ma 2007

Table 1 List of Bacterial strains used in this study.

2.1.2 Plasmids

All of the constructs were made on pHSG575 a low copy plasmid.(42)

Plasmid Name	Genotype	Reference
pHSG575		Hashimoto-Gotoh et. al. 1981
pITS23	*fepA*$^{+}$ on pHSG575 (full promoter)	Scott et al. 2001
pFepβ	*fepA*Δ17-151	Scott et al. 2001
pFepN	*fepA*1-151	Scott et al. 2001

Plasmid Name	Genotype	Reference
pHSG575		Hashimoto-Gotoh et. al. 1981
pITS23	*fepA*$^{+}$ *on* pHSG575(Full promoter)	Scott 2001
pQBT7-GFP	*gfp*$^{+}$	Qbiogene
pGT	*gfp:tonB*on pHSG575	This study
pGLT	*gfp:6α-hlix linker:tonB* pHSG575	This study
pTpG	*tonBpromoter:gfp* on pHSG575	This study
pTPG	*tonBpromoter:gfp* on pUC18	This study
pT23	*tonB*$^{+}$ on pHSG575	Scott 2001
pSTON	pMalp2 malE::tonB 170-239	Scott 2001
pSTON104	pMalp2 *malE::tonB* 104-239	Scott 2001
pSTONRIG	pMalp2 *malE::tonB* 69-239	Scott 2001
pSTONFull	pMalp2 *malE::tonB 1-239*	Scott 2001

Table 2 Plasmids used in this study.

2.1.3 Preparation of Competent Cells for Transformation

The transformation process required competent cells that are first started with 5mL of an overnight culture in LB with the appropriate antibiotics was subcultured 1/100 into 50 mL of LB with the appropriate antibiotics. The cells were allowed to grow until mid-log phase and then collected by centrifugation in a Beckman JA-20 XP centrifuge in a JA-14 rotor at 3,000xg for 5min. The cell pellet was then resuspended in 1.5mL of ice cold double distilled water and then spun down at maximum speed in a Beckman GS-15R tabletop centrifuge. The cells were then washed 3 more times with ice cold double distilled water and then once with a 10% glycerol solution. The cells were then resuspended to a final volume of 200µl in 10% glycerol, separated into 40µl aliquots and then stored at -80˚C until used for transformation.

2.1.4 Transformation via Electroporation

For electroporation 1-5µl of DNA was added to 40µl of competent bacteria cells and then added to pre-chilled electroporation cuvettes. The mixture was then pulsed with 2.5V and then immediately 1mL of SOC buffer was added. The mixture was then transferred to small 13 x 100mm test tubes and then incubated with shaking at 37˚C for 1 hour. The cells were then streaked on LB agar plates with the appropriate antibiotics.

2.1.5 Media and Growth Conditions

Strains were grown in Luria-Bertani (LB) (70) prior to purification of plasmid DNA, prior to colicin B and siderophore nutrition assays. For purification of

membrane extracts, cells were first grown in LB and then in MOPS media (73). Bacterial lawns for colicin susceptibility were prepared using LB top Agar. Siderophore nutrition assays were perfumed using Nutrient Broth (DIFCO). For the purification of Enterobactin T-media was used. (68).

Media	**Reference**
Luria-Bertani Broth	Miller, 1972
T-Media	Klebba et. al. 1982
MOPS	Neiderhardt et. al. 1974

Table 3 List of Media with References used in this study.

2.1.6 Fluorescent Labeling

The site directed Cys residues were covalently modified in live cells. The live cells were grown overnight in 10mL of LB media with the streptomycin at a concentration of 100μg/mL and chloramphenicol at a concentration of 20μg/mL at 37˚C with shaking in a New Brunswick series 25 incubator shaker. The cells were than subcultured into MOPS minimal media at a 1 to 100 dilution and grown to mid-log phase at an $O.D._{600}$ of between 0.5 and 0.6. The cells were collected using a Beckman JA-20 centrifuge with a JA-14 rotor at 5,000xg for 5mins. The cells were then washed twice with ice-cold tris buffer saline (10mM Tris, 1.37M NaCl pH 7.4)(TBS). The cells were then resuspended in cold TBS at a pH of 7.2 containing 0.4% glucose. After the cells were resuspended they were incubated either in the presence or absence of FeEnt at concentrations ranging from 0.0001-200μM and or the presence or absence of the energy inhibitor sodium azide at a concentration of 10mM. Fluorescein-5-

Maleimide (FM) was diluted into dimethyl formamide and then based on its extinction coefficient of 81,500 M^{-1} further diluted to a concentration between 5 and 20μM. The cells were incubated in the dark with the FM at 37˚C between 1 and 15mins. Cysteine was added to a concentration of 1mM after the incubation with FM to quench the binding reaction. The cells were washed an additional three times with 1mL of ice-cold TBS and finally resuspended in ice-cold TBS. The number of cells in these samples was then quantitated via $O.D._{600}$ then $1x10^8$ cells were resuspended in SDS-PAGE sample buffer, boiled and then run on SDS-PAGE.

2.1.7 Membrane Separations

2.1.7.1 Sucrose Density Gradient

Cells were grown overnight in 15mL of LB. Cells were then subcultured into 1L of MOPS and grown to mid-log phase (OD_{600} 0.5-0.9). Cells were then pelleted by centrifugation in a Beckman JA-20 centrifuge using a JLA 8.1 rotor at 3000xg for 10min. Cells were resuspended in 25mL of 10mM HEPES buffer pH 7.4. 1mg of DNAse and RNAse was added and cell suspensions were passed through a French press three times at 14000psi. Lysate was spun using a Beckman JA-20 centrifuge with a JA-17 rotor at 3000xg for 5min to remove unlysed cells and debris. Supernatant containing the lysed membranes were pelleted using a Beckman LB-M ultracentrifuge in a 45Ti rotor at 40,000rpm for 1hour. Membrane pellets were then resuspended in 3mL of 10mM HEPES buffer pH 7.4. The resuspended membranes were then layered on top of sucrose trilayer gradients. The sucrose trilayer gradients

consisted of 4.6mL of 2.02M sucrose in 10mM HEPES buffer pH 7.4, followed by 16mL of 1.44M sucrose in 10mM HEPES buffer pH 7.4 and finally 12.4mL of 0.77M sucrose in 10mM HEPES buffer pH 7.4. The trilayers was made in Beckman Ultra-Clear centrifuge tubes 25 x 89 mm. The sucrose trilayers were then placed in an SW27 swinging bucket rotor and spun down at 26,000rpm for 16hrs. The inner membrane (IM) fraction settled between the 0.77M sucrose and the 1.44M sucrose layer and the outer membrane (OM) fraction settled between the 1.44M sucrose and the 2.02M sucrose. The membrane fractions were then removed using a needle and syringe and transferred to Beckman Quick-Seal centrifuge tubes 25 x 89mm. The tubes were then balanced using 10mM HEPES buffer pH 7.4, sealed and spun down in a Beckman LB-M ultracentrifuge with a 70Ti rotor at 60,000rpm for 1hr (107). The pelleted membrane fractions were then resuspended in 1mL of 10mM HEPES buffer pH 7.4 assayed for protein concentration using the Lowry protein concentration determination assay and then 30μg of protein of each sample was added to SDS-PAGE gels.

2.1.7.2 Sarkosyl Extraction

A 5mL culture of bacteria was grown overnight with shaking at 37˚C. This culture was then subcultured 1 to 100 into 50mL of MOPS media and then grown to mid-log phase (OD_{600} 0.5-0.9). The cells were then collected via centrifugation in a Beckman JA-20 centrifuge in a JA-17 rotor at 5,000xg for 3min. The cells were then resuspended in TBS buffer with DNAse and RNAse and then lysed in a French Pressure cell three times at 14,000 psi. The lysate was centrifuged using a Beckman GS-15R tabletop centrifuge 12,000rpm for 5min to remove unlysed cells and debris.

The supernatant was pelleted using a Beckman GS-15R tabletop centrifuge 14,000rpm for 45min. The pellet was resuspended in 500µL 50mM Tris pH 7.4 and then an additional 500µL of 2% sarkosyl in Tris buffer was added. The mixture was incubated for 20min at 25˚C on a rotary microshaker. The mixture was then centrifuged at 14,000rpm for 45min in the Beckman GS-15R tabletop centrifuge. The supernatant which contains the inner membrane was collected and stored in a -20˚C freezer. The pellet containing the outer membrane fraction was resuspended in 100µL of 50mM Tris pH 7.4.

2.1.8 Fluorescence Imagery

After resolution of either cells or membrane fractions on SDS-PAGE, the gels were rinsed in distilled water and then transferred to a STORMSCAN PhosphorImager. The gels were then scanned for fluorescence emission and the densities of the protein bands were quantitated using ImageQuant 5.2 (Molecular Dynamics).

2.1.9 Western Blot Analysis

After resolution of cell lysates and membrane fractions on SDS-PAGE the protein samples were then transferred to nitrocellulose with a pore size of 0.45microns. After transfer of the proteins to the nitrocellulose the nitrocellulose was incubated in TBS 1%gelatin for one hour. The TBS 1% gelatin was removed and then the nitrocellulose was incubated overnight at 4˚C in a solution containing monoclonal antibody 45 (Mab45) which recognizes FepA in TBS plus 1% gelatin. Mab45 was

removed and the nitrocellulose was then washed five times for five minutes in TBS plus 1%tween-20. The nitrocellulose was then incubated for two hours with an anti-mouse anti-body with alkaline phosphatase conjugated to it. The nitrocellose was then washed five times as before with TBS plus 1% tween. After the final wash the nitrocellulose was expose to a solution containing 5mM $MgCl_2$ 0.1M NaCl 0.1M Tris, 3.7nM p-nitro blue tetrazolium (NBT) and 4nM 5-bromo-4-chloro-3-indolyl phosphate (BCIP).

2.1.10 Complementation Assays

2.1.10.1 Colicin Susceptibility

Cells were grown overnight in 10mL of LB media with the appropriate antibiotic. 100µl of cells were placed in test tubes along with 100µg/mL streptomyocin and 20µg/mL chloramphenicol. 3mL of pre-heated LB top agar was added to the tubes mixed and then plated onto 25mL LB plates. Colicin B was diluted in 96 well titer plates that were prepared by making 1/10 dilutions of purified colicin B and then ½ dilutions of these dilutions across. A clone master was used to spot test the colicin B dilutions onto the LB plates. Results are expressed as the reciprocal of the dilution that was able to clear bacterial growth.

2.1.10.1.1 Colicin B Purification

The bacterial strain DM1187/pCLB1 was inoculated in 5mL of LB with 100µg/mL streptomycin and 20µg/mL chloramphenicol let grow overnight. Subcultured the overnight culture at a 1 to 100 ratio into 30mL LB with 100µg/mL

streptomycin and 20μg/mL chloramphenicol let grow for 8 hours until culture reached late-log phase. The 8 hour culture was subcultured at a 1 to 100 ratio into 30L LB with 100μg/mL streptomycin and 20μg/mL chloramphenicol. The culture was then spun down in a Beckman JA-20 XP centrifuge with a JLA 8.1 rotor for 5min at 3000xg. The Cells were then washed two times with 250mL of 10mM phosphate buffer pH 7.4. The cells were then resuspended in 100mL final volume in 10mM phosphate buffer pH 7.4 with DNAse and RNAse and then passed through a French pressure cell twice at a 14,000psi. The lysate was then was spun down using a Beckman JA-20 centrifuge with a JA-17 rotor at 3000xg for 5min to remove unlysed cells and debris. Supernatant containing the lysed membranes as well as periplasmic and cytoplasmic contents separated using a Beckman LB-M ultracentrifuge in a 45Ti rotor 40,000rpm for 1hour. The supernatant was collected and subjected to a 41% ammonium sulfate precipitation. The precipitation was centrifuged in a Beckman JA-20 XP centrifuge in a JA-14 rotor for 30min at 10,000xg. The supernatant was subjected to a 48% ammonium sulfate precipitation and then centrifuged in a Beckman JA-20 XP centrifuge in a JA-14 rotor for 30min at 10,000xg. The pellet was then resuspended in 50mM Tris pH 7.4 and then dialyzed using Spectra/Por molecularporous membrane tubing (Spectrum Laboratories, Inc.) against 4L of 50mM Tris pH 7.4. The dialyzed solution was then loaded onto a DE-52 anion exchange resin equilibrated with 50mM Tris pH 7.4. The column was washed with 10 column volumes of 50mM Tris pH 7.4 and then subjected to a 0-0.2M sodium chloride gradient. Fractions were assayed for

protein concentration and colicin B activity. Peak fractions were then run on SDS-PAGE gel to analyze purity of protein.

2.1.10.2 Siderophore Nutrition Assay

Strains were grown overnight in 10mL of LB media with the appropriate antibiotic at 37˚C. 100µl of cells were placed in test tubes along with 100µg/mL streptomyocin, 20µg/mL chloramphenicol and 1mM bipyridal. 3mL of pre-heated nutrient top agar was added to the tubes mixed and then poured into 6 well Falcon tissue culture plates with low evaporation lids. Once the agar had solidified blank BBL paper discs with 6 mm diameters were added to the top. To the discs 10µl of a 50µM solution of FeEnt was added. After overnight incubation the diameters of the halos of growth around the disc were measured. Results are expressed as the diameter of the halo of growth observed around the center of the disc.

2.1.10.2.1 Purification of Enterobactin

AN102 (115) was used for the purification of Enterobactin (Ent). 5mL of AN102 were grown overnight in LB broth with 50µl of a 10mg/mL solution of streptomycin. The next morning the AN102 overnight culture was subcultured one to one hundred into 150mL LB broth with 100µg/mL of streptomycin and grown for 8hrs. This was then inoculated into 15L of T media and grown overnight in a 35˚C water bath with aeration. After the bacteria reached stationary phase (15 hours) the culture was spun down at 5,000xg in an Avanti JA-20 XP centrifuge in a JLA 8.1 rotor. The supernatant was then extracted once with 150mL of ethyl acetate and then

two more times with 100mLs ethyl acetate. The organic layer was collected and then concentrated using Brinkman rotovapor R110 in a one liter tear drop flask at a temperature of 28˚C. The concentrated ethyl acetate extract was then transferred to a new container and extracted once with 100mM citrate pH 5.5 one to ten dilution, then extracted with 10mL dH_2O. The extract was then dried overnight with anhydrous magnesium sulfate. The magnesium sulfate was then filtered off and the extract concentrated using a rotovapor to a final volume of 10mL. Hexanes was added slowly dropwise to until crystals formed after which the extract was then centrifuged in 25mL corex tubes in a JA-17 rotor in a Avanti JA-20 XP centrifuge at 9,000xg. The supernatant was discarded and the pellet containing the Ent dried.

2.1.10.2.2 Formation of Ferric Enterobactin

1-2mg of enterobactin was dissolved in 500µl methanol and then mixed with 500µl 4mM ferric sulfate in dilute hydrochloric acid. For the preparation of ^{59}Fe-enterobactin 0.05mCi of $^{59}FeCl_3$ was added to the ferric sulfate prior to its addition to the Ent. The mixture was then incubated at room temperature for 1hour after which 500mM sodium phosphate, monobasic, monohydrate at a pH of 6.9 was added to a final concentration of 10mM. The solution was then passed through a Sephadex LH20 column equilibrated with 10mM phosphate buffer. The dark red fractions containing Ferric Enterobactin (FeEnt) were pooled and the concentration of the pooled fractions determined by measuring the absorbance at 495nm on a Beckman DU 640 spectrophotometer, using the extinction coefficient of $5.6mM^{-1}$ (86). The purity of the

FeEnt was measured by looking at the ratio of absorbance at 395nm to 495nm (395/495). The pooled fractions were stored on ice and then if necessary re-purified on the Sephadex LH20 column.

2.1.11 Protein Concentration Determination

To determine the protein concentrations of membrane containing protein samples a modified version of the Lowry method (63) was used involving the addition of 1% SDS to all samples. For all other protein concentration determinations the original Lowry method was used.

2.1.12 Purification of H8

100µl of an 8 hour culture of OKN3/pits23 was added to 50mL of LB containing 100µg/mL streptomycin, 20µg/mL chloramphenicol, and 100µl of phage at a titer of 10^7 pfu. This infection was propagated at 37˚C in a shaker at 200RPM. In the morning RNAse (1µg/µL) and DNAse (1µg/µL) were then added to the culture which was allowed to shake at 37˚C for 20min. The solution was passed through a 1µm filter (Gelman Science Extra Thick), sodium chloride was added to a final concentration of 0.5M with stirring at room temperature until dissolved, finely ground PEG 6000 to an initial 2% concentration was slowly added with stirring at room temperature, until dissolved. The mixture was centrifuged in a Beckman Avanti JA-20 XP centrifuge, in a JA-14 rotor at 10,000xg for 10min. The supernatant was transferred to a fresh container and finely ground PEG 6000 was added with stirring at room temperature to 6% weight/volume. The solution was stirred at 4˚C for an additional 30min, and

centrifuged in an Avanti JA-20 XP centrifuge and JA-14 rotor at 10,000xg for 10min. The supernatant was discarded and the pellet was resuspended in 1mL T5 buffer (0.5M sodium chloride, 0.1M tris base, 0.001M calcium from calcium chloride dehydrate, final pH 8). The resuspended pellet was passed through an AcA22 (LKB 100,000-1,200,000) resin gel filtration column and eluted with T5 buffer. (44)**.**

2.1.13 Phage Infection Assays

The bacteria were grown overnight in 5mL of LB with appropriate antibiotics at 37˚C. Ten fold serial dilutions were made of a 10^{10} PFU per mL stock of H8. 10µL of these dilutions were added to 50µL of overnight bacterial culture and incubated at room temperature for 2mins. Molten top agar was mixed with these solutions and plated out on LB plates with the appropriate antibiotics. The plates were incubated overnight at 37˚C, and the number of plaques on each plate was counted.

2.1.14 Phage binding competition experiments with FeEnt

10^5 PFU of H8 was mixed in 0.5ml of LB (10µM $CaCl_2$), either in the presence or absence of FeEnt ranging from a concentration of 0.04µM to 20µM. The solution was mixed with 10^8 cells of OKN3/pITS23 in 0.5ml of LB (10µM $CaCl_2$). After incubation for 40min at 37˚C the samples were centrifuged at 8,000xg for 5mins at 4˚C in a BECKMAN GS-15R tabletop centrifuge. The supernatant was diluted in 10 fold increments and mixed with $5x10^6$ cells of OKN3/pITS23 plated out on LB+Cm plates. The plates were incubated overnight at 37˚C overnight. The number of PFU's on each plate was counted and used to determine the number of unbound PFU's.

2.1.15 Preparation of H8 DNA

A single plaque of H8 from infection plate using KDF541/pITS449 was picked with a sterile stick and mixed in 0.5mL of LB broth. This phage suspension was diluted 1 to 10 into 1mL of 0.01M $MgCl_2$ 0.01M $CaCl_2$ and added to 2 x 10^8 cells of KDF541/pITS449 in 50µL of LB broth. The suspension was incubated for 15mins at 37˚C and diluted again into 50mL of LB broth and incubated overnight with shaking at 37˚C. The solution was centrifuged in sterile Corex tubes in a JA-17 rotor at 3,000rpm for 20min. This supernatant was placed in an ultracentrifuge in a 70-Ti rotor and centrifuged for 1hour at 45,000rpm. The phage pellet was resuspended in 180µL of Tris HCl (50mM pH 8.0), extracted twice with phenol, and then with chloroform. The final DNA was precipitated with two volumes of ice cold 100% ethanol, and the precipitated pellet was resuspended in 10mM Tris HCl, 1mM EDTA.

2.2 Construction of GFP TonB Hybrid proteins

2.2.1 Polymerase Chain Reaction:

The pGT and pGLT constructs were generated using PCR amplification of enhanced green fluorescent protein (EGFP) from plasmid QBT7-GFP and tonB from pT23. The procedure for the PCR reaction was as follows: each reaction contained 1µl of Midi-Prep of plasmid 10-60ng of plasmid for template, 1µl of a 10µM solution of dNTP mix, 10µl of each primer at 10µg/µl, 10µl of 10X pfu buffer (Stratagene) and 1µl of pfu polymerase (Stratagene). The following cycling parameters were used except when specified otherwise, a 95˚C denaturation step for 5min, 30cycles of denaturation at 95˚C for 30 sec, primer annealing at 55˚C for 1min, 2min times the

length in kilobases of the target DNA at 72˚C, after the 30cycles of denaturation, annealing and extension a final identical extension at 72˚C and finally a 4˚C cooling reaction until subsequent reactions would be performed.

2.2.2 Agarose gel electrophoresis

DNA samples were mixed with at a 1part DNA loading buffer (50% glycerol, 0.1M EDTA, 1%SDS and 0.1%Bromophenol Blue Newton 1995) 5part DNA ratio. Samples were then added to 1% Agarose gels (1% UltraPure Agarose (invitogen)) in TAE buffer (0.4MTris 0.2MAcetate 0.2MEDTA). The samples were then electrophoresed through the Agarose gel for separation after which the separated DNA was visualized via UV illumination.

2.2.3 GFP attached to the C-terminus of TonB

Dr. Danny Scott constructed a fusion between GFP and TonB in which GFP was attached to the C-terminus of TonB (pTG). This fusion would contain GFP in the periplasmic space. Interestingly his construct was functional but not fluorescent. To achieve fluorescence, the signal sequence of this protein was altered to encode for a TAT (twin arginine translocation pathway) consensus sequence that would presumably allow this fusion protein to be fluorescent in the periplasm (pTGTat) twin arginine (99). However this did not result in a fluorescent protein. Finally the signal sequence of *tonB* was deleted completely conceivably containing the C-terminal TonB:GFP fusion protein in the cytoplasm where it could be fluorescent (pTGΔSS).

This fusion protein was also not fluorescent leading to the construction of an N-terminal GFP fusion protein.

2.2.4 Construction of pGT and pGLT

The construction of the GFP:TonB fusions was created by PCR amplifying three regions: the TonB promoter region, the enhanced GFP gene and TonB. The plasmid pT23 was used as a template for the replication of the TonB promoter and TonB gene and the plasmid pQBI-T7-GFP (Qbiogene) was used as a template for replication of the GFP gene. pT23 was constructed by PCR amplifying the structural gene for TonB from pRZ540 (89), including 333bp upstream of the start codon and 229bp downstream of the stop codon. The PCR product was then ligated into pHSG575 using an EcoRI site upstream of the start codon and a HindIII site downstream of the stop codon.

The *tonB* promoter was amplified using M13 forward, which anneals on pHSG575 on the 5'end of the *tonB* insert including the EcoRI site and the 333bp upstream of the *tonB* start codon and a second primer that anneals to the 3'end of the *tonB* promoter directly upstream of the TonB gene incorporating an XbaI restriction site on the 3' end. This gave a 333bp product with an EcoRI site on the 5'end and a BglII site on the 3'end.

GFP was cloned from the Qbiogene plasmid pQBI-T7-GFP. The plasmid pQBI-T7-GFP contains the gene for enhanced GFP. Enhanced GFP contains an **F64L** mutation giving the enhanced GFP greater solubility, protein folding and fluorophore

formation at 37˚C, the **S65C** mutation giving a single excitation peak at 474nm and the **I167T** mutation which enhances the excitation peak at 474nm (http://www.qbiogene.com/products/gene-expression/hidden/afp.shtmL). The *gfp* fragment was PCR amplified with an XbaI restriction site on the 5'end and BglII restriction site on the 3'end giving a 717bp fragment.

The *gfp* and *tonB* promoter fragments were digested with XbaI, then ligated together. Giving a product of 1050bp, this fragment consists of the *tonB* promoter followed by *gfp* with a BglII site on the 3'end of *gfp* an EcoRI site on the 5'end of the *tonB* promoter. This ligation product was then PCR amplified using M13 reverse and the 3'primer used for the previously mentioned GFP amplification. This PCR product was cleaned on agarose gel and digested with BglII. The TonB fragment was PCR amplified using M13 forward, which anneals to the pT23 plasmid incorporating 229bp downstream of the *tonB* stop codon and another primer that anneals to the first 21bp of *tonB* attaching a BglII site to the beginning of tonB. This *tonB* fragment was digested with BglII, cleaned and ligated with the previously mentioned *tonB*promoter:*gfp* fragment giving a final 2117bp *tonB*promoter:*gfp:tonB* product. This final product was then digested with HindIII and EcoRI along with the host plasmid pHSG575 and then ligated together to give the final construct pGT.

For the construction of pGLT a linker region was designed using the 5 amino acid sequence EAAAK (3) Quickchange mutagenesis was used to alter the N-

terminal sequence of TonB from TLDLPRR to AEAAAKA. This places a small helix forming peptide linker between GFP and TonB.

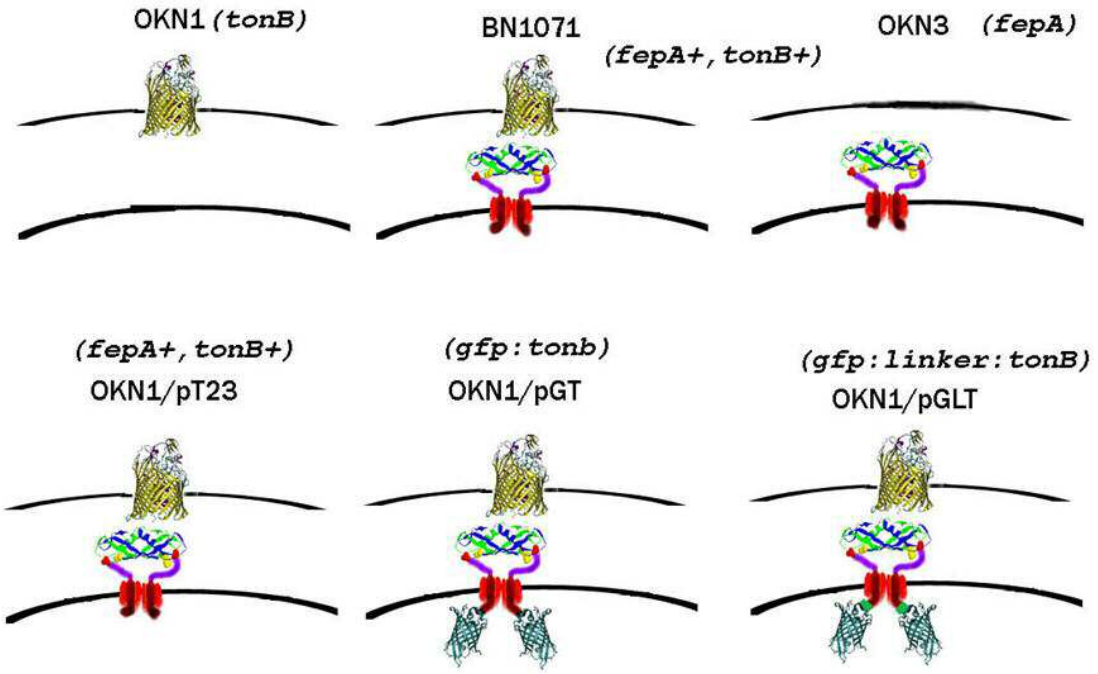

Figure 4 Constructs used in this study. In each of the figures the extracellular space is located at the top of the figure and the periplasmic space is located on the bottom of the figure. The single top line represents the outer membrane and the single bottom line represents the cytoplasmic membrane. FepA is located in the outer membrane, the dimerized C-terminal domain of TonB (22) is seen in the periplasmic space connected by the rigid central region (purple) and the transmembrane domain (brown). GFP is located in the cytoplasmic space.

2.2.5 Construction of C-terminal 69 residues of GFP:TonB fusion.

Plasmid pGT was used to construct a fusion protein in which the C-terminal 69 amino acids of TonB were removed. This would leave GFP in the cytoplasm anchored to the cytoplasmic membrane via the N-terminal domain of TonB. However without the C-terminal 69 amino acids which have been shown to dimerize the GFP: TonBΔ170-239 should not dimerize and there should be an increase in fluorescence due to a lack of quenching by GFP molecules held in close proximity to each other via the dimerized C-terminus.

To delete the C-terminal 69 amino acids Quick-change mutagenesis was used to alter the end of the tonB gene (downstream SacI site) and at position 170 (upstream SacI site) into a SacI site. The constructs were digested with SacI to verify the incorporation of the site. The upstream construct was then digested with EcoRI and SacI giving a fragment containing the TonBpromoter GFP and TonBΔ170-239 and then the rest of the plasmid. The small fragment had a size of 1.563 Kb and was purified using agarose gel electrophoresis and the Zymoclean gel clean up kit. The downstream was digested with EcoRI and SacI giving a fragment of 4.137Kb which was composed of the plasmid, this larger fragment was purified as described above and then both fragments were ligated together to form the final construct.

2.3 Binding of Ferric Enterobactin

The binding of FeEnt was measured using ^{59}FeEnt. For the induction of the iron regulated genes *fepA* and *tonB*, strains were grown overnight in 5mL LB with the

appropriate antibiotic and subcultured one to one hundred into MOPS and grown to mid-log phase. In the case of OKN1 and OKN13 due to their lack of vigorous growth they were grown for 24 hours in LB prior to subculturing into MOPS, then once subcultured into MOPS grown in MOPS for 12 hours prior to their use in binding studies. Prior to experimental work the strains were incubated on ice for one hour. 100µl of cells was added to a 50mL test tube on ice to this a mixture of 10mL MOPS at 4˚C containing ^{59}FeEnt at the various concentrations was added to the cells and incubated for 5 seconds after which the solution was filtered through 0.45-µm nitrocellulose. The nitrocellulose was then washed with 10mL ice cold 0.9% lithium chloride and then placed in a 5mL polystyrene round-bottom tube and counted in a Packard Cobra gamma counter. Each concentration was performed in triplicate. OKN3 the FepA-deficient strain was used as the negative control and binding observed in this strain was subtracted from the other samples. Binding data were analyzed using the Bound versus Total equation of Grafit version 5.0.12 (Erithacus Ltd., Middlesex, UK).

2.4 Transport of Ferric Enterobactin

Strains were grown to mid-log phase as mentioned earlier and then kept at room temperature during transport experiments. 100µl of cells was added to a 50mL test tube in a 37˚C water bath. 10mL MOPS with various concentrations of ^{59}FeEnt at 37˚C were then added to the cells and incubated at 37˚C for 1 min. The mixture was then filtered through 0.45-µm nitrocellulose filters. The nitrocellulose was then washed with 10mL ice cold 0.9% lithium chloride and then placed in a 5mL

polystyrene round-bottom tube and counted in a Packard Cobra gamma counter. Each concentration was performed in triplicate. In order to account for background due to binding the counts per minute (cpm) from the binding experiments were subtracted from the final cpms from the 1min transport experiments. The kinetic parameters of K_m and V_{max} were determined from initial rates of uptake. OKN3 the *ΔfepA* strain was used as a negative control. Transport data were analyzed using the Michaelis-Menten equation of Grafit version 5.0.12 (Erithacus Ltd., Middlesex, UK).

2.5 Fluorescence Microscopy

Cells were grown overnight in 10mL of LB media with the appropriate antibiotics at 37˚C with shaking. The cells were then subcultured into 10mL of MOPS media with the appropriate antibiotic at 37˚C with shaking to mid-log phase at an $O.D._{600}$ between 0.5-0.6. 300µL of cells were mixed with 15µL of a 25µg/mL poly-L-lysine solution. This mixture was spread out onto cover slips and incubated at room temperature for 5mins. The cover slips were then rinsed with phosphate buffer saline at a pH of 7.4 (PBS). 5µL of PBS was spotted onto a 3" X 1"microscope slide and then the coverslips were placed on top. An Insight black and white spot camera mounted on an Olympus BX50 microscope through a UPlanFI X 100/1.3 oil immersion objective was used for all cell photography.(59)

2.6 Fluorescence Intensity and Anisotropy Measurements

An overnight culture of bacteria grown in 10mL of LB media with the appropriate antibiotics was subcultured into MOPS media at a one to one hundred

dilution and grown to an $O.D._{600}$ of 0.7 to 0.8. at 37˚C with shaking. One of two energy poisons was then added either sodium azide or CCCP at a final concentration of 10mM or no poison was added. If an energy inhibitor was added the cells were placed back at 37˚C with shaking for an additional 40mins. The cells were than diluted to a final concentration of 4×10^7 cells per mL in TBS in either a 2mL quarts cuvette or in a 96 well TECAN fluorescence reading plate.

Fluorescence intensities were first measured in the TECAN Genios Pro with the following parameters: measurement mode: Fluorescence Top, excitation wavelength: 485nm, emission wavelength: 535nm, gain: optimal, number of reads: 10, integration time (40μs), lag time (0μs), mirror selection: Automatic, shake duration: Linear, settle time: 1s and units set to RFU. The average fluorescence intensity from two reads was averaged and the fluorescence intensity of BN1071/pT23 was subtracted from all other strain values to give the final fluorescence intensity measurement. Fluorescence intensities were then measured in an SLM aminco 8000 upgraded to 8100 specifications at an excitation wavelength of 474nm and an emission wavelength of 509nm. The fluorescence intensity of BN1071/pT23 was subtracted from the intensities of the other strains for the final fluorescence intensity measurement.

Fluorescence anisotropy was measured in an SLM aminco 8000 upgraded to 8100 specifications at an excitation of 474nm and an emission of 509nm. at an excitation wavelength of 474nm and an emission wavelength of 509nm. The

fluorescence intensities of BN1071/pT23 was subtracted from the intensities of the other strains for the final fluorescence intensity measurement for use in the anisotropy calculations.

Chapter 3

3. Ball-and-chain mechanism for Ferric Enterobactin Transport through FepA

3.1 Introduction

FepA has two domains, the C-terminal β-barrel and the N-terminal domain that resides in the barrel; understanding their interaction with one another is crucial to finding the mechanism for FepA. There are currently two models available. The first model is that FeEnt moves through FepA from sites of increasing affinity through a transient pore. This model is called the sequential model and is modeled from other transport proteins such as the acetylcholine receptor, potassium and chloride channels, bacteriorhodopson, ATPase, general porins and specific porins.

There are problems in the sequential model. The first is that FeEnt transport is not driven by mass action like the substrates of the specific porins. The second is that in order for sequential transport to take place there needs to be a disruption of the initial binding site and a creation of sequential binding sites.

The second model is that the N-terminus changes conformation and moves to create a channel within the barrel. This is termed the concerted transport model. The concerted model is broken into two separate mechanisms. The first is that the N-domain folds inside the β-barrel of FepA to allow for transport. Evidence for this is that the N-domain is a unique fold and therefore functions in a unique way. Upon the binding of FeEnt the N-domain folds into a loaded state. This loading in turn changes the conformation of the N-domain from a structure that occludes the β-barrel to one

that allows for transport. The second mechanism is that the whole plug, consisting of the N-terminal 151 residues, leaves the β-barrel completely. This is termed the Ball and Chain mechanism. As the N-domain leaves the β-barrel it needs to break over 50 H-bonds which hypothetically reform with water or other residues and possibly FeEnt. The breaking of these bonds would take approximately 100kCal of energy assuming 2kCal/Mol for a single H-bond. Therefore it would take 10ATP to disrupt these bonds. The interior of the β-barrel is hydrophilic composed of charged, polar and uncharged residues. This means that the β-barrel is likely a water filled channel. This was seen in the crystal structure of FepA with water bridges.

3.2 Results

3.2.1 Deletion of OM Receptor Proteins

Chromosomal fragments of ferric siderophore receptor genes and mutants of these receptor genes expressed on plasmids may complement each other resulting in artifactual interpretation of the mutant phenotypes (110). Therefore, we generated an isogenic series of complete, precise deletions of *tonB*, *fepA*, *cirA*, *fhuA*, and *fiu* in BN1071 (F-, *trp*, *entA*-) (65) OKN3 contains a precise in-frame deletions, of the *fepA* gene, and OKN7 contains a precise in-frame deletion of the *fhuA* gene. These host strains are resistant to colicins and phage that require *fepA* and *fhuA*, respectfully, demonstrating the absence of FepA and FhuA. After OKN3 was transformed with pITS23 ($fepA^+$ (105) it became vulnerable to colicins B and D, bacteriophage H8 infection, and it acquired the ability to bind and transport FeEnt (Figure 6). Similarly

when OKN7 was transformed with pITS11 (*fhuA*+) (105), it recovered its vulnerability to colicin M and T5, and its ability to transport ferrichrome. Furthermore, when OKN3 was transformed with p*fepA*S271C, fluorescence spectroscopy of fluorecein maleimide (FM)-labeled S271C demonstrated its ability to transport FeEnt. The results in these experiments were identical to those observed in earlier work (20), showing that in general, the noted complementation did not cause pervasive artifacts in our prior experiments (97). Along with the deletions of *fepA* and *fhuA* we constructed other deletions: *tonB* (OKN1), *fecA* (OKN2), *cirA* (OKN5), and *ybiL* (OKN9). I separated the inner and outer membrane fractions of these complete and precise deletions using sucrose density gradients and then ran the outer membrane fraction on SDS-PAGE to verify the deletion (Figure 5).

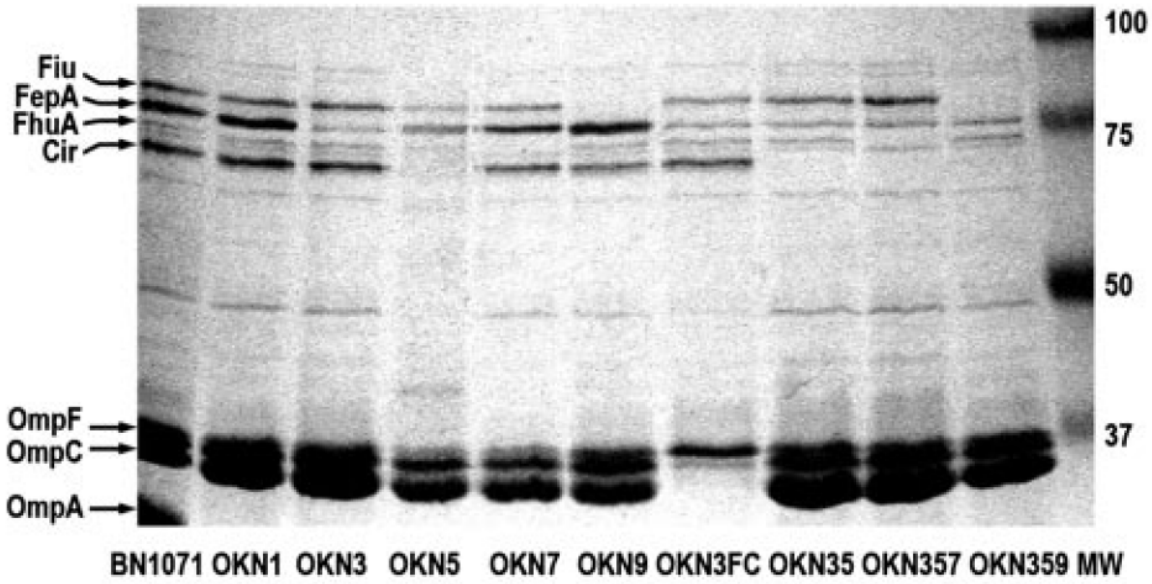

Figure 5 Outer membranes of *E. coli* strains with site-directed deletions of siderophore receptor proteins. Genetically engineered *E. coli* K12 strain BN1071 (*entA*) to introduce individual deletions of *tonB, fecA, fepA, cir, fhuA*, and *ybiL* (strains OKN1, -2, -3, -5, -7, and -9, respectively). In addition, we transduced the defective *ompF*::*Kn* and *ompC*::*Tc* genes from HN705 into OKN3 (OKN3FC) and generated multiple combinations of the individual deletions (OKN35: Δ*fepA*, Δ*cir*; OKN357: Δ*fepA*, Δ*cir*, Δ*fhuA*; OKN359: Δ*fepA*, Δ*cir*, Δ*ybiL*; and OKN2357: Δ*fecA*, Δ*fepA*, Δ*cir*, Δ*fhuA*). Sarkosyl-extracted OM fractions of selected strains, which were grown in MOPS media, show the identity of the siderophore receptor proteins and their absence in the mutant bacteria (65).

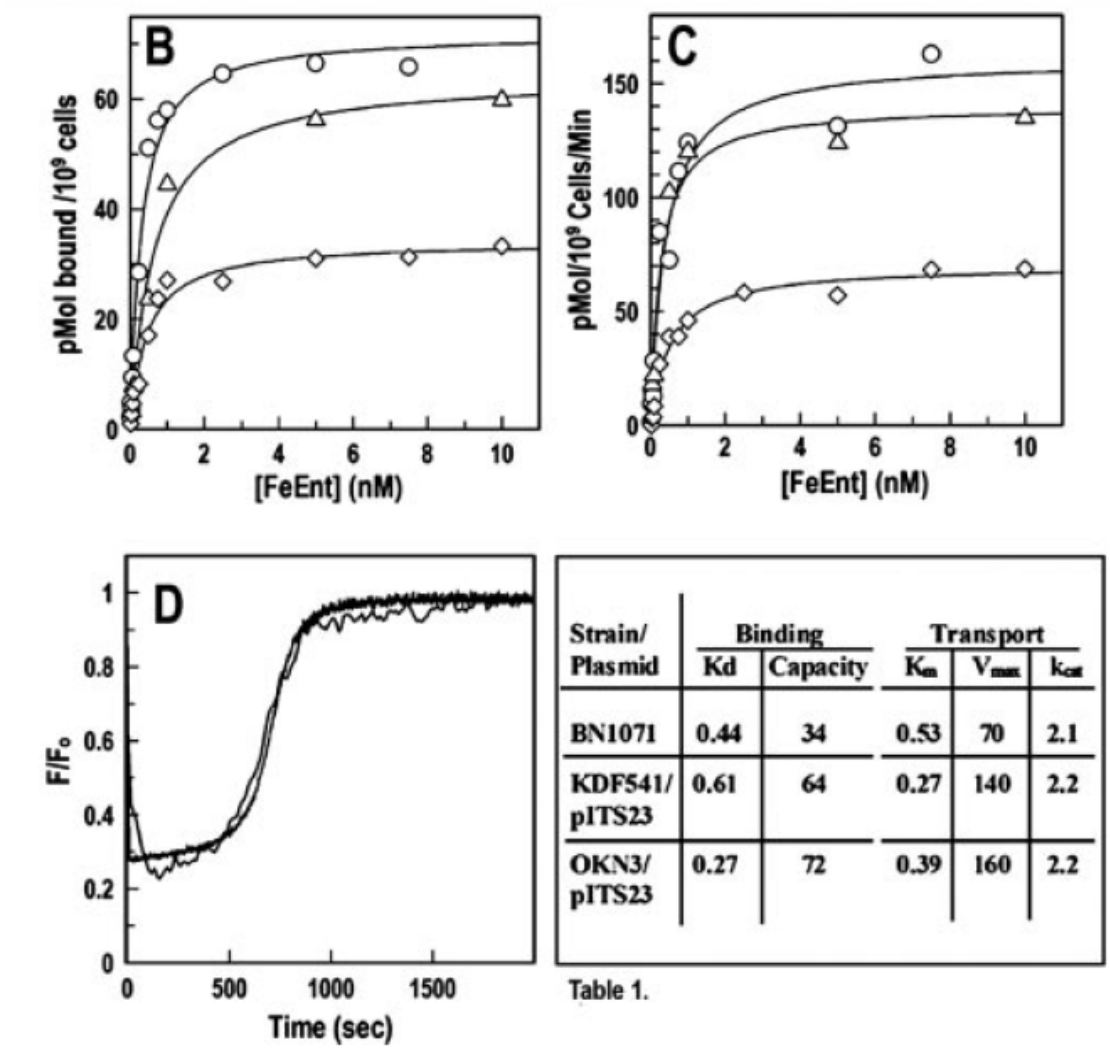

Strain/ Plasmid	Binding		Transport		
	Kd	Capacity	K_m	V_{max}	k_{cat}
BN1071	0.44	34	0.53	70	2.1
KDF541/ pITS23	0.61	64	0.27	140	2.2
OKN3/ pITS23	0.27	72	0.39	160	2.2

Table 1.

Figure 6 *B* and *C*, 59FeEnt binding and transport by OKN3/pITS23. Ability of FepA encoded on the plasmid pITS23 transformed into the strain OKN3 to bind (*B*) and transport (*C*) 59FeEnt, in comparison to BN1071 which contains the chromosomaly encoded FepA and KDF541/pITS23 (38). KDF541 (48) contains a spontaneous deletion of the 381 C-terminal amino acids of FepA (45). (*D*) spectroscopic measurements using fluorescence to observe FeEnt uptake using FM labeled FepA. FeEnt uptake (47) by OKN3/pFepAS271C (*thin line*) was compared to KDF541/ pFepAS271C (*heavy line*; data from Ref. 47). Table 1 summarizes the binding and transport data of the different host strains. *Kd* and *Km* (nM), capacity (pmol/109cells), *V*max (pmol/109 cells/min), *k*cat (expressed as turnover number, molecules transported/receptor/min) (65)

3.2.2 FM labeling of Cellular Proteins

After creating a new genetic system (i.e., the Δ*fepA* host), we began experiments on the mechanism of FepA transport. A total of 25 residues in FepA were genetically engineered to cysteine via QuikChange™ mutagenesis. All of these mutants are under the regulation of the native *fepA* promoter, and all were expressed at wild-type levels (data not shown). These mutants were tested for their susceptibility to colicins and bacteriophage and their ability to transport FeEnt. All of the mutants transported FeEnt like wild-type FepA in siderophore nutrition tests. They also showed normal susceptibility to colicin B (data not shown). Therefore, these mutations did not alter FepA's ability to perform its function at a wild-type level.

We used cysteine substitution mutagenesis to test the accessibility of the sites in FepA's tertiary structure to FM modification. If the cysteines were labeled, as seen by SDS-PAGE and fluorimetry, then it showed that these residues were accessible to FM in their local environment. The susceptibility of these residues in FepA was dependent on their location. Cysteines in the surface loops of FepA (216, 271, 322, 383, 482 and 550) were labeled at much higher levels than residues located in the lower region of FepA next to the periplasm (14, 33, 300 and 666) and the one cysteine located on the N-domain (54). The labeling intensity of residues 14, 54, 322, 383 and 550 changed when incubated with FeEnt, indicating that the ligand altered the labeling of these residues. G54C is a residue located on the interior of FepA on the surface of the N-domain, in the center of the pore. G54C was labeled with FM but

residues located in the wall of the β-barrel C-domain that were located in close physical proximity (G565C, S569C, and T585C) were not. This labeling of G54C was not as intense as the labeling on the surface loops, but it was distinct and reproducible.

During the fluorescent labeling of live *E. coli* several other proteins other than cysteine containing FepA mutants were labeled. Seven proteins in total showed clear reproducible labeling (Figure 7). This labeling was dependent on the external concentration of FM and also the duration of the labeling reaction. In order to reduce this background labeling the following conditions were used: concentration of FM 5μM, labeling reaction time of 15min at 37˚C and a pH of 7.2. These labeling conditions decreased non-specific labeling of the seven proteins previously labeled as well as wild-type FepA which contains no genetically engineered cysteines.

The intensity of cysteine reactivity was at its highest point on residue S216C at 45% of the total cellular labeling. Residue S271C showed 26% of total cellular labeling, and this labeling showed no change in the presence of FeEnt. S271C was used as a standard control to compare labeling on other sites due to extensive previous work done on it.

G54C when compared to other residues that were considered showed lower levels of labeling at levels between 5 and 9% of total cellular labeling.

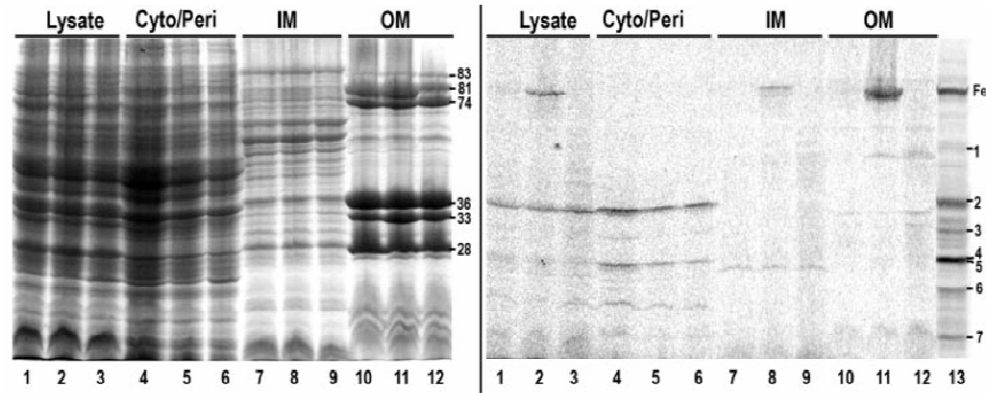

Figure 7 Fractionation via Sucrose density gradient of FM labeled bacteria. OKN3 (fepA) harboring pITS23 ($fepA^+$; lanes 1, 4, 7, and 10) or pFepAG54C (lanes 2, 5, 8, and 11) and OKN13 (fepA, tonB)/pITS23 (lanes 3, 6, 9, and 12) were grown in MOPS media to late log, pelleted by centrifugation and lysed in a French press. Their cytoplasm/periplasm (cyto/peri), IM and OM fractions were collected, resolved by SDS-PAGE, scanned for fluorescence (right panel), and the same gel was then stained with Coomassie Blue (left panel). The molecular weights of the outer membrane proteins Fiu (83 kDa), FepA (81 kDa), CirA (74 kDa), OmpF/C (36 kDa), and OmpA (denatured (33 kDa) and native 28 kDa)) are shown (respectively, top to bottom). Lane 13 shows a fluoresceinated lysate of OKN3/pFepAG54C, without any fractionation. OKN3 (fepA) harboring pITS23 ($fepA^+$; lanes 1, 4, 7, and 10) or pFepAG54C

3.2.3 Accessibility of cysteines during FeEnt Binding and Transport

During the binding and transport of FeEnt the labeling of G54C was altered. Approximately 90% of the fluorescently labeled G54C mutant was seen in the OM and the rest was found in the IM suggesting a preprocessed form of FepA. Interestingly it showed an increase in labeling during the binding and transport of FeEnt. G54C was one of the most weakly labeled residues at 5% and 9% of total cellular labeling; and it still constituted more than 90% of the total fluorescence of the OM fraction. (Figure 8).

3.2.4 Inhibition of FM labeling by FeEnt

A total of six cysteine mutants were tested under varying conditions for their accessibility to FM. These conditions were an exposure to FM for 15min at 37˚C with or without FeEnt, in *tonB*$^{+}$ or *tonB* cells and in the absence or presence of sodium azide. The concentration of FeEnt was used at a concentration of 10μM. Of the sites that were studied (I14C, G54C, S271C, G300C, G565C, and T585C) G54C showed the most interesting labeling pattern. G54C reacted with FM in the *tonB*$^{+}$ and the *tonB* cells in the absence of FeEnt but not in the presence of FeEnt. This data suggests that FepA remains open (106) and that G54C is accessible from the surface of FepA unless FeEnt is being transported (Figure8). When FeEnt is being transported, the loops of FepA close and block FM from entering into the pore of FepA, thus preventing FM from labeling G54C. Cells that are deficient in TonB bind FeEnt but do not transport FeEnt and this closes the loops of FepA. The closed loop conformation closes the

interior of FepA off to molecules from the exterior or periplasmic environments. This preferential occupation of FepA by FeEnt should exclude FM from the barrel of FepA. However G54C is labeled by FM in the presence of FeEnt and TonB with no energy inhibitor. This can be explained if FM accessed G54C from the periplasmic side when the N-domain left the barrel. This also accounts for why FM does not label residues that are located in the barrel in the same region as G54C. These other residues are located deeper in the barrel and are not accessible from the periplasm even with the removal of the N-domain. This result supports the hypothesis that the N-domain leaves the barrel during transport thus exposing itself to the periplasmic space and therefore FM (Figure 8).

Sodium azide inhibits energy metabolism in the bacteria and results in the loss of FeEnt transport, closing FepA; this also eliminated the FM labeling of G54C. In the absence of FeEnt FepA has an open loop conformation that allows for the access of G54C by FM. In contrast S271C is a cysteine located in the L3 loop of FepA, and this residue was consistently labeled in the presence or absence of FeEnt, in the presence and absence of the energy inhibitor sodium azide and also with or without the expression of TonB. This residue is located on the surface of FepA and therefore it is reasonable that this site is accessible to FM labeling from the outside of the cell. This further indicates that the labeling of G54C is interfered with by FeEnt binding and transport.

Labeling of residues that reside on the periplasmic interface of FepA (I14C, A33C, G300C and T666C) further indicate that G54C is labeled from the periplasmic side during transport of FeEnt. I14C and G300C were labeled more strongly in the presence of FeEnt. This could be due to a conformational change of these residues during the binding and transport of FeEnt. Since I14C and G300C are located around the TonB box region next to the barrel wall, this data further implicates this region in the transport mechanism of FepA (23, 34, 61).

Located on the interior surface of the β-barrel of FepA are residues G656C, S569C and T585C; all of these residues were not labeled by FM under any conditions. These residues are located directly opposite G54C inside the β-barrel of FepA. Since these residues were not labeled but G54C was labeled this further implies that G54C is labeled when the N-domain it resides on is moved during a conformational change to the periplasmic space. This argues against the transient pore model further supporting the ball-and-chain model. FM differentially labels cysteines at residues 14 and 54. Labeling of G54C occurs when FepA is unoccupied by FeEnt, but when FepA is occupied by FeEnt then FM is unable to bind to this site. Residues such as T585 and G565 are not labeled even though they reside directly across from G54C on the β-barrel. The lack labeling of these residues give further evidence that the labeling of G54C in the presence of FeEnt is from the periplasmic side (Figure 8).

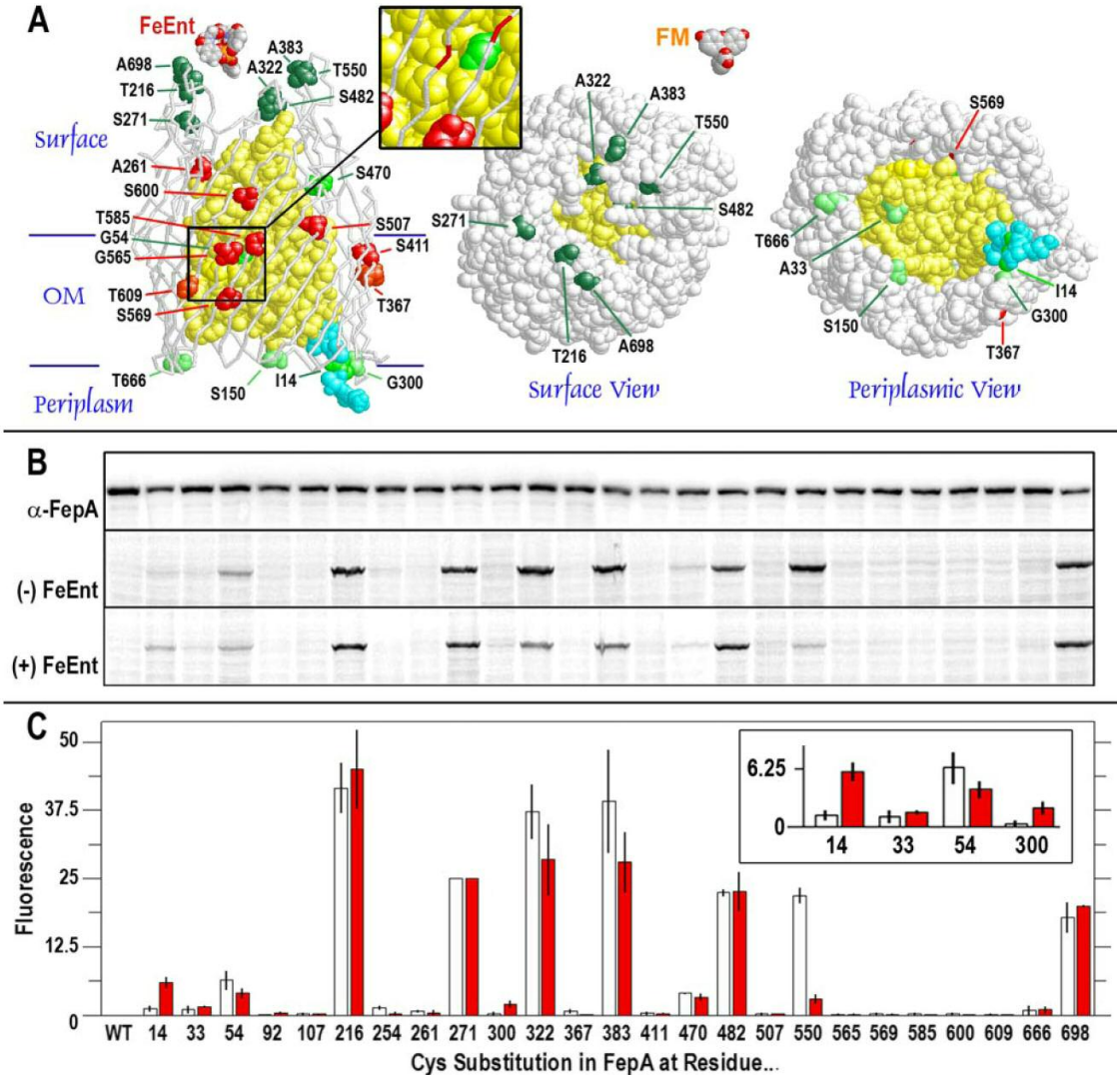

Figure 8 FM labeling of genetically engineered Cys residues in FepA. *A*, N-domain (*yellow)*, C-domain (*white*) and TonB-box (amino acids 11-17) (*cyan). Left*, positions of the 25 Cys substitutions used for fluoresceination. Residues reactive to FM are colored *dark green, green*, and *light green* in relation to the intensity of their fluoresceination and unreactive Cys substituted residues (*red*). The *inset* is a magnification of the region near residues the center of FepA surrounding G54C. *Center* (cell surface) and *right* (periplasm) space-filling models of FepA showing the accessibility of Cys substitutions to extrinsic fluors based on the relative sizes of FeEnt and fluorescein. *B* (expression) when visualized by anti-FepA (monoclonal antibody 45) immunoblots, developed with [^{125}I]protein A. *C* (FM modification) of FepA and FepA Cys visualized by fluorescence scans of lysates from cells expressing single Cys mutants substitution mutants. *C*, The amount of fluoricination was quantitated from fluorescence imaging data of SDS-PAGE gels depicted by the *bar graph* the percentage of total cellular labeling is expressed as a mean of two experiments and the standard error of the means (*vertical bars*) in the absence (*white*) or presence (*red*) of FeEnt. (65)

3.2.5 Complementation of Fepβ by FepN

The data seen in the previous fluorescence labeling experiments of residues G54C and I14C indicated the expulsion of the globular N-domain from the β-barrel of FepA into the periplasmic space. To further investigate this expulsion of the N-domain from the β-barrel into the periplasmic space, the two separate domains of FepA were expressed on two separate plasmids. The N-domain was expressed in the high copy pUC18 vector (pFepN) and the β-barrel on the low copy vector pHSG575 (pFep β). These two constructs were expressed alone and together in the *fepA* strain OKN3 and in the *tonB, fepA* strain OKN13. The first point of interest is the rates of growth of the bacteria when the constructs were expressed together in OKN3. There was a increase in the doubling time of the bacteria from 35mins as seen in OKN3/pITS23 to 10hrs for OKN3/ pFepN pFep β. Interestingly after 8hrs in LB broth, the doubling time of OKN3/ pFepN pFep β shifted to a higher rate of 75mins until reaching late log phase when the density of bacteria did not increase.(Figure 9)

The activity of the constructs was tested using colicins B and D. During the initial slow growing stage of growth, the expression of the two fragments did not recover sensitivity of FepA activity to these toxins. However once the cells reached the later phase after 10hrs of growth the sensitivity to both toxins was restored. (Table 4).

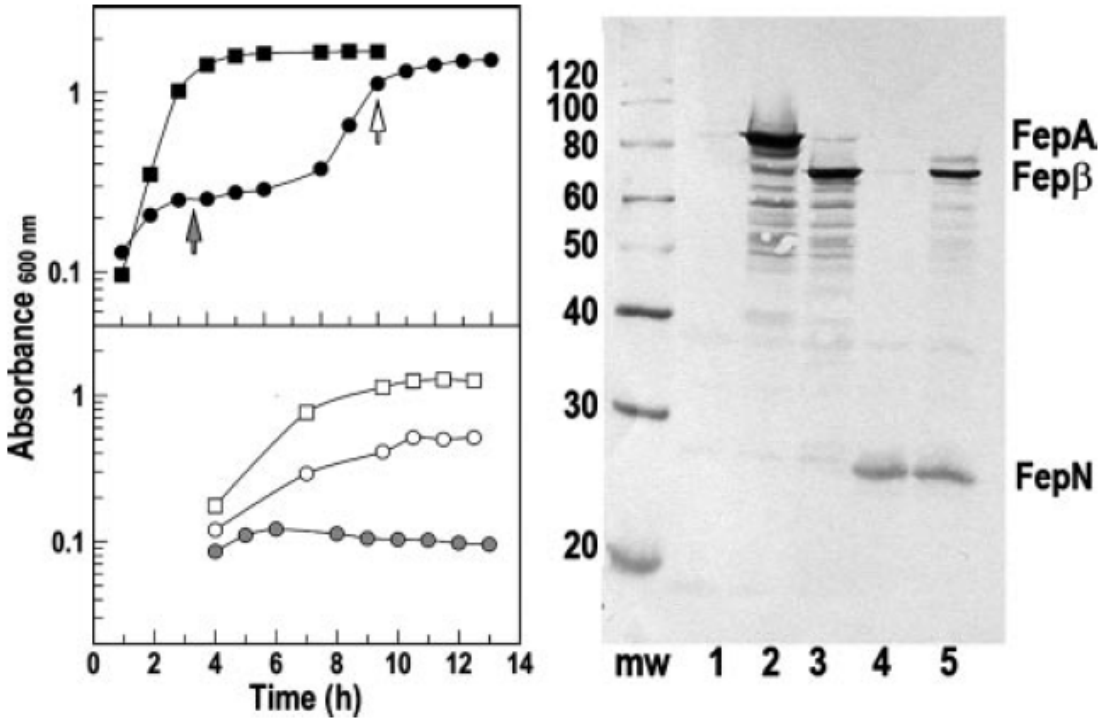

Figure 9 Expression of FepA, FepN, and Fepβ in OKN3. *Left*, growth in LB broth and MOPS minimal media. *Top*, OKN3 harboring pITS23 (*squares*) or pFepNpFepβ (*circles*) was inoculated into LB broth at 37 °C and shaken at 250 rpm. When expressing wild-type FepA, it grew without a lag and had a doubling time of 35 min; when separately synthesizing the N- and C-domains of FepA, OKN3 showed a first phase with doubling time of ~10 h, and a second phase with doubling time of 75 min. *Bottom*, if subcultured from the first phase of LB growth into MOPS media (at the *filled arrow*), OKN3/pFepNpFepβ did not grow (*filled circles*), but when subcultured from the second phase (*unfilled arrow*), it had a doubling time of 3 h (*open circles*), only slightly slower than that of OKN3/pITS23 (2 h, *open squares*). *Right*, expression of FepA, FepN, and Fepβ (*lane 5*) in OKN3. After growth in LB or MOPS media for 6 h, lysates of OKN3 (*lane 1*) harboring pITS23 (*lane 2*), pFepβ (*lane 3*), pFepN (*lane 4*), and pFepN pFepβ (*lane 5*) were separated on SDS-PAGE gels and immunoblotted with anti-FepA MAbs 45 and 41 (recognize epitopes in surface loop 4 (near residue 329)and the N-domain (residues 100-142) respectively. The immunoblot derives from bacteria grown in LB broth, but expression of FepA and its fragments was the same in all conditions, despite physiological differences in the two media at different stages of growth. (65)

Host strain/plasmids[a]	Allele[b]	ColB[c]	ColD[c]
OKN3	*fepA*	R	R
OKN3/pITS23	*fepA*$^+$	10^6	10^5
OKN3/pFepN	*fepN*-(1–151)	R	R
OKN3/pFepβ	*fep*β-(1–17; 151–724)	R	R
OKN3/pFepNpFepβ	*FepNfep*β	4×10^4	3×10^3
OKN13	*tonBfepA*	R	R
OKN13/pITS23	*fepA*$^+$	R	R
OKN13/pFepNpFepβ	*fepN*fepβ	R	R

Table 4 Co-expression of FepN and Fepβ *E. coli* strain OKN3, alone or harboring plasmids, was tested for FepA-dependent functions.[a] OKN3 contains an engineered deletion of the *fepA* structural gene ("Experimental Procedures"), pITS23 and pFepβ are derivatives of the low copy number vector pHSG575, and pFepN is a derivative of pUC18 [b] The *fepN* allele encodes residues 1–150 of wild-type FepA, under the control of its natural promoter; *fep*β (*fepA*Δ18–150) encodes residues 1–17 followed by a deletion of residues 18–150 and continues with residues 151–724 [c] Purified colicin was diluted in a microtiter plate over a 10^8-fold range, and 5 µl of each dilution was transferred to an LB agar plate, previously coated with 2.5×10^8 bacterial cells in LB top agar. The plates were incubated overnight at 37 °C. The tabulated values are the reciprocal of the final dilution that showed visible clearing of the bacterial lawn. (65)

3.3 Discussion

The data shown by the differential labeling of Cys residues by FM reveals the accessibility of these regions of FepA to the extracellular surface as well as the periplasm. The environment indicates the state in which the structure of FepA is in, specifically the location of the N-domain. The labeling of these sites was TonB dependent as well as dependent on energy produced via proton motive force. FM was able to pass through the outer membrane of the bacteria and label FepA sites from the periplasm. This was due to the fact that FM has a molecular weight of 427Da which is small enough to pass through the 600Da barrier of outer membrane. The transport of FM through the outer membrane was most likely through the OmpF/C porins. This was indicated in the decrease of 70% in the labeling of the periplasmic residue I14C in the absence of OmpF/C. Since the labeling seen on I14C is from the periplasmic side, the previously shown data clearly indicates a change in this residues environment.

This change in the environment of I14C was clearly seen when comparing the labeling in the presence and absence of FeEnt. The binding and transport of FeEnt to FepA allowed for the labeling of I14C. The presence and absence of TonB and also in the presence and absence of the energy inhibitor sodium azide gave a bigger clue to I14C's disposition. In the absence of TonB or in the presence of the energy inhibitor sodium azide FeEnt can bind to FepA but transport will not occur. I14C is located on the TonB-box and when FeEnt was present but in the absence of TonB or the presence

of the energy inhibitor I14C is labeled. This indicates a conformational change of I14C upon the binding of FeEnt to FepA.

Of even greater interest is the reactivity of G54C since it is present on the N-domain inside the β-barrel. Directly across form G54C are residues T585 and G565. T585 and G565 are located on the β-barrel whereas G54C is on the N-domain. G54C is labeled only when transport of FeEnt occurs. That is only in the presence of FeEnt, TonB and in the absence of the energy inhibitor was G54C labeled.

The goal of this labeling was to study the mechanism of FepA in relation to the current hypothesized models of FepA transport. The preferential labeling of I14C and G54C in the periplasm indicates a ball-and-chain mechanism. This leads to the conclusion that the N-domain does in fact exit the barrel when transport occurs.

The final piece of evidence presented here in favor of the ball-and-chain mechanism is in the complementation of the two domains of FepA. When the N-domain is expressed separately from the β-barrel there is still activity seen in the sensitivity to colicins B and D. The ball-and-chain mechanism hypothesizes that the N-domain needs to exist and then re-enter the pore of FepA during the activity of FepA. The ability for there to be FepA function with the N-domain expressed separately from the β-barrel, shows that the N-domain can be outside the β-barrel and enter it to perform FepA's function. The slow initial rate of growth of the strain containing both the β-barrel and the N-domain was perhaps due to improper folding of

the N-domain in the β-barrel until hour 10 at which point the folding occurred correctly.

Chapter 4

4. Bacteriophage H8

4.1 Introduction

Transmission electron microscopy taken of H8 revealed that its structure is similar to T5 (Figure 12). Bacteriophage T5 requires the ligand gated porin FhuA. H8 was recently discovered to require FepA for infection of *E. coli*. To further investigate this existing phenomenon, we tested *fepA* constructs to determine the regions of the receptor protein responsible for the interaction with H8. The significance of different regions of FepA to H8 reception was tested using several mutants of *fepA*. The β-barrel alone (*fepA*Δ1-151) and the N-terminus alone (*fepA*Δ151-724) did not confer infectious susceptibility by H8. Neither did chimeric proteins containing either the β-barrel from FepA and the N-domain from FhuA, or the β-barrel from FhuA and the N-domain from FepA, allow for H8 infection. Strains harboring plasmids with either of the chimera proteins lacked the ability to be infected by H8 (Table 5).

Strain[b] or allele[c,d]	Susceptibility to H8 (%)[e]	Activity with FeEnt[f]			Susceptibility to ColB killing (%)[g]	Reference or source
		K_d (μM)	K_m (μM)	Halo diam (mm)		
KDF541 (*fepA*)	R	NB	NT	0	R	81
GUC12 (*tonB*)	R	NB	NT	0	R	33
KDO23 (*tonB*)	R	NB	NT	0	R	90
OKN1 (*tonB*)	R	NB	NT	0	R	58
fepA$^{+b,c}$	100	0.4	0.2	18	100	5
fepA$^{+b,d}$	100	0.3	0.4	19	100	89
fepA$^{+b,d,h}$ (+FeEnt)	9 (2)	NA	NA	NA	ND	This study
Class I strains (resistant)						
fhuA^{b,d} *fhuA*Δ1–160	R	NB	NT	0	R	89
fepA^{b,d} *fepA*Δ1–150	R	0.6	1.5	20	0.4	89
fepA^{b,d} *fepN fhu*β	R	NB	NT	0	R	89
fepA^{b,d} *fhuN fep*β	R	0.2	1.7	25	0.01	89
fepA^{b,c} ΔL2 (199–206)	R	1453	8912	11	0.3	62
fepA^{b,c} ΔL4 (315–326)	R	651	1092	28	100	62
fepA^{b,c} ΔL7 (467–497)	R	NB	NT	0	R	62
fepA^{b,c} ΔL9 (592–603)	R	6	354	25	3	62
fepA^{b,c} ΔL11 (681–708)	R	236	3360	22	10	62
Class II strains (<15% susceptibility)						
fepA^{b,c} ΔL5 (383–401)	7 (1)	251	964	25	0.6	62
fepA^{b,c} ΔL8 (546–560)	7 (5)	NB	NS	12	R	62
fepA^{b,c} ΔL10 (630–654)	4 (7)	945	446	23	0.5	62
Class III strains (16 to 50% susceptibility)						
fepA^{b,d} ΔNL1 (60–67)	28 (8)	7	119	25	10	4
fepA^{b,d} ΔNL2 (98–105)	24 (11)	12	163	25	10	4
fepA^{b,c} ΔL3 (269–280)	38 (23)	22	930	26	100	68

Table 5. Comparison of Deletions between FepA and H8 infection

a FepA susceptibility to H8 infection for *E. coli* strains lacking functional *fepA* or *tonB*, containing *fepA* alleles encoded on plasmids, tested on LB agar plates. The percentage of wild-type susceptibility to H8 infection was used to designate each Class.
b KDF541 (*F_ pro leu trp thi entA fepA fhuA cir*) was used as host strain(97).
c pUC18 derivative pITS449 (4) carrying *fepA*$^+$ or mutant derivatives of *fepA* under Fur-mediated regulation.
d pSC01 derivative pHSG575 (43), a carrying *fepA_* or its mutant derivatives under Fur-mediated regulation.
e Percent infection relative to wild type determined by counting the number of plaques on bacteria carrying *fepA*$^+$ or mutant *fepA* alleles on plasmids. Values shown in parentheses are the standard deviation of three separate trials. R indicates strain is resistant to H8 infection.
f Binding (*Kd*), transport (*Km*) reactions and siderophore nutrition halo diameter (mm) to evaluate interaction of FepA with FeEnt and the affinity of this interaction. NA (not applicable), NB (no binding), NT (no transport) NS (nonsaturable transport).
g Killing by colicin B determined as the reciprocal of the highest dilution of a preparation of the toxin that gave visible clearing of the agar on an LB plate spread with the bacteria being tested (75). The results shown are the percentage of wild-type activity. R (resistant) ND (no data).
h Bacteria were incubated with 10 μMFeEnt, diluted phage or colicin lysate was added, followed by incubation for 20 min at room temperature and pelleted by centrifugation. The bacteria were plated on LB agar and the number of PFU(103). (92)

We also tested the individual surface loops of FepA for their importance in H8 binding and killing. Loop deletions showed the most significant changes to H8 infection compared with other mutations in FepA. The affect of these loop deletions was different than that found for the other ligands for, FeEnt and colicins B and D (75). Loops, 2, 4, 9 and 11, participated in the transport of FeEnt and killing by colicins B and D. These loops were also important for H8, because without them FepA was no longer capable of H8 reception. None of the ligands were able to perform their function with the deletion of loop seven in FepA, emphasizing the importance of this loop. On the other hand loops 1 and 2 on the N-domain did not effect H8 infection to the extent of the other loop deletions, implying that these loops are involved in a secondary binding role. All of the eleven loops in FepA affected H8 infection to some extent. The levels of their effects were categorized into three groups: Group I= no infection, these loop deletions give complete resistance to H8, Group II=10% of wild-type infection levels and finally group III=10-50% of wild-type infection levels. Group I consisted of the deletion of loops 2, 4, 7, 9 and 11, group II consisted of the deletion of loops 5, 8 and 10 and group III consisted of loop 3 as well as loops 1 and 2 from the N-domain.

The natural ligand of FepA, FeEnt, binds to FepA through aromatic and basic residues found on the receptor through interaction with catecholate and anionic groups found in FeEnt (2, 19, 74). Ala substitutions for aromatic residues involved in FeEnt

binding in the outer loop regions of FepA showed some effect on phage binding as well suggesting similarities in the binding of FeEnt and H8 to FepA. Of the sixteen Ala substitutions for aromatic residues in FepA, only three had any effect on H8 infection: F329A, Y478A, and Y553A. Fifteen Ala substitutions for Lys were constructed and of these only two showed changes in infection of H8 (K328A and K483A). These two substitutions showed a level 10% of wild-type. However, residues located deeper within FepA showed a stronger inhibition of susceptibility to H8 infection, binding and transport of FeEnt, and colicin B and D. Two of these residues are arginines (R286A and R316A) which have previously been shown to be important in the transport of FeEnt (74). These same residues are also important in the infection of bacteria by H8. Y260, which resides even deeper within FepA, is of particular interest since its substitution with Ala reduces colicin B activity 10-fold, FeEnt affinity 100-fold and H8 infection 50-fold (Figure 11).

Strain[a]/*fepA* allele [b, c]	H8 [d]	FeEnt [e]			ColB [f]	Reference
		K_d	K_m	Nutrition		
KDF541	R	NB	NT	0	R	(80)
GUC12	R	"	"	0	R	(33)
KDO23	R	"	"	0	R	(90)
OKN1	R	"	"	0	R	This study
fepA^{+} [a, b]	100	0.4	0.2	18	100	(5)
fepA^{+} [a, c]	100	0.3	0.4	19	100	(89)
fepA^{+} [a, c, g] (+ FeEnt)	9 (2)	NA	NA	NA	ND	This study
Class DI (Resistant to H8)						
fepA[a, c] *fhuAΔ1-160*	R	NB	NT	0	R	(89))
" *fepAΔ1-150*	R	0.6	1.5	20	0.4	"
" *fepNfhu*β	R	NB	NT	0	R	"
" *fhuNfep*β	R	0.2	1.7	25	0.01	"
fepA[a, b] *ΔL2 (199-206)*	R	1453	8912	11	0.3	(62)
" *ΔL4 (315-326)*	R	651	1092	28	100	"
" *ΔL7 (467-497)*	R	NB	NT	0	R	"
" *ΔL9 (592-603)*	R	6	354	25	3	"
" *ΔL11 (681-708)*	R	236	3360	22	10	"
Class II (< 15% of wild-type susceptibility to H8)						
" *ΔL5 (383-401)*	7 (1)	251	964	25	0.6	"
" *ΔL8 (546-560)*	7 (5)	NB	NS	12	R	"
" *ΔL10 (630-654)*	4 (7)	945	446	23	0.5	"
Class III (16-50%)						
fepA[a, c] *ΔNL1 (60-67)*	28 (8)	7	119	25	10	(4))
" *ΔNL2 (98-105)*	24 (11)	12	163	25	10	"
fepA[a, b] *ΔL3 (269-280)*	38 (23)	22	930	26	100	(68)

Figure 10 Loop deletions of FepA and their affect on H8 infection, Kd, Km, siderophore Nutrition, and colicin B sensitivity (92).

Host strain /fepA allele	H8 [e]	FeEnt [f]			ColB [g]	Reference [h]
		K_d	K_m	Nutr		
RWB18-60 or KDF541	0	NB	NT	0	R	(81)
fepA [a, c] +	100 (7)	0.1	0.3	18	100	(67)
fepA [b, c] +	100 (14)	0.2	0.5	19	100	(68)
fepA [b, d] +	100 (10)	0.3	0.4	18	100	(4)
Ala substitutions: Class I (Resistant to H8)						
" ***R313AR316A***	R	ND	ND	21	20	(64)
" ***Y260A/F329A***	R	126	367	25	50	"
" ***Y260A/Y272A***	R	33	128	25	50	"
Ala substitutions: Class II (H8 susceptibility < 15% of fepA+)						
fepA [a, c] ***R286A***	7 (9)	ND	ND	22	100	(67)
" ***R286AR316A***	1 (1)	ND	ND	17	2	"
" ***R316AR274A***	12 (12)	ND	ND	20	20	"
fepA [b, c] ***Y260A***	2 (1)	10	33	23	10	(16)
" ***F329A***	5 (7)	0.2	5.5	19	50	"
" ***E319A***	11 (3)	0.3	9.2	22	100	"
" ***Y260A/Y309A***	14 (13)	ND	ND	19	1	"
fepA [b, d] ***K483A***	10 (2)	1.3	ND	"	10	(90)
" ***K328A***	9 (4)	ND	ND	"	100	"
Class III (16 - 50%)						
fepA [a, c] ***R316A***	24 (13)	0.4	16	21	20	(16)
" ***R274A***	48 (53)	ND	ND	20	100	"
" ***R286AR313A***	17 (9)	ND	ND	21	100	(64)
" ***R283AR316A***	38 (19)	ND	ND	21	10	"
" ***R283AR286A***	37 (24)	ND	ND	21	100	"
" ***Y260A/R316A***	29 (7)	17	133	23	2.5	"
fepA [b, c] ***Y260A/Y309A***	14 (13)	ND	ND	19	1	(16)
" ***R316A/F329A***	20 (5)	83	486	24	2.5	"
fepA [b, d] ***Y478A***	39 (14)	0.8	167	21	10	(90)
Class IV (51-80%)						
" ***R286AR274A***	63 (32)	ND	ND	20	100	(64)
fepA [b, d] ***K332A***	69 (3)	ND	ND	"	100	(90)
" ***K634A***	68 (14)	ND	ND	"	100	"
" ***K635A***	65 (36)	ND	ND	"	100	"
" ***Y553A***	56 (16)	0.4	2	21	2.5	"

Figure 11 Single and double Alanine substitutions in FepA and their affect on H8 infection, Kd, Km, siderophore Nutrition, and colicin B sensitivity (92).

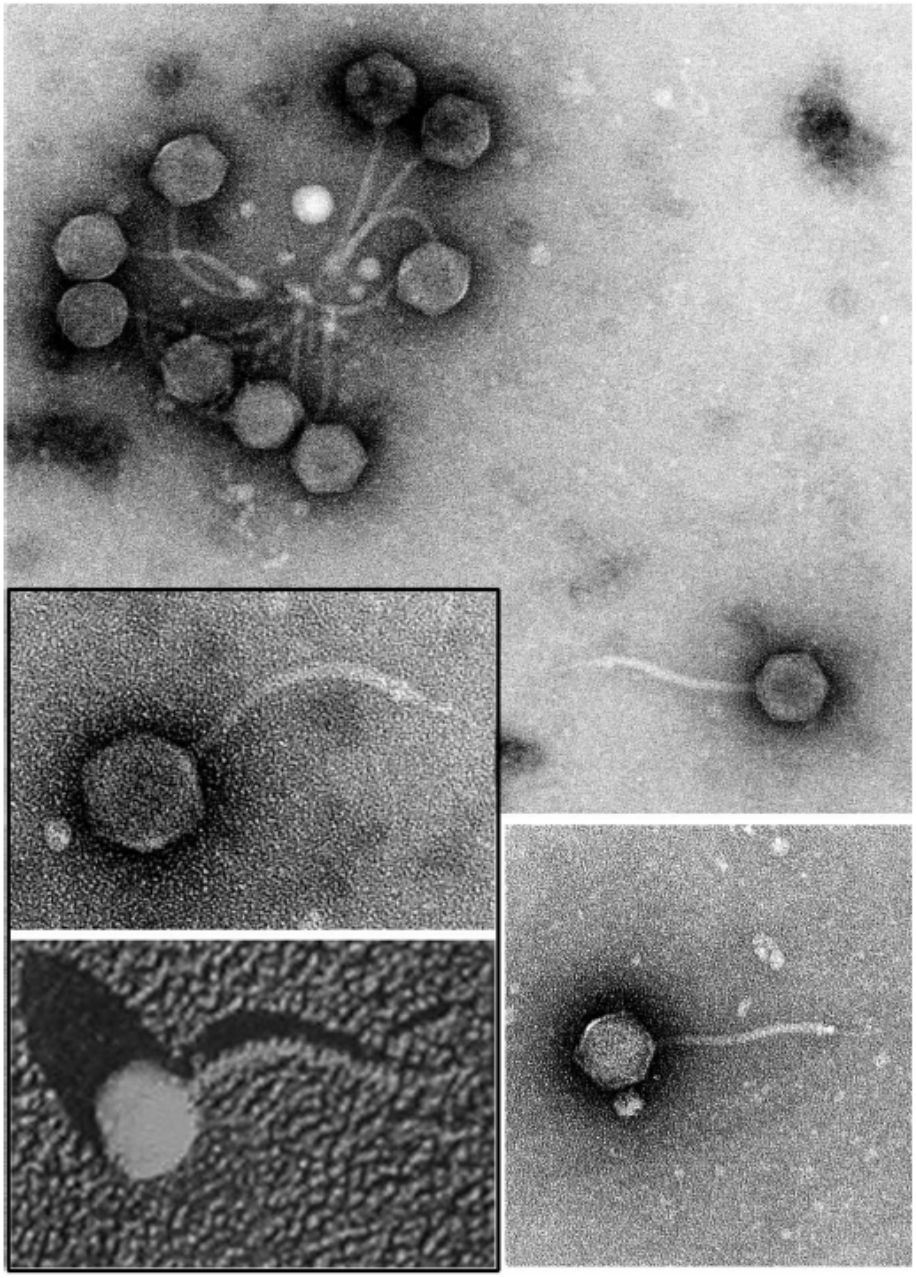

Figure 12 Bacteriophage H8 morphology. H8 particles were observed by transmission electron microscopy at a magnification of 100,000. The inset at the bottom left shows T5, observed by metal-shadowed transmission electron microscopy at magnification 93,150.

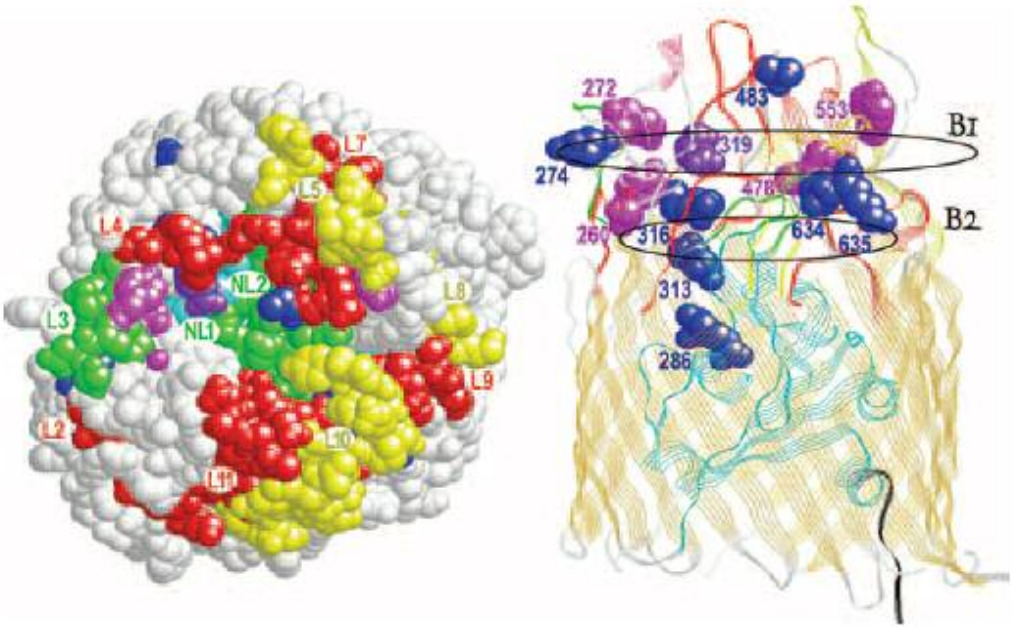

Figure 13 Analysis of FepA mutants. (Left) The space-filling model shows a view looking down onto the surface of the protein from the exterior. The N-terminal domain is colored cyan, and the TonB box region is black. Other colored regions or residues indicate sites that affected H8 infection. Residues removed by class I loop deletions (L4, L7, L9, and L11), class II (L5, L8, and 10), and class III (NL1, NL2, and L3) are colored red, yellow, and green, respectively. Site-directed Ala substitution mutations for individual basic, aromatic, and acidic residues are colored blue, magenta, and purple, respectively. (Right) In the ribbon model the protein was rotated _90◦ along its *x* axis to show the location of individual substitution mutations within the loops. The figure also depicts the B1 and B2 regions of the FepA surface vestibule, which participate in the initial and secondary stages of ligand binding. The bacteriophage utilizes sites that are broadly distributed across the outer, B1, region of the receptor protein, but single substitutions in the inner, B2, region also impair H8 infection, as well as FeEnt transport and colicin B/D killing. (92)

4.2 Results

4.2.1 FepA Specificity

Experiments conducted in collaboration with Li Ma showed that the infectivity of H8 is dependent on the expression of FepA and the expression of TonB. This was shown using OKN3, a strain of *E. coli*, that contains a precise in-frame deletion of *fepA*. OKN3 was found to be completely resistant to H8 infection as demonstrated by the lack of formation of plaques when the strain was exposed to H8 phage particles. Besides *E. coli* several other strains of Gram-negative bacteria were tested for H8 susceptibility. Of the strains tested, *Salmonella, Shigella, Citrobacter,* and *Serratia* were infected with H8 in liquid and solid LB media. Several strains of Gram-negative bacteria were found to be entirely resistant to H8; these include all strains of *Enterobacter, Klebsiella, Morganella, Proteus*, and *Yersinia* that were tested. Furthermore, H8 infection was restored in *fepA E. coli* strains OKN3, KDF541, and RWB18-60 that contained plasmid encoded expression of FepA. The plasmid encoded expression also increased the susceptibility of the host strain from that of wild-type BN1071 as evidenced by the increase in titer. It was also demonstrated that the other ferric catecholate receptor proteins, Cir, Fiu and Iron are not involved in phage uptake.

H8 is very similar to T5, and T5 uses FhuA as its receptor for infection. The idea that H8 could use FhuA as a receptor was evaluated and it was clearly shown that this is not the case. This was demonstrated through the use of strain OKN73, a strain

of *E. coli* that contains precise chromosomal deletions of both *fhuA* and *fepA*. This strain, when transformed with a plasmid containing the *fhuA* gene (pITS11) (105), did not become sensitive to H8. However, when OKN73 was transformed with pITS23, a plasmid that is *fepA*$^+$ H8 sensitivity was restored.

The TonB dependence of H8 was studied using the *E. coli* strains GUC12, KDO23, and OKN1. All three of these strains are *fepA*$^+$ *tonB*. All three of these strains were resistant to H8. TonB dependence was also shown in *S. enterica* S1001 and *S. enteritidis* WR1529.

The *exbB* dependence of H8 infection was studied using *S. enterica* WR1829 and *E. coli* H1. The loss of *exbB* alone failed to prevent H8 infection. When both *exbB* and *TolQ/R* are not present as in *E. coli* H2 and H10, then H8 was unable to infect the bacteria.

The level of FepA expression in the host cell influenced the level of infection for H8. This was seen when the *fepA* strain of *E. coli* OKN3 was transformed with either pUC18 (pITS449, pITS944), a high copy plasmid containing *fepA*, or pITS23 and low copy plasmid (3-5 copies per cell) containing *fepA*. The number of plaque forming units (pfu's) changed according to the level of expression of FepA. FepA expressed on the low copy plasmid showed a higher number of pfus when compared to FepA expressed on the high copy plasmid. H8 infected the cells containing FepA on the high copy plasmid at 18% less and at 81% less when expressed from the chromosome in the BN1071 strain.

4.2.1.1 Presence of FeEnt

Competitive inhibitions studies were done to look at the competition between FeEnt and H8. When FeEnt at a concentration of 10μM was pre-incubated with *E. coli* OKN3 containing pITS23, the number of pfus was 9% of what it was in the absence of FeEnt. The IC_{50} of FeEnt was determined to be 98nM. This indicates that FeEnt and H8 share binding sites on FepA (Figure 14) (92).

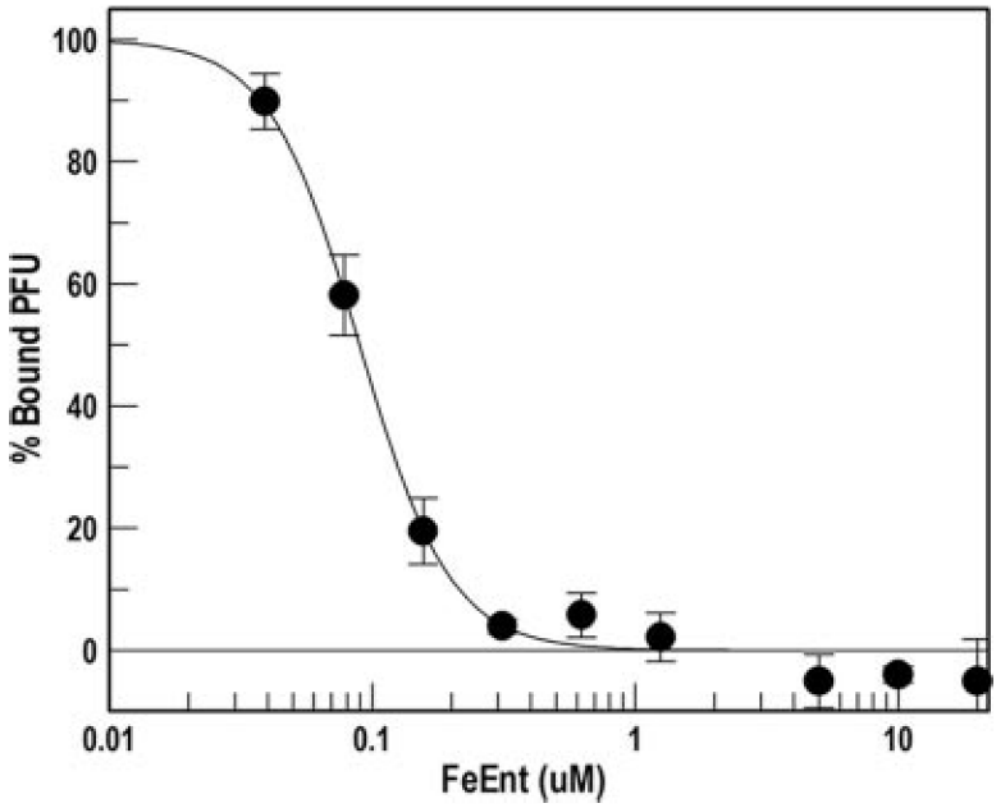

Figure 14 **Inhibition of H8 binding by FeEnt**. OKN3/pITS23 the *E. coli* strain containing the precise in frame deletion of *fepA* harboring the *fepA* plasmid pITS23 was grown overnight in LB broth and exposed to H8 (10^5 PFU) in the absence or presence of increasing concentrations of FeEnt. The bacteria were incubated for 45 min at 37°C, centrifuged to remove bound phage and bacteria from the supernatant, the number of non-bound phage in the supernatant was determined by serial dilution and plaque assays. The number of phage bound was calculated by subtracting the number of non-bound phage from the total number of phage. The percent bound in the presence of FeEnt was calculated by dividing the number of bound phage in the presence of FeEnt by the number of bound phage in the absence of FeEnt and then multiplying this number by 100%. The IC50 algorithm of Grafit 5.013 (Erithacus Ltd., Surrey, United Kingdom) was used to analyze the data giving an IC50 value of 0.098 μM for FeEnt (92).

4.2.2 H8 Genome

The 101kB chromosome of H8 contained 141 open reading frames NCBI accession number AC171169). Of these open reading frames, six contained loci located around the 20kB region encoding the tRNA for arginine, glycine, isoluecine, methionine, serine and threonine. The genome of H8 revealed a close relationship between H8 and T5, as demonstrated by the fact that the majority of translated proteins from these open reading frames were highly homologous to known T5 proteins. A total of 127 of the 141 predicted proteins in H8 had homologs in T5, with 84.2% identity and 88.7% similarity. Predicted proteins that shared homology with other phage include BF23, Felix 01, and RB16. These phage are of the Order *Caudovirales* and the Family *Siphoviridae*; phage in this group include BF23, λ, Φ81 and T1. These viruses have either isometric or prolate capsids with long non-contractile tails. H8 has morphology similar to this, as shown by electron microscopy. T5 is a double stranded DNA virus that lacks an RNA stage for reproduction. T5 infects *E. coli* through FhuA, another outer membrane siderophore receptor similar to FepA.

Orfs starting at 12629, 2472, 3086, 30849, 41390, 68191, 68393 and 94792 bp encode for nine potentially unique genes found in the H8 chromosome. These predicted proteins ranged in length from 133 to 724 amino acids. PSORT predicted that four of these genes would be cytoplasmic, four would be inner membrane and one outer membrane/periplasmic, ranging from 11-80kD (Figure 15).

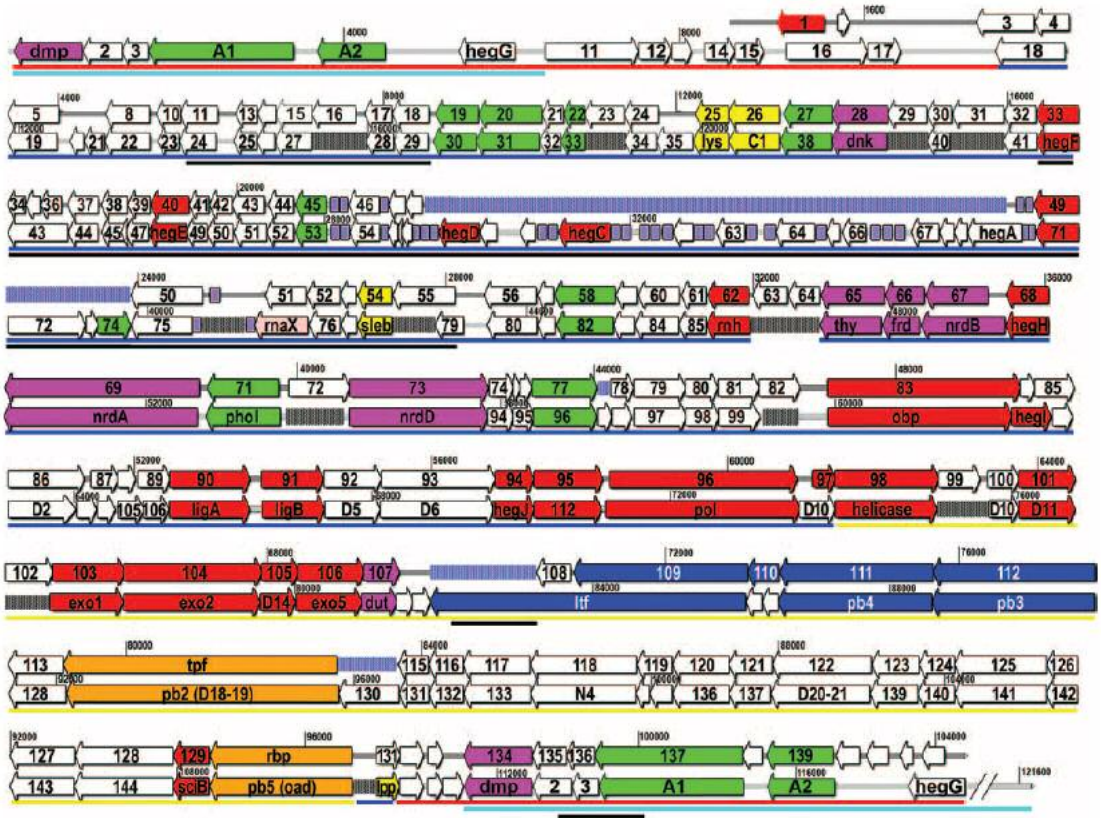

Figure 15 Comparison of the overall genomic structure of H8 and T5. ACT4 (**http://www.sanger.acuk**) was used for the alignment of the annotated genomes. NCBI(**http://www.ncbi.nlm.nih.gov/genomes**) accession number NC005859 was used for the source of the annotated T5 genomic sequence. The homology between the DNA sequences (vertical bars of graded color) between the genomes of H8 (accession no. AC171169) and T5 from a minimum identity value of 70% (white) to a maximum identity of 100% (red). Pre-early (red), early (blue), late regions (yellow) and deletable regions (cyan) underlines mark these regions in the T5 genome. For both T5 and H8 genomes DNA replication and repair, (red) nucleotide metabolism (magenta) host interaction (yellow) other enzymes, (green) structural proteins, (blue) unknown function (white) arrows indicate direction of transcription. ORFs encoding the receptor-binding and pore-forming and tail proteins (orange). Gaps in the H8 chromosomerelative to that of T5 (blue stippled boxes) gaps in the T5 chromosome relative to that of H8 (black stippled boxes). (92)

BLAST analysis of the H8 genome identified a predicted receptor binding protein (rbp) at 91.8kB and a pore-forming tail protein at 76.2kB. This was based on homology to the experimentally identified receptor binding protein pb5 (45, 71) and the pore-forming protein pB2 (11, 35) of bacteriophage T5 (113). The receptor binding protein (Rbp) found in H8 was one of the least conserved proteins found in the H8 genome, with only 26% identity and 41% similarity in comparison to its T5 homolog. The differences in sequence similarity between these two proteins is most likely due to the fact that these receptor proteins are designed to interact with different outer membrane receptors (Figure 16).

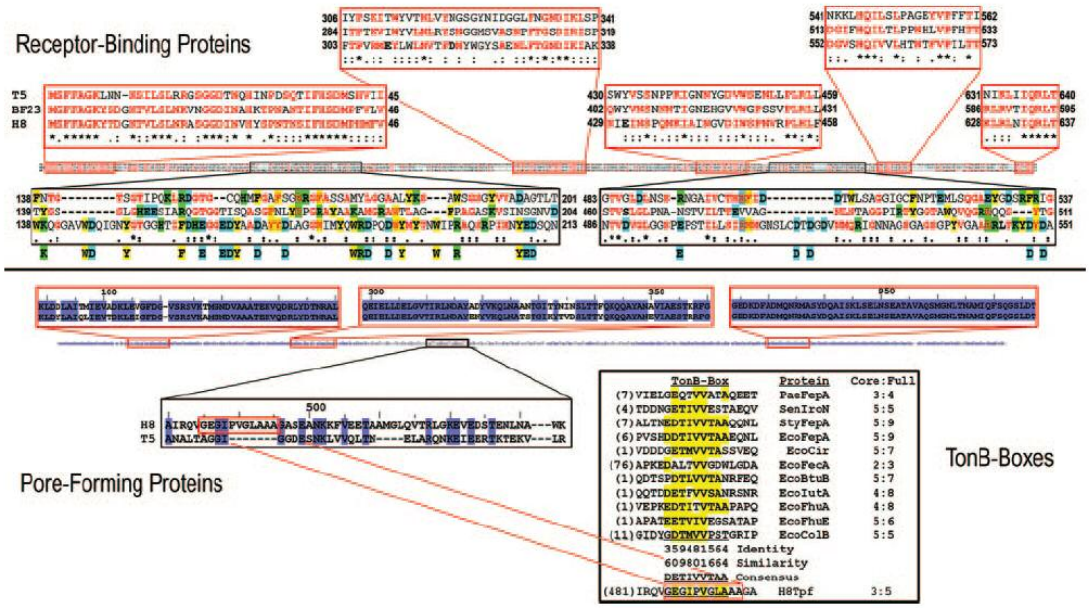

Figure 16 **Putative receptor-binding and pore-forming proteins of bacteriophage H8**

(Top) Alignment of the tail receptor-binding proteins of bacteriophages T5 (protein pb5 or Oad) and BF23 (Hrs) with the putative receptor binding protein (Rbp) of H8 using CLUSTAL W. Analysis revealed five regions of similarity (red boxes), with identical (marked with a star below) and similar (BLOSUM 62 matrix; marked with a colon or dot below) residues in the sequences (red). The alignment also showed two variable regions (boxed in black). H8's variable region contained several acidic residues (cyan), basic residues (green) and aromatic residues (yellow). This region may participate in adsorption to FepA (19, 75, 106). Listed below the alignment are the charged and aromatic amino acids that are unique to H8.
(Bottom) Alignment of the tail pore-forming protein of T5 with its H8 homolog (ORF 114, encoded by *tpf*) revealed a high level of homology between the T5 and H8 sequences (66% identity; 72% similarity), regions highlighted in blue show prominent similarities. Alignment between the two sequences showed the most homology close to the N and C termini; this homology decreases toward the central region. Enlarged elements of the sequence boxed in red show the three regions with the most homology between the proteins. The region boxed in black contains a region of greater variability of in the central region. The pore-forming protein of H8 contains a sequence similar to the consensus TonB box regions (GEGIPVGLA) located near the N-termini of the siderophore receptor proteins. The TonB box sequence of FepA is DDTIVVTAA. There is considerable variability in these regions as seen in this comparison of TonB boxes. The proteins in the TonB-box comparison are listed from top to bottom (*Pseudomonas aeruginosa* (PaePfeA), *S. enterica* serovar Typhimurium (StyIron and StyFepA), *E. coli* (EcoFepA), (EcoCir, EcoFecA, EcoBtuB, EcoIutA, EcoFhuA, and EcoFhuE) are *E. coli* LGP paralogs) (92).

4.2.2.1 Bacteriophage Comparisons

H8's overall genome structure is very similar to T5 as both are arranged according to their life cycles. Sequence homology to other phage genes was used as a basis for the genomic annotation in the absence of genetic and physiological data from this new bacteriophage. Of the 135 predicted proteins in the H8 genome, 49 were annotated as enzymes involved in the replication and repair of phage DNA, nucleotide metabolism, or structural proteins. H8's genome also contains several large areas not found in T5; these areas are located at 17.2, 20.7 and 21.5 kB on the T5 chromosome and range from 2 to 7.7 kB in length. The three regions are homologous to regions in T5 that are not required for the function of T5 (67, 114). Inside of these regions are areas encoded for ORFs, including 24 tRNA genes, two HNH-homing endonucleases, and one putative endonuclease (Figure 15).

Although H8 is similar to T5 in genomic and phenotypic structure, H8 requires TonB whereas T5 does not. This difference might be related to the lack of homology between the tail proteins of H8 and T5. This lack of homology includes the tail fiber protein at 67.8kB on the H8 chromosome which was only 24% identical and 29% similar to the tail fiber protein (Ltf) T5 protein. Comparing the genome of H8 to the genome of the bacteriophage T1, a bacteriophage that is also TonB-dependent, revealed similarity to Orfs in the T1 genome encoding proteins involved in binding or transport of the phage in T1.

4.2.2.2 Tail pore-forming protein

A total of five phage/receptor systems are known: H8/FepA, T5 and T1/FhuA, BF23/BtuB, and λ/LamB. The complete genomic sequences of all of these bacteriophage are known with the exception of BF23. Yet, although not complete, the proteins that encode some of the tail proteins of BF23 are known from previous work (71). The predicted homolog protein to pb5 from H8 showed homology to Hrs, a protein found in BF23. Sequence comparisons between the pb5 protein in H8 and those of its homologs found in T5 and BF23 identified five regions along BF23's tail binding protein with significant identity/similarity. Of these regions, the N-terminus contained the highest level of conservation. In the N-terminus, the first 45 residues of the three homologs were 49% identical and 91% similar, as compared with scores of 17%/81%, 21%/89%, 33%/71% and 50%/90% for the other four regions. Variable regions were also found in these sequence comparisons; these regions in H8 had a high amount of acidic residues and, as shown in previous work, it is likely that these residues are involved in phage adsorption to basic residues found in FepA (74, 106). The H8 tail pore-forming protein (tpf) is structurally related to the pore-forming tail proteins of T5, T1, and λ. Of these proteins tpf is most similar to the pore-forming tail protein of T5. It is 66% identical and 72% similar to this T5 protein. There is a key similarity though to the T1 pore-forming protein. Both H8 and T1 are TonB-dependent and they both contained sequences the look like the TonB-box regions found on the N-domain of TonB dependent LGPs. In H8 the sequence is GIPVGLAAAGA and TIGDVVAIA in T1 (FepA DETIVVTA). These TonB-box like sequence's are found

in the most variable regions of H8's and T1's primary structure. It is this TonB-box region that is believed to be the most crucial connection between TonB and the receptors it serves (Figure 14).

4.3 Discussion

OM porins often serve a multifunctional role of nutrient receptor, transporter and receptors for bacteriocins and bacteriophages. The first example of this was BtuB, the OM LGP responsible for the transport of vitamin B12, which has been shown to be required in the killing activity of E-group colicins (30) and binding and infectivity of the BF23 phage (12). Bacteriocins and bacteriophages usually require OM porins. Later FhuA was shown to function in this multi-purpose role. Now FepA has been shown to transport H8, a bacteriophage, and therefore completing its requirement to join this group of proteins. Unlike several of these proteins, the ability of FepA to yield infection by H8 is dependent on TonB. This is unlike fellow bacteriophage T5 and BF23 which do not require TonB even though H8 shares homology to them.

Susceptibility of *E. coli* to H8 was found to have at similar level among host strains carrying *fepA* in their genome or on plasmids. The plating efficiency of H8 for these strains are different however and dependent on the level of expression of FepA in the OM. A higher level of expression of FepA in the OM as seen in strains carrying *fepA* on pITS23 gave more pfus per H8 lysate then strains carrying *fepA* on pITS449. Even though pITS23 is a low copy vector, it produces more FepA on then the high copy pITS449. This is due to the partial truncation of the Fur-regulated promoter on

pITS449. As a result pITS23 produces roughly twice the amount of FepA per cell than pITS449 (4). It has also been observed that cells harboring pITS23 have a higher capacity and V_{max} when compared to pITS449 (2).

The infection of *E. coli* by H8 was inhibited by the same mutations that negatively affect binding and/or uptake of FeEnt and colicin. H8 was unable to infect cells carrying the N-domain deletion version of FepA or the FhuA N-domain FepA β-barrel protein. Deletion of N-domain loops had less of an impact on H8 infection than deletions of loops on the β-barrel. The β-barrel loops are the more external loops, suggesting an initial biding between H8's tail-fiber assembly and these loops. Without these surface loops, H8 may be unable to bind irreversibly before it dissociates.

Individual residues in FepA do not have as great an effect on the binding of H8 as the surface loops, but several residues were found to be important for H8 infection. A total of 46 residues in the loop extremities were studied for their role in H8 infection. These residues were either aromatic or basic and were substituted with alanine to study their role in H8 infection. The extent of this decrease in infection varied from residue to residue. H8 infection was affected by a total of 8 randomly distributed residues in the surface loops of FepA. The two residues that had the greatest effect on infection were F329 and K483. When F329 (19) was substituted with alanine H8 infection decreased by 95% and when K483 was substituted with alanine H8 infection decreased by 91%. Other residues were also observed to have an affect on H8 infection; these were R274, K332, Y478, Y553, K634, and K635.

Alanine substitution of these residues only decreased infection by roughly 2-fold. This shows that the H8 phage tail interacts with a broad range of residues in the outer loops of FepA. Studies of the binding of FeEnt and colicins B and D showed similar deleterious effects from the alteration of these residues (2). However regions deeper in FepA's vestibule show a hierarchy in their effect on FeEnt, colicin (19, 74) and H8 interactions with FepA. For example colicin killing is decreased 2-fold by Y260A but FeEnt binding and transport shows a 100-fold increase in K_D and K_M. Whereas transport affinity and colicin B and D susceptibility were equally reduced 50-fold. The combination of mutations R286A and R316A had an even greater impact with 1000-fold. The infection of *E. coli* by H8 was reduced 98%, 93%, and 76% by Y260A, T286A and R316A respectively. The double mutant R286AR316A decreased infection by 99%. This indicates the importance of these residues for H8 infection and as mentioned earlier these same residues have importance in FeEnt binding and colicin susceptibility as well. F329 and K483 are residues located in the initial binding region for FeEnt in FepA. These residues are also important in binding of FeEnt to FepA and H8 infection. These residues are located over a wide range of the surface of FepA indicating that H8's initial interaction takes place over a greater portion of the receptor's surface and then FeEnt. Later on in the infection reaction H8 as the phage begins to inject its DNA and penetrate the OM it requires many of the same core basic amino acids that are required for FeEnt transport. This is supported by the competitive inhibition of H8 infection by FeEnt (Figure 11).

The metal complexes that are transported through LGPs differ in net charge. FeEnt is acidic with a net charge of negative three at physiological pH which is very different from the charge found on cyanocobalamin (+1) and ferrichrome (neutral). It is believed that the phage mimics the substrate for these LGPs to enter them. If this is the case, then it would be expected to see a large amount of amino acids on the surface of the binding protein of H8 to have a negative charge at physiological pH, whereas the binding protein of T5 should have amino acids with a positive charge at physiological pH on the surface of its binding protein. As mentioned earlier H8 uses FepA, T5 uses FhuA and BF23 uses BtuB. A comparison of their receptor-binding tail fiber proteins showed many areas of significant homology along their sequences but also revealed two regions of variability in between them from residues 138-213 and 486-551. In H8 these regions of variability contain a significant amount of negative charge. The first region from 138-213 has a net charge of negative eight and the second region from 486-551 has a net charge of negative six. These two regions are the main set of residues that differ from the T5 and BF23 homologs. This suggests that this is the main source for selectivity for at least H8, giving H8 its unique ability to use FepA as a source of entrance into the bacterial cell.

H8 and T1 unlike T5 and λ are TonB dependent. This TonB dependence is coupled to an energy requirement that is seen for the transport of chelated metals, bacteriocins and bacteriophage. It is still unclear what the link is between TonB and energy, as it is still unclear what the true function of TonB really is. A central theme in

the TonB process is the TonB box region that is found in all LGPs. It is a short 7-11 residue segment found on the N-domain of LGPs that is highly conserved among LGPs and some colicins as well. A look at the H8 and T1 genomes reveals sequences within the variable regions of the tail-pore forming protein that share homology to the TonB box. These regions are not found in the T5 or λ phage genomes suggesting that these regions could play a role in the TonB dependence of these phage (Figure 16).

Chapter 5

5. TonB Hybrid Proteins

5.1 Introduction

It is believed that structural transitions in TonB are required for the transduction of energy from the inner membrane to the LGPs of the outer membrane. There is as of yet no actual structural model for this; only the C-terminal structure of TonB has been solved. The structure has been solved using X-ray crystallography (22) and NMR (82). The crystal structure shows the C-terminus in a dimerized conformation whereas the NMR structure suggests that the C-terminus is a monomer in solution. However either model has yet to be proven *in vivo*.

The idea that TonB forms a dimer has been explored and there is evidence that supports this conclusion (100). This was shown with the construction of fusion proteins containing either full length TonB or truncated versions of TonB synthesized with the cytoplasmic fragment of the ToxR protein (1-182) on the N-terminus of TonB. The cytoplasmic region of ToxR activates the transcription of *ctx*, the cholera toxin gene. The transcription of the *lacZ* gene was placed under the *ctx* promoter leading to an indication of dimerization through the expression of *β*-galactosidase. As a positive control ToxR was fused to PhoA and ToxR fused to MalE was used as a negative control. The TonB ToxR fusion was 78% as active as the ToxR PhoA fusion in *β*-galactosidase activity represented in Miller units. This evidence supports the conclusion that TonB does form a dimer. Of further interest is that these functional

fusion proteins have a large polypeptide (ToxR) on the cytoplasmic side of the inner membrane on the N-terminus of TonB. This presents evidence against the shuttle model of transport (100).

One view of the function of TonB is that it is an energy transducer which shuttles between the IM and OM (88). This was based on association of TonB with both the inner and outer membranes, when the cell envelope was fractionated. It dictates that TonB captures energy from the proton motive force of the cytoplasmic membrane, and then uses this transduced energy to facilitate ligand gated porin transport by a protein-protein interaction that opens the closed channels of OM metal transporters. This model postulates that TonB complexes with ExbB and ExbD to capture energy derived from the proton gradient, causing a conformational change in TonB's structure. The structure of this energized conformation has not been observed or demonstrated, and there are no theories on what this conformation looks like or the mechanism by which it would transduce energy. The energized conformation then transmits, or transports energy across the periplasmic space to the OM LGPs. Once at the OM, TonB recognizes receptor proteins with the ligands bound on the outer surface, through the TonB box region, and physically transmits the stored energy to the LGP to allow for transport. This changes the conformation of TonB protein to a non-energized form that then returns to the inner membrane to repeat this cycle. This interaction by TonB with the outer membrane LGPs is what allows for the

internalization of ligands such as siderophores, vitamin B_{12}, colicins and phage (Figure 17).

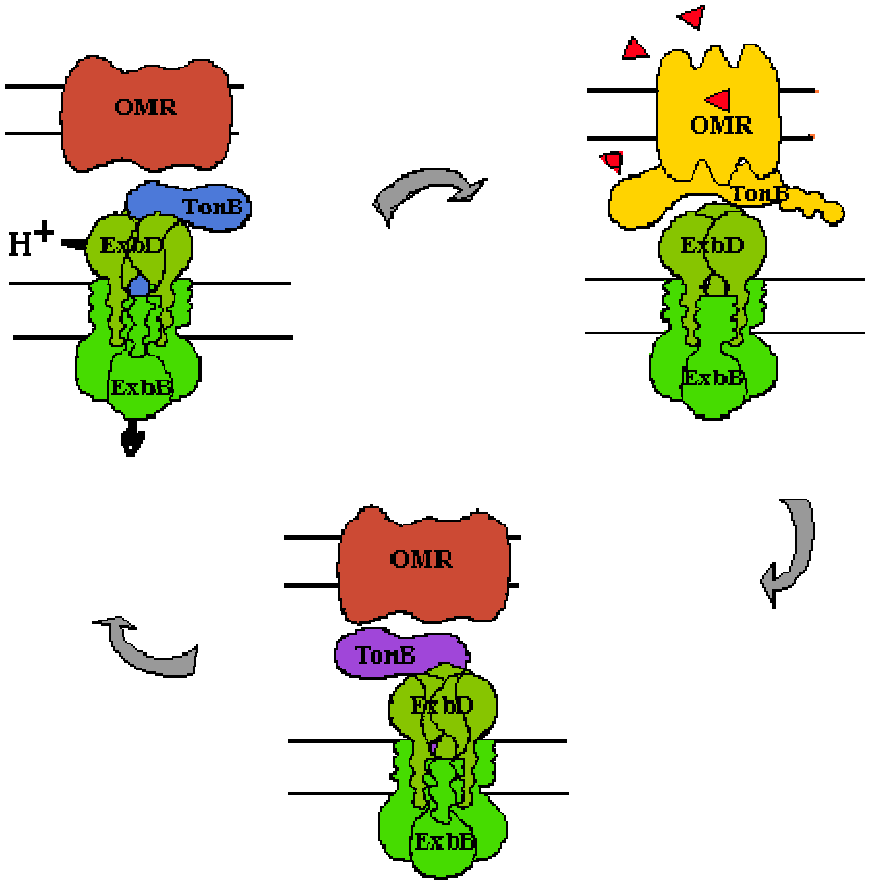

Figure 17 TonB shuttle model.), Non-energized TonB (purple) begins in inner membrane associated with ExbB (light green), ExbD (olive green), proton motive force changes the conformation of TonB to energized TonB (blue), the energized TonB shuttles across the periplasm to the non-energized outer membrane receptor (OMR) such as FepA (orange), TonB binds to the OMR forming an energized OMR with TonB (yellow) complex resulting in the transport of substrate (red triangle). TonB then returns to the inner membrane and its initial non-energized form (88). (60)

The *in vivo* evidence for the TonB LGP association (5, 16, 17, 25, 32, 33, 69, 83) conceptually and experimentally has significant gaps. These gaps open a lot of deficiencies in the TonB-mediated energy transduction hypothesis. These gaps can be broken down into three categories: the number of TonB molecules present in the cell, TonB's connection with energy metabolism and lastly TonB's structural similarities to any known proteins that are involved in energy metabolism.

The number of TonB molecules varies from 300-3000 (120) copies per cell whereas the proteins that it is required to facilitate are produced at levels close to 30,000 copies per cell and there are at least six of these proteins CirA, FepA, FhuA, IutA, FecA and BtuB. This creates a large stoichiometric difference between TonB and the molecules that require it for their function.

TonB has not been directly linked to energy metabolism. The theory that TonB is linked to energy metabolism originated with genetic inference and was furthered by cross-linking analysis. TonB is not known to pump protons, accept or donate electrons or to utilize or synthesize ATP, GTP or any other tri-phosphate in any way.

One of the unique features of TonB is the central rigid region 66-100 is not required for TonB function. The idea that the transmembrane alpha helix serves as an anchor and the lack of the necessity of the central rigid region lead to a focus on the C-terminus and its interaction with LGP.

Studies of the last 69 residues of the TonB C-terminus revealed that it folds into a globular form that it spontaneously inserts into liposomes (51). The C-terminus also has a general affinity for OM proteins including proteins that do not contain a TonB-box found in the multi-active transport of LGPs and do not require TonB for their function. These results involving the C-terminus clarify several ideas on the disposition of the C-terminus in the Gram-negative bacterial membrane. The first is that the TonB C-terminus does not require the TonB-box to adsorb to FepA as shown by the TonB C-terminus binding to the N-terminal deletion of FepA. The second is that TonB has a general affinity for outer membrane proteins not just the LGP's.

TonB is unique and has no structural similarity to other membrane proteins associated with membrane proteins involved in bio-energetic processes. It requires no chromophores, prosthetic groups or co-factors and contains no metal centers. And although it cross-links at low levels to other cell envelope proteins, it presumably exists as a 58 kD dimer, with each monomer consisting of three regions, a transmembrane alpha helix followed by a central proline rich rigid region with a C-terminal β-α-β domain that links the two monomers together. It is believed that ExbB and ExbD are needed to form a proton channel with TonB.

As mentioned earlier one of the other systems that uses a proton pump is the bacterial flagellar motor system, and comparisons to the flagellar motor system lead to another hypothesis for the mechanism of TonB. This hypothesis known as the rotational model proposes that TonB's mechanism involves spinning of the dimer in

the IM bilayer TonB. This model of TonB has two premises: that two TonB molecules form a dimer and are in association with ExbB/D, and that movement of protons through ExbB/D leads to rotation of TonB. Based on these assumptions, the overall system can take 2 conformations (Fig 18).

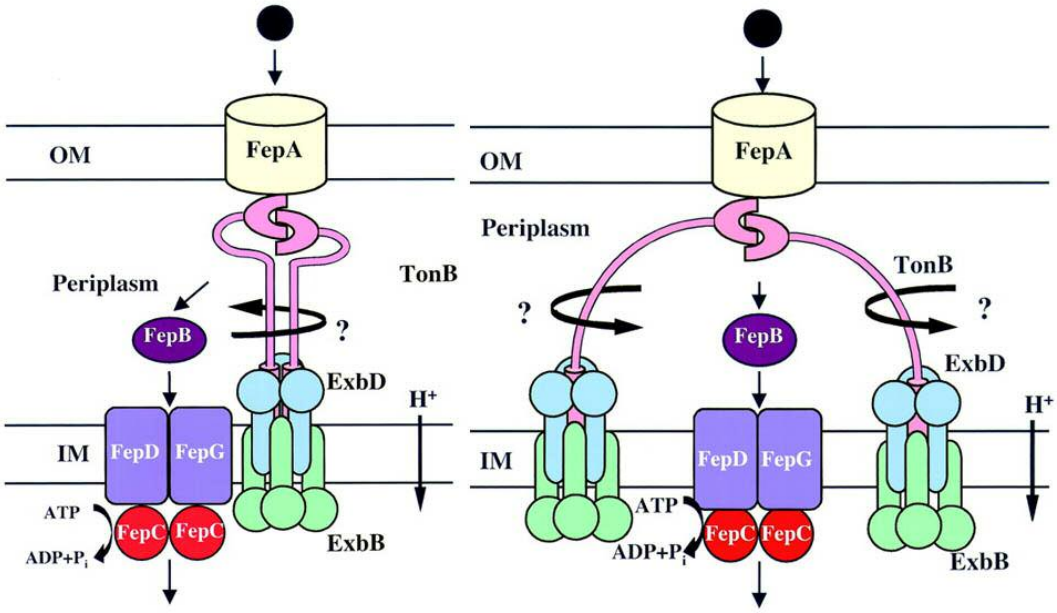

Figure 18 Rotational models of TonB. (Left) model of TonB in which two TonB molecules are dimerized and associated with a single ExbB/D complex. (Right) model of TonB in which the two TonB molecules are associated with two separate ExbB/D complexes (22).

5.2 Results

5.2.1 Activity of Hybrid Proteins

5.2.1.1 Siderophore nutrition

Both fusion proteins pGT and pGLT expressed in OKN1 showed a halo diameter of 15mm, which is equivalent to wild-type represented by pT23 expressed in OKN1. Also the density of growth is equivalent between the fusion proteins and wildtype indicating that bacteria containing the fusion proteins successfully bound and utilized FeEnt with the same affinity as wildtype. This show's that the addition of GFP to the N-terminus of TonB had no effect on ability of the bacteria to use FeEnt (Table 6) (Figure 19).

Strain	Halo diameter
OKN3	0
OKN1	0
OKN1/pT23	15mm high density growth
OKN1/pTpG	0
OKN1/pGT	15mm high density growth
OKN1/pGLT	15mm high density growth
BN1071	17mm high density growth
BN1071/pT23	15mm high density growth
BN1071/pTpG	15mm high density growth
BN1071/pGT	15mm high density growth
BN1071/pGLT	15mm high density growth

Table 6 . Results of Siderophore Nutrition Assay of Hybrid proteins. The utilization the siderophore ferric enterobactin (FeEnt) was measured using OKN3(*ΔfepA*), OKN1(*ΔtonB*) for the negative controls and OKN1/pT23(*ΔtonB* with *tonB* expressed on the low copy plasmid pHSG575) and BN1071 representing the wildtype controls. pTpG(GFP expressed under the *tonB* promoter on the low copy plasmid pHSG575), pGT(GFP attached to the N-terminus of tonB expressed under the *tonB* promoter on the low copy plasmid pHSG575) and pGLT(GFP attached to the N-Terminus with a 6 amino acid α-helix linker region between the N-terminus of TonB and GFP). The halo diameter represents the halo of growth surrounding the disc containing 10µl of a 50µM solution of FeEnt.

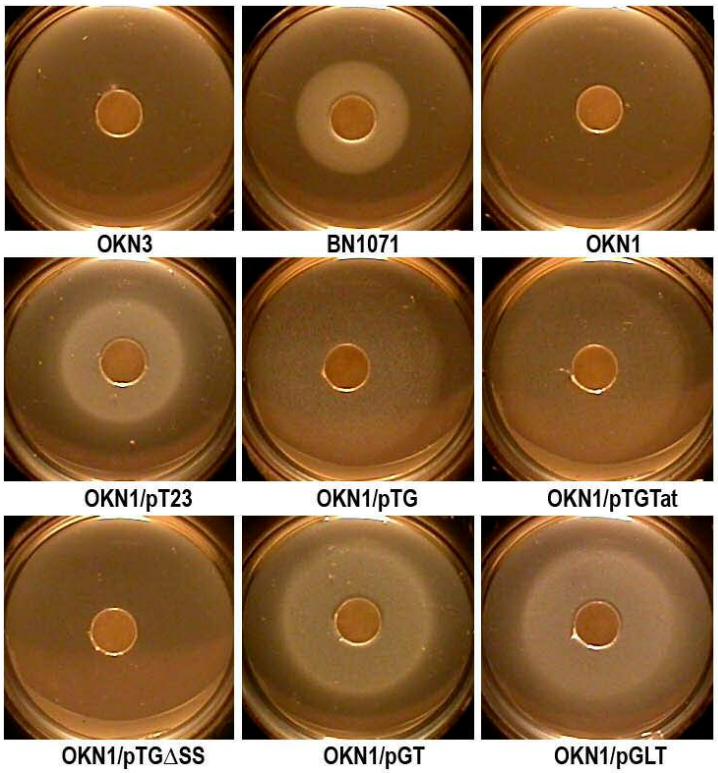

Figure 19 Siderophore Nutrition of relevant strains. (Top) OKN3 (*fepA*), BN1071 (*entA)* and OKN1 (*tonB)*. (Middle) OKN1 transformed with plasmids encoding for *tonB* (pT23), *tonB:gfp* (pTG) and *tonB:gfp* with a modified signal sequence in which the original signal sequence of *tonB* was replaced by a consensus TAT signal sequence (pTGTat). (Bottom) OKN1 transformed with plasmids encoding for *tonB:gfp* with the signal sequence of *tonB* deleted (pTGΔSS), *gfp:tonB* (pGT) and *gfp:*linker*:tonB* (pGLT). The bacteria were plated out in nutrient broth top agar with the appropriate antibiotics, 100μM bipyridal with 10μL of 50μM FeEnt added to a paper disc on the center of the plate.

5.2.1.2Colicin Sensitivity:

Both pGT and pGLT showed wild-type activity with respect to colicin B sensitivity (Table1). There is no difference in colicin B sensitivity between the wild-type represented by OKN1/pT23 and the two constructs pGT and pGLT. This indicates that TonB remained functional with respect to colicin B susceptibility even though it is attached to the 30kDa GFP (Table 7).

Strain	Colicin B susceptibility
OKN3	R
OKN1	R
OKN1/pT23	100
OKN1/pTpG	R
OKN1/pGT	100
OKN1/pGLT	100
BN1071	100
BN1071/pT23	100
BN1071/pTpG	100
BN1071/pGT	100
BN1071/pGLT	100

Table 7 Colicin B susceptibility was measured using OKN3(*ΔfepA*), OKN1(*ΔtonB*) for the negative controls and OKN1/pT23(*ΔtonB* with *tonB* expressed on the low copy plasmid pHSG575) and BN1071 representing the wildtype controls. pTpG(GFP expressed under the *tonB* promoter on the low copy plasmid pHSG575), pGT (GFP attached to the N-terminus of tonB expressed under the *tonB* promoter on the low copy plasmid pHSG575) and pGLT (GFP attached to the N-Terminus with a 6 amino acid α-helix linker region between the N-terminus of TonB and GFP). Susceptibility is a percent comparison to wildtype BN1071 (100 is equal to 100% susceptibility, R is completely resistant).

5.2.1.3 Flow Cytometry

Flow cytometry was used to measure the fluorescence intensity of each of the strains. OKN1, OKN1/pT23 and BN1071 were used as non-fluorescent negative controls. Their fluorescence intensities never reached more than roughly 1/3 the fluorescence intensity of the fluorescent fusions (Table 8). The fusion proteins expressed in the *ΔtonB* strain OKN1 had fluorescent levels more than ten times higher than for the negative non-fluorescent controls. When GFP was expressed alone from the *tonB* promoter (pTpG), its fluorescence levels were lower than the fusion proteins. These low levels of fluorescence are still higher than the negative controls by at least three fold. The fluorescence levels of the fusion proteins increased when they were transformed in the wildtype BN1071 strain.

Strain	%population	Fluorescence intensity
OKN3		
OKN1	100%	0.178
OKN1/pT23	100%	0.163
OKN1/pTpG	75.2%	0.645
OKN1/pGT	78.8%	1.80
OKN1/pGLT	84.8%	2.54
BN1071	99.9%	0.173
BN1071/pT23	100%	0.152
BN1071/pTpG	75.3%	1.05
BN1071/pGT	78.8%	2.10
BN1071/pGLT	84.5%	2.66

Table 8 Flow Cytometry data of the different constructs.

5.2.2 Expression of Hybrid Proteins

The fusion proteins were expressed as seen by Western blot using a polyclonal α-TonB antibody. The molecular weight of the fusion proteins are at the correct molecular weight of 60kDa (30kDa for TonB in addition to 30kDa for GFP) (Figure 20).

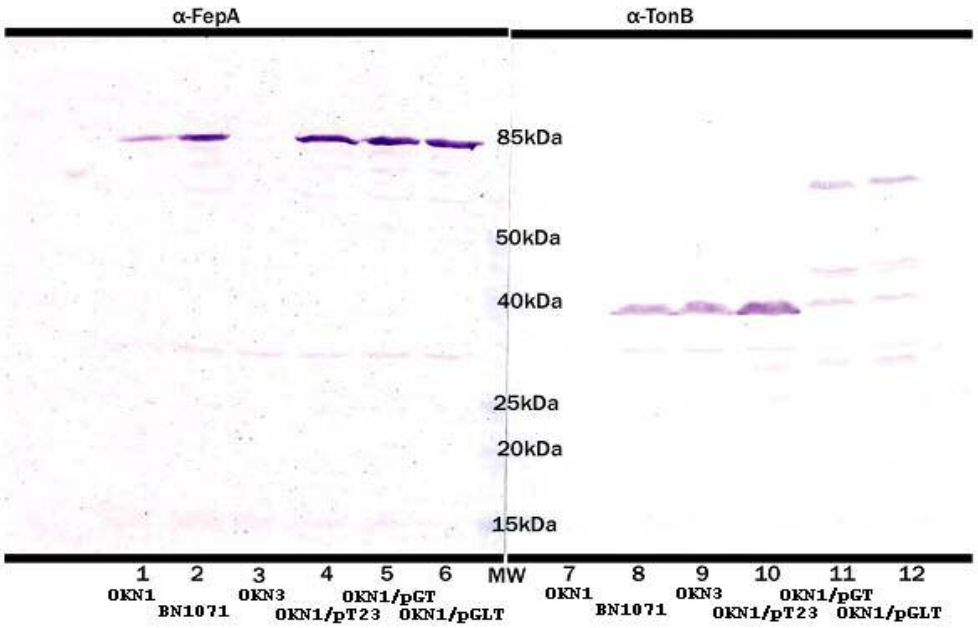

Figure 20 Western Blot of hybrid proteins post Binding and Transport experiments. Each lane contains $1x10^8$ cells that were resuspended in SDS-PAGE sample buffer, boiled for 5mins and spun at 14,000rpm in an Beckman GS-15R tabletop centrifuge.

5.2.3 Transport of FeEnt

The construction of the two hybrid proteins was used to evaluate the association of TonB in the inner membrane and determine if TonB leaves the inner membrane to perform its function. As shown above both hybrid proteins show phenotypes similar to wild-type in the nutrition tests. These tests measure the ability of the bacteria to bind and transport FeEnt, however this is a qualitative result. The larger the halo of growth, the lower the affinity for FeEnt the strain has. The halo diameters of the hybrid proteins are both larger than those seen for wild-type. This is a quantitative measurement of binding and transport radio labeled ^{59}FeEnt is used as mentioned in the methods above. Both of the GFP fusion proteins transported FeEnt at levels similar to wild-type.

The hybrid proteins have higher V_{max} and K_m values when compared to wild-type BN1071 and TonB expressed in the plasmid pHSG575 OKN1/pT23 (Table 9 and 10) (Figure 21). This agrees with the siderophore nutrition assays that show larger halos. The larger halo in the siderophore nutrition test indicates that the strain transports and binds FeEnt at a lower rate and with less affinity. Strains expressing wild-type FepA from the chromosome or from a plasmid show halos with small diameters and higher densities. Although the strains that contain the hybrid proteins do not transport at perfect wild-type levels, they bind and transport nonetheless. This

indicates that TonB is functional even though it is connected to GFP, a protein equal in size.

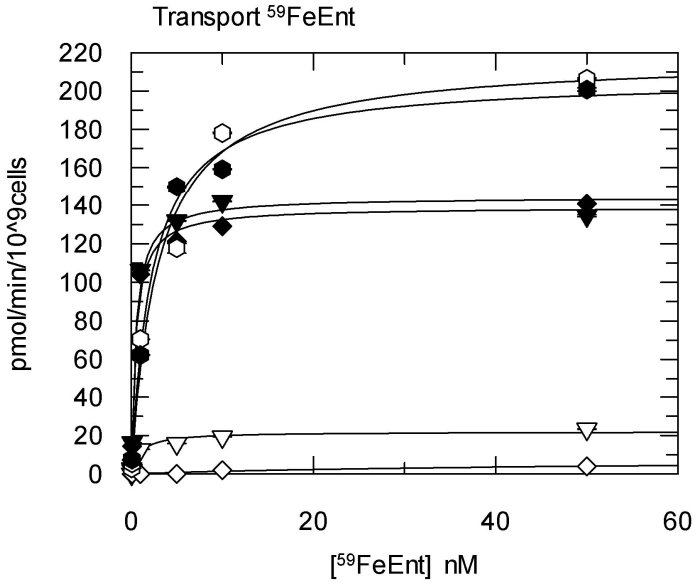

Figure 21 Transport of FeEnt by hybrid proteins. Wild-type TonB expressed from the chromosome (◥) BN1071, chromosomal deletion of FepA (∗) OKN3, chromosomal deletion of TonB (∗) OKN1, (∎) TonB expressed from pHSG575 in *tonB* strain OKN1/pT23, GFP:TonB hybrid protein expressed from pHSG575 in *tonB* strain(∗) OKN1/pGT, GFP:TonB protein expressed from pHSG575 in *tonB* strain(●) OKN1/pGLT. Six concentrations of ^{59}FeEnt were used to determine the concentration dependence of transport. The enzyme kinetics equation from GraFit 5.0.13 (Erithracus) was used to analyze and plot the data.

Strain	[a]Km	[b]Vmax
OKN1	0	0
OKN1/pGT	2.9207	217.3811
OKN1/pGLT	2.2362	206.3607
BN1071	0.4808	144.1819
OKN3	0	0
OKN1/pT23	0.4860	138.9292

Table 9. Binding and transport data of GFP hybrid proteins. Binding and transport was determined using six concentrations of ^{59}FeEnt from 0.05nM to 50nM. [(a)] K_m (nM) [(b)] V_{max} was determined using Enzyme Kinetics from GraFit 5.0.13 (Erithacus).

Strain/plasmid	Nutrition	ColB	K_m	V_{max}	V_{max}/K_m	Cytometry
BN1071	17	100	0.5	144	288	0.14(100)
OKN3	0	0	NT	NT	NT	0.15(100)
OKN1	0	0	NT	NT	NT	0.18(100)
OKN1/pT23	18	100	0.5	139	278	0.16(100)
OKN1/pTG	25	15	ND	ND	ND	0.14(100)
OKN1/pTGTat	25	20	ND	ND	ND	0.15(100)
OKN1/pTGΔSS	0	0	ND	ND	ND	ND
OKN1/pTpG	0	0	ND	ND	ND	0.77(70)
OKN1/pGT	21	100	2.9	217	74.8	1.80(79
OKN1/pGLT	22	100	2.2	206	93.6	2.54(85)

Table 10 Combined data for constructs

5.2.4 Localization of GFP Hybrid Proteins

5.2.4.1 Fluorescence Microscopy

To study the localization of TonB, I made two hybrid proteins containing TonB with GFP attached to the N-terminus. TonB is known to localize in the inner membrane of *E. coli*, and it was expected that these fusion proteins would localize in the membranes of the cells. TonB is a protein that is expressed in a low abundance with approximately 335 +/- 78 copies per cell in iron replete conditions (100 μM) and 1070 +/- 345 copies per cell in iron limiting conditions (>0.1 μM) (46). The hybrid proteins were expressed under the *tonB* promoter. The cells containing the plasmids encoding for the fusion proteins showed normal rod-shaped morphology grown in MOPS media. This implies that the attachment of GFP to the N-terminus of TonB does not affect cell morphology. The GFP hybrid proteins were fluorescent as seen by fluorescence microscopy. It is clear that when compared to GFP expressed in the cytoplasm under the *tonB* promoter (OKN1/pTG), both of the hybrid proteins have different localization properties. The fact that the hybrid proteins are fluorescent demonstrates that GFP is located in the cytoplasm since GFP cannot fold in the periplasmic space, therefore, it is not fluorescent in the periplasm (26) unless the TAT signal peptide sequence is attached to the N-termninus (99). The fluorescence in bacteria expressing the hybrid proteins is localized in a pattern that is confined to the cytoplasmic membrane in the poles. The fluorescence microscopy also demonstrates that these proteins do contain a functional GFP protein (Figure 22).

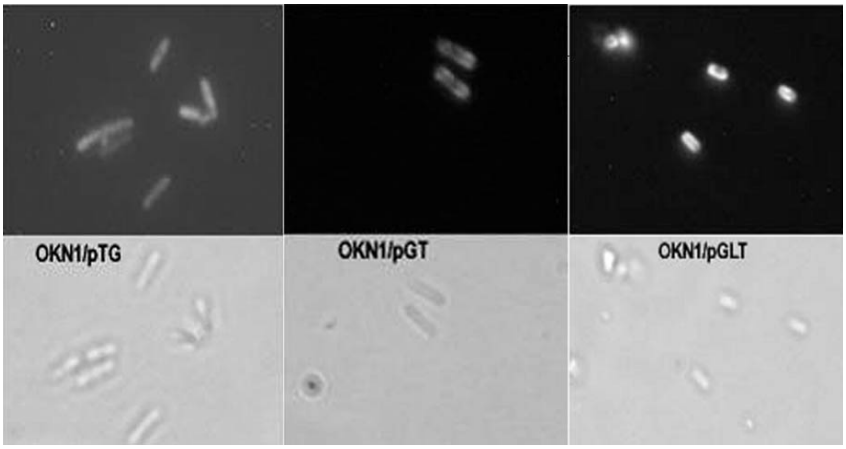

Figure 22 Fluorescence Microscopy. OKN1 containing plasmids encoding for GFP under the *tonB* promoter (pTG), the GFP:TonB hybrid protein (pGT) and the GFP:linker:TonB hybrid protein (pGLT). Strains were grown to mid-log phase in MOPS media at 37˚C with shaking at 220rpm. (Top) GFP fluorescence microscopy. (Bottom) Light microscopy.

5.3 Fluorescence Intensity and Anisotropy

The fluorescence intensities varied between each construct with the Qbiogene GFP having the highest fluorescence intensity (Figure 21). The fluorescence intensities of pGTdel and pTpG had the lowest intensities whereas the fluorescence intensity of pGT and pGLT were higher then pGTdel and pTpG(Figure 21).

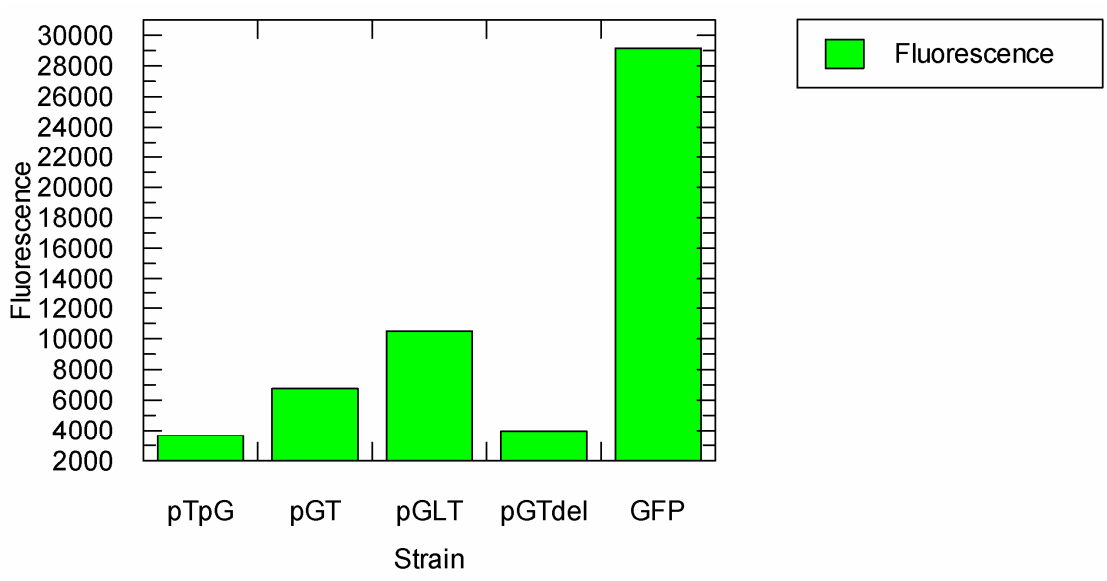

Table 11 Fluorescence intensity of strains.

The anisotropy of the constructs was similar for each of the strains with the exception of pGTdel with no poison. The trend indicated that GFP expressed alone in the cytoplasm (pTpG, and GFP (pQB-T7-GFP)) had lower anisotropy then GFP fused to TonB (pGT, pGLT and pGTdel) (Table 12).

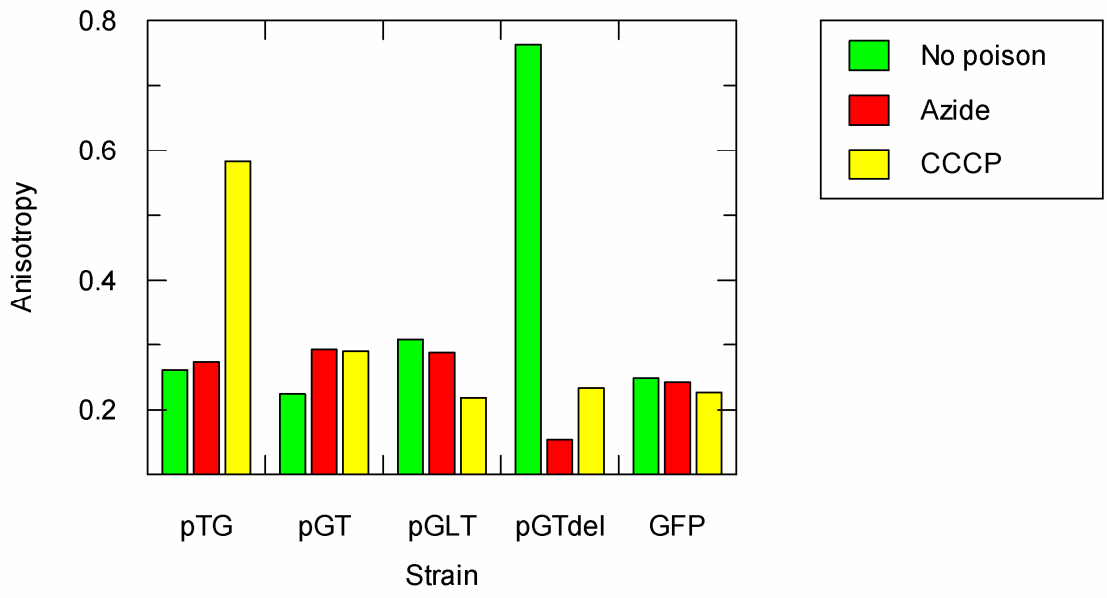

Table 12 Anisotropy of Constructs in the presence and absence of energy inhibitors.

5.4 Discovery of ycfS

Upon examination of the outer membrane sarkosyl extract of strain OKN1 (*tonB)* a distinct band was present at a molecular weight of roughly 40kDa (Figure 21). The presence of this band indicated the overexpression of this protein in the absence of TonB. The band containing this protein was excised from the gel and submitted for protein sequencing at the Insitute de Pasteur under the supervision of Alan Charbit. The sequence data identified the protein to be YcfS a protein of unknown function containing a LysM domain. The LysM domain has been implicated in the binding of peptidoglycan (49) and was named after the bacterial lysin proteins that contain this domain (87). The crystal structure of the LysM domain from *E. coli* membrane-bound lytic murein transglycosylase D (MltD) was solved (7) giving a

βααβ secondary structure which shows no similarity to other bacterial cell surface domains with the two α-helices packed on the same side of the antiparallel β-sheet (Figure 22).

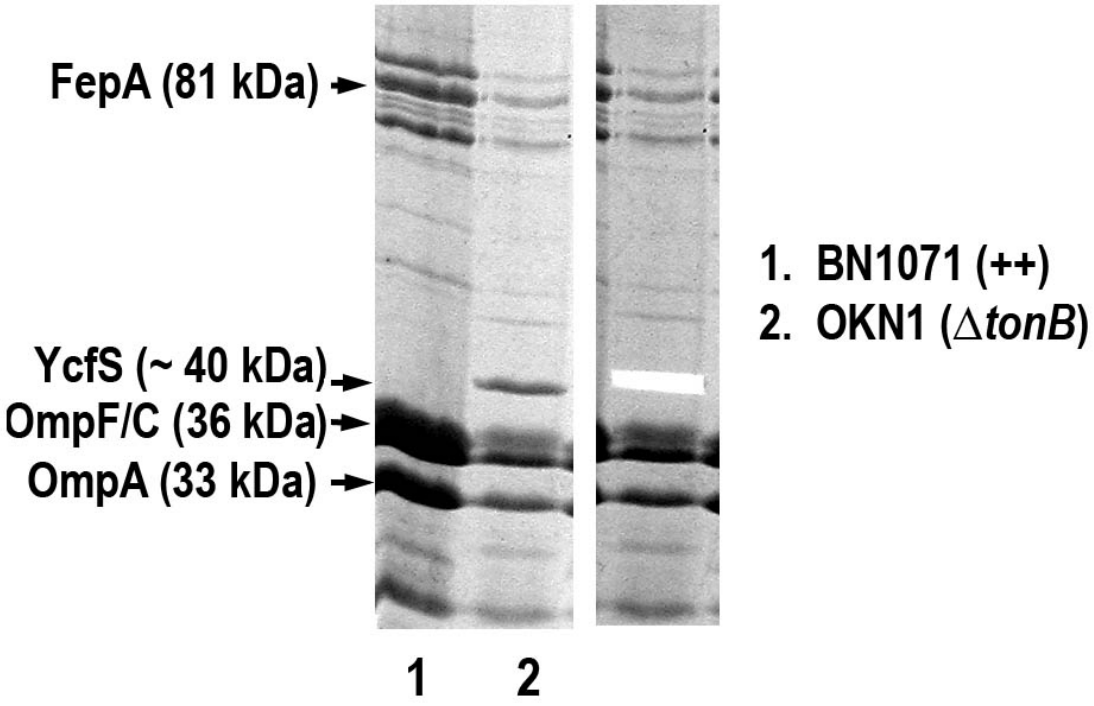

Figure 23 Isolation of ycfS.

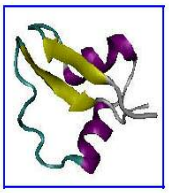

EcoYcfS protein sequence and the **LysM motif**

KFHVVENDGGSLEAIAKKYNVGFLALLQANPGVDPYVPRAGSVLTIP

MMIKTRFSRWLTFFTFAAAVALALPAKANTWPLPPAGSRLVGEN**KFHVVENDGGSLEAIAKKYNVGFLALLQANPGVDPYVPRAGSVLTIP**LQTLLPDAP
REGIVINIAELRLYYYPPGKNSVTVYPIGIGQLGGDTLTPTMVTTVSDKRANPTWTPTANIRARYKAQGIELPAVVPAGLDNPMGHHAIRLAAYGGVYLL
HGTNADFGIGMRVSSGCIRLRDDDIKTLFSQVTPGTKVNIINTPIKVSAEPNGARLVEVHQPLSEKIDDDPQLLPITLNSAMQSFKDAAQTDAEVMQHVM
DVRSGMPVDVRRHQVSPQTL

320 amino acids, 27 proline (8.4%)
Molecular Weight = 34635.83 Da

EcoTonB protein sequence

MTLDLPRRFPWPTLLSVCIHGAVVAGLLYTSVHQVIELPAPAQPISVTMVTPADLEPPQAVQPPPEPVVEPEPEPEPIPEPPKEAPVVIEKPKPKPKPKP
KPVKKVQEQPKRDVKPVESRPASPFENTAPARLTSSTATAATSKPVTSVASGPRALSRNQPQYPARAQALRIEGQVKVKFDVTPDGRVDNVQILSAKPAN
MFEREVKNAMRRWRYEPGKPGSGIVVNILFKINGTTEIQ

239 amino acids, 40 proline (16.7%)

Figure 24 Top Left Crystal structure of LysM motif from *E. coli* membrane-bound lytic murein transglycosylase D (MltD) (7) **Below comparison of E. coli YcfS protein Top and E.coli TonB protein bottom.** (green) hydrophobic regions found in YcfS and TonB on their N-terminus (blue) LysM motif (yellow) proline residues.

To analyze whether or not YcfS is involved in any activities associated with TonB or FepA a complete deletion of YcfS from the host strain BN1071 was constructed. The deletion of YcfS did have an effect on the uptake of FeEnt and Fc as shown by siderophore nutrition assay (Figure 23 and 24).

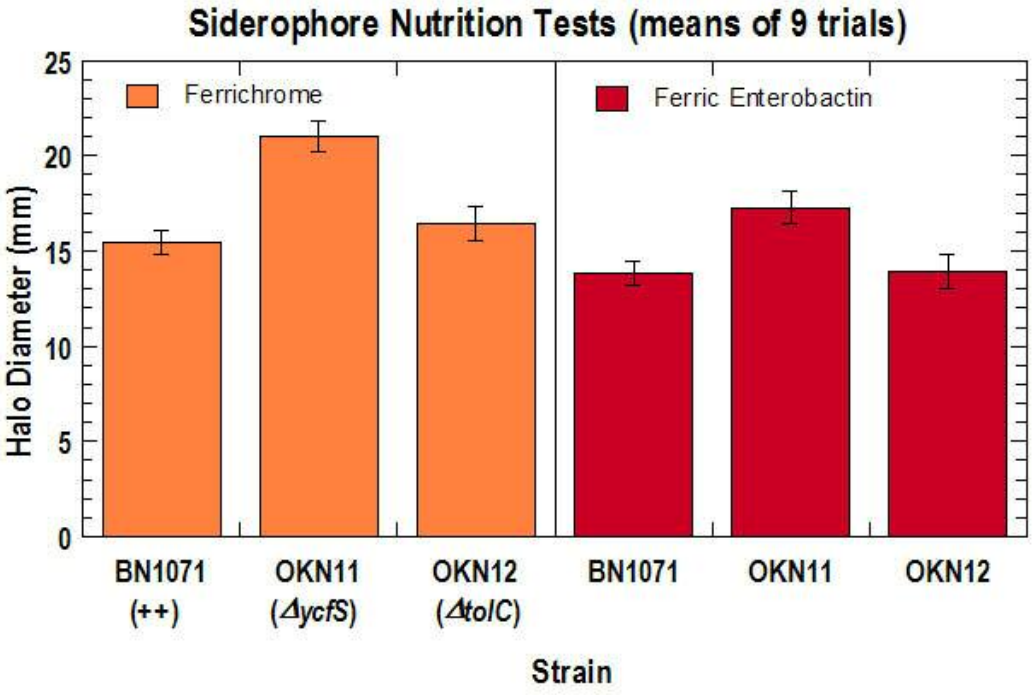

Figure 25 Average growth halo in mm for siderophore nutrition of Ferrichrome and Ferric Enterobactin.

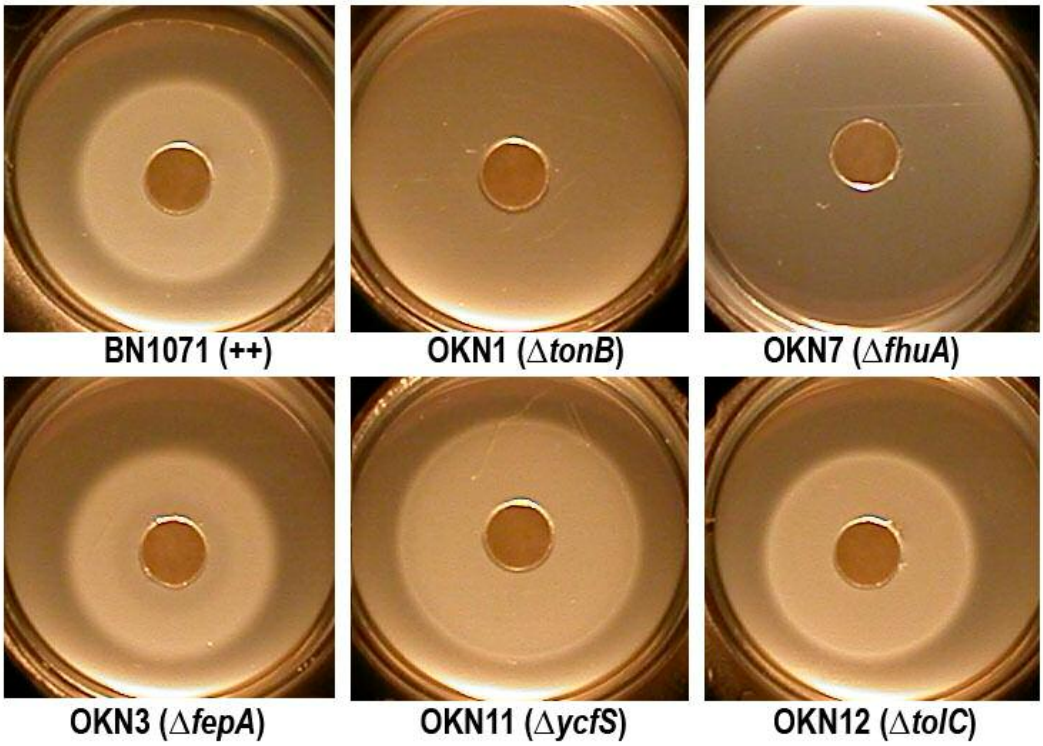

Figure 26 Siderophore Nutrition assay of BN1071, OKN1, OKN7, OKN3, OKN11(ΔycfS), OKN12(ΔtolC)

Analysis of the outer membrane fraction from sarkosyl extraction of the YcfS deletion on SDS-PAGE the overproduction a new distinct band was scene (Figure 25). This new band was sent for sequencing to OSU. The results of the sequencing determined that this protein is TolC.

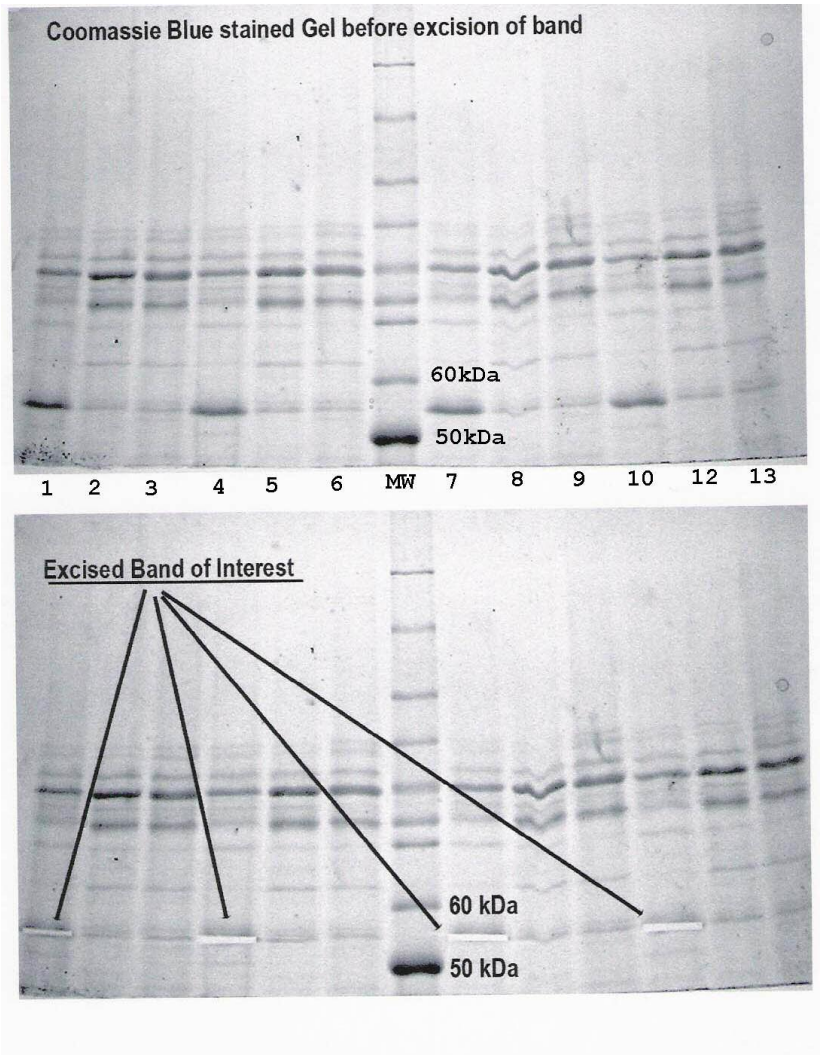

Figure 27 SDS PAGE of sarkosyl extractions of outer membranes. OKN11 (lanes, 1, 4, 7 and 10), BN1071 (lanes, 2, 5, 8, and 12) and OKN1 (lanes 3, 6, 9, and 13). Before band excision (Top) after band excision (bottom).

5.5 Discussion

The data shown here demonstrates that TonB does not need to leave the inner membrane to perform its function. The previously mentioned fractionation experiments established the idea that the intact TonB protein naturally partitions in both the inner and outer membrane of *E. coli*. In light of the new data presented here it may be that TonB forms a permanent link between the inner and outer membranes. The fact that the last 69 residues of TonB naturally partition into liposomes and that these residues have a general affinity for OM proteins including OmpA (104) leads to the conclusion that TonB has a general interaction with the outer membrane bilayer. The one thing that the outer membranes have in common is their β-barrel structure. Perhaps TonB recognizes this as the main feature for its interaction.

There is a protein similar to TonB found in the inner membrane of Gram-negative that has been found to be a structural necessity of the bacteria, TolA. TolA is a component of the TolQRAB system that is involved in the maintenance of outer membrane integrity. This system like the TonB system is required for the infection of certain bacteriophages (f1, M13, fd, and Ike) and also the group A colicins (E1, E2, E3, A, K, L, and N). The experiments involving the C-terminal 69 residues of TonB build further evidence towards this conclusion of TonB as a structural component of the Gram-negative bacterial cell envelope.

When a *tolA* strain is transformed with a vector that allows for the overexpression of the C-terminal domain of TolA, the strain does not recover its

TolA-dependent activities. However when this same C-terminus of TolA is incorporated into a *tolA*$^{+}$ strain, the cells increase in resistance to group A colicins. This increase in resistance does not occur in the case of the group B colicins. This data emphasizes the importance of a full length TolA protein for proper cell function and also the competition the C-terminus of TolA may have. This is very similar to the TonB system. There has also been a direct link between the translocation domains of colicins E1 and A, and truncations in the C-terminus of TolA prevented this interaction. Components of both Tol and Ton systems may also be able to substitute for each other as demonstrated by leaky phenotypes in *exbB* and *exbD* strains. ExbB and ExbD are the homologous proteins of the TolA system TolQ and TolR which are capable of substituting for ExbB and ExbD in the TonB system for TonB dependent processes. (13). In conclusion the similarity of these two systems leads to a model of TonB that is similar to TolA, in that TonB is a structural component of the cell envelope.

References

1. **Anderson, E. H.** 1946. Growth Requirements of Virus-Resistant Mutants of Escherichia Coli Strain "B". Proc Natl Acad Sci U S A **32:**120-8.
2. **Annamalai, R., B. Jin, Z. Cao, S. M. Newton, and P. E. Klebba.** 2004. Recognition of ferric catecholates by FepA. J Bacteriol **186:**3578-89.
3. **Arai, R., H. Ueda, A. Kitayama, N. Kamiya, and T. Nagamune.** 2001. Design of the linkers which effectively separate domains of a bifunctional fusion protein. Protein Eng. **14:**529-32.
4. **Armstrong, S. K., C. L. Francis, and M. A. McIntosh.** 1990. Molecular analysis of the Escherichia coli ferric enterobactin receptor FepA. J Biol Chem **265:**14536-43.
5. **Bassford, P. J., Jr., C. Bradbeer, R. J. Kadner, and C. A. Schnaitman.** 1976. Transport of vitamin B12 in tonB mutants of Escherichia coli. J Bacteriol **128:**242-7.
6. **Bassford, P. J., Jr., C. A. Schnaitman, and R. J. Kadner.** 1977. Functional stability of the bfe and tonB gene products in Escherichia coli. J Bacteriol **130:**750-8.
7. **Bateman, A., and M. Bycroft.** 2000. The structure of a LysM domain from E. coli membrane-bound lytic murein transglycosylase D (MltD). J Mol Biol **299:**1113-9.
8. **Bauer, K., M. Struyve, D. Bosch, R. Benz, and J. Tommassen.** 1989. One single lysine residue is responsible for the special interaction between polyphosphate and the outer membrane porin PhoE of Escherichia coli. J Biol Chem **264:**16393-8.
9. **Benz, R., A. Schmid, and R. E. Hancock.** 1985. Ion selectivity of gram-negative bacterial porins. J Bacteriol **162:**722-7.
10. **Benz, R., A. Schmid, and G. H. Vos-Scheperkeuter.** 1987. Mechanism of sugar transport through the sugar-specific LamB channel of Escherichia coli outer membrane. J Membr Biol **100:**21-9.
11. **Bohm, J., O. Lambert, A. S. Frangakis, L. Letellier, W. Baumeister, and J. L. Rigaud.** 2001. FhuA-mediated phage genome transfer into liposomes: a cryo-electron tomography study. Curr Biol **11:**1168-75.
12. **Bradbeer, C., M. L. Woodrow, and L. I. Khalifah.** 1976. Transport of vitamin B12 in Escherichia coli: common receptor system for vitamin B12 and bacteriophage BF23 on the outer membrane of the cell envelope. J Bacteriol **125:**1032-9.
13. **Braun, V.** 2006. Energy transfer between biological membranes. ACS Chem Biol. **1:**352-4.
14. **Braun, V., R. Burkhardt, R. Schneider, and L. Zimmermann.** 1982. Chromosomal genes for ColV plasmid-determined iron(III)-aerobactin transport in Escherichia coli. J Bacteriol **151:**553-9.
15. **Buchanan, S. K., B. S. Smith, L. Venkatramani, D. Xia, L. Esser, M. Palnitkar, R. Chakraborty, D. van der Helm, and J. Deisenhofer.** 1999. Crystal structure of the outer membrane active transporter FepA from Escherichia coli [see comments]. Nat Struct Biol **6:**56-63.

16. **Cadieux, N., C. Bradbeer, and R. J. Kadner.** 2000. Sequence Changes in the Ton Box Region of BtuB Affect Its Transport Activities and Interaction with TonB Protein. J Bacteriol **182:**5954-5961.
17. **Cadieux, N., P. G. Phan, D. S. Cafiso, and R. J. Kadner.** 2003. Differential substrate-induced signaling through the TonB-dependent transporter BtuB. Proc Natl Acad Sci U S A. **100:**10688-93. Epub 2003 Sep 4.
18. **Cao, Z., and P. E. Klebba.** 2002. Mechanisms of colicin binding and transport through outer membrane porins. Biochimie **84:**399-412.
19. **Cao, Z., Z. Qi, C. Sprencel, S. M. Newton, and P. E. Klebba.** 2000. Aromatic components of two ferric enterobactin binding sites in escherichia coli fepA. Mol Microbiol **37:**1306-17.
20. **Cao, Z., P. Warfel, S. M. Newton, and P. E. Klebba.** 2003. Spectroscopic observations of ferric enterobactin transport. J Biol Chem **278:**1022-8.
21. **Cascales, E., S. K. Buchanan, D. Duche, C. Kleanthous, R. Lloubes, K. Postle, M. Riley, S. Slatin, and D. Cavard.** 2007. Colicin biology. Microbiol Mol Biol Rev **71:**158-229.
22. **Chang, C., A. Mooser, A. Pluckthun, and A. Wlodawer.** 2001. Crystal structure of the dimeric C-terminal domain of TonB reveals a novel fold. J Biol Chem **276:**27535-40.
23. **Chimento, D. P., A. K. Mohanty, R. J. Kadner, and M. C. Wiener.** 2003. Substrate-induced transmembrane signaling in the cobalamin transporter BtuB. Nat Struct Biol **10:**394-401.
24. **Chu, B. C., R. S. Peacock, and H. J. Vogel.** 2007. Bioinformatic analysis of the TonB protein family. Biometals **16:**16.
25. **Coggshall, K. A., N. Cadieux, C. Piedmont, R. J. Kadner, and D. S. Cafiso.** 2001. Transport-defective mutations alter the conformation of the energy-coupling motif of an outer membrane transporter. Biochemistry **40:**13964-71.
26. **Cormack, B. P., R. H. Valdivia, and S. Falkow.** 1996. FACS-optimized mutants of the green fluorescent protein (GFP). Gene **173:**33-8.
27. **Cowan, S. W., T. Schirmer, G. Rummel, M. Steiert, R. Ghosh, R. A. Pauptit, J. N. Jansonius, and J. P. Rosenbusch.** 1992. Crystal structures explain functional properties of two E. coli porins. Nature **358:**727-33.
28. **Cox, G. B., F. Gibson, R. K. Luke, N. A. Newton, I. G. O'Brien, and H. Rosenberg.** 1970. Mutations affecting iron transport in Escherichia coli. J Bacteriol **104:**219-26.
29. **Dargent, B., J. Rosenbusch, and F. Pattus.** 1987. Selectivity for maltose and maltodextrins of maltoporin, a pore-forming protein of E. coli outer membrane. FEBS Lett **220:**136-42.
30. **Di Masi, D. R., J. C. White, C. A. Schnaitman, and C. Bradbeer.** 1973. Transport of vitamin B12 in Escherichia coli: common receptor sites for vitamin B12 and the E colicins on the outer membrane of the cell envelope. J Bacteriol **115:**506-13.
31. **Evans, J. S., B. A. Levine, I. P. Trayer, C. J. Dorman, and C. F. Higgins.** 1986. Sequence-imposed structural constraints in the TonB protein of E. coli. FEBS Lett **208:**211-6.

32. **Fanucci, G. E., N. Cadieux, C. A. Piedmont, R. J. Kadner, and D. S. Cafiso.** 2002. Structure and dynamics of the beta-barrel of the membrane transporter BtuB by site-directed spin labeling. Biochemistry **41:**11543-51.
33. **Fanucci, G. E., K. A. Coggshall, N. Cadieux, M. Kim, R. J. Kadner, and D. S. Cafiso.** 2003. Substrate-induced conformational changes of the periplasmic N-terminus of an outer-membrane transporter by site-directed spin labeling. Biochemistry **42:**1391-400.
34. **Ferguson, A. D., E. Hofmann, J. W. Coulton, K. Diederichs, and W. Welte.** 1998. Siderophore-mediated iron transport: crystal structure of FhuA with bound lipopolysaccharide [see comments]. Science **282:**2215-20.
35. **Feucht, A., A. Schmid, R. Benz, H. Schwarz, and K. J. Heller.** 1990. Pore formation associated with the tail-tip protein pb2 of bacteriophage T5. J Biol Chem **265:**18561-7.
36. **Frost, G. E., and H. Rosenberg.** 1975. Relationship between the tonB locus and iron transport in Escherichia coli. J Bacteriol **124:**704-12.
37. **Garavito, R. M., and J. P. Rosenbusch.** 1980. Three-dimensional crystals of an integral membrane protein: an initial x-ray analysis. J Cell Biol **86:**327-9.
38. **Gratia, A., and P. Fredericq.** 1946. Diversite des souches antibiotiques de Bacterium coli et etendue variable de leur champ d'action. C. R. Soc. Biol. (Paris) **140:**1032-1033.
39. **Gratia, J. P.** 1964. Ann. Inst. Pasteur (Paris) **107:**132-151
40. **Hancock, R. W., and V. Braun.** 1976. Nature of the energy requirement for the irreversible adsorption of bacteriophages T1 and phi80 to Escherichia coli. J Bacteriol **125:**409-15.
41. **Hantke, K., and V. Braun.** 1975. Membrane receptor dependent iron transport in Escherichia coli. FEBS Lett **49:**301-5.
42. **Hashimoto-Gotoh, T., F. C. Franklin, A. Nordheim, and K. N. Timmis.** 1981. Specific-purpose plasmid cloning vectors. I. Low copy number, temperature-sensitive, mobilization-defective pSC101-derived containment vectors. Gene **16:**227-35.
43. **Hashimoto-Gotoh, T., A. Kume, W. Masahashi, S. Takeshita, and A. Fukuda.** 1986. Improved vector, pHSG664, for direct streptomycin-resistance selection: cDNA cloning with G:C-tailing procedure and subcloning of double-digest DNA fragments. Gene **41:**125-8.
44. **Hayward, G. S., and M. G. Smith.** 1972. The chromosome of bacteriophage T5. I. Analysis of the single-stranded DNA fragments by agarose gel electrophoresis. J Mol Biol **63:**383-95.
45. **Heller, K. J.** 1984. Identification of the phage gene for host receptor specificity by analyzing hybrid phages of T5 and BF23. Virology **139:**11-21.
46. **Higgs, P. I., R. A. Larsen, and K. Postle.** 2002. Quantification of known components of the Escherichia coli TonB energy transduction system: TonB, ExbB, ExbD and FepA. Mol Microbiol. **44:**271-81.
47. **Hilsenbeck, J. L., H. Park, G. Chen, B. Youn, K. Postle, and C. Kang.** 2004. Crystal structure of the cytotoxic bacterial protein colicin B at 2.5 A resolution. Mol Microbiol **51:**711-20.

48. **Jacob, F., L. Simmonvitch, and E. Wollman.** 1953. Definition de quelques termes relatifs a la lysoenie. . Ann Inst. Pasteur (Paris) 222-224.
49. **Joris, B., S. Englebert, C. P. Chu, R. Kariyama, L. Daneo-Moore, G. D. Shockman, and J. M. Ghuysen.** 1992. Modular design of the Enterococcus hirae muramidase-2 and Streptococcus faecalis autolysin. FEMS Microbiol Lett **70:**257-64.
50. **Kamio, Y., and H. Nikaido.** 1976. Outer membrane of Salmonella typhimurium: accessibility of phospholipid head groups to phospholipase c and cyanogen bromide activated dextran in the external medium. Biochemistry **15:**2561-70.
51. **Kaserer, W., Scott D. C., Schuerch D. W., Xiao Q, Jian X., Bauler M, Newton S., Klebba P. E. .** 2007. Analysis of TonB Hybrid Proteins in FepA-Mediated Transport. In preparation.
52. **Klebba, P. E.** 2003. Three paradoxes of ferric enterobactin uptake. Frontiers in Bioscience **8:1422-1436**.
53. **Klebba, P. E., M. Hofnung, and A. Charbit.** 1994. A model of maltodextrin transport through the sugar-specific porin, LamB, based on deletion analysis. Embo J **13:**4670-5.
54. **Klebba, P. E., and S. M. Newton.** 1998. Mechanisms of solute transport through outer membrane porins: burning down the house. Curr Opin Microbiol **1:**238-247.
55. **Klebba, P. E., S. M. Newton, A. Charbit, V. Michel, D. Perrin, and M. Hofnung.** 1997. Further genetic analysis of the C-terminal external loop region in Escherichia coli maltoporin. Res Microbiol **148:**375-87.
56. **Kodding, J., F. Killig, P. Polzer, S. P. Howard, K. Diederichs, and W. Welte.** 2005. Crystal structure of a 92-residue C-terminal fragment of TonB from Escherichia coli reveals significant conformational changes compared to structures of smaller TonB fragments. J Biol Chem. **280:**3022-8. Epub 2004 Nov 2.
57. **Korteland, J., de Graaf, P. and Lugtenberg, B.** 1984. PhoE protein pores in the outermembranes of *E. coli* K-12 not only have a preference for phosphate and phosphate containing solutes but are general anion preferring channels. Biochim Biophys Acta**:**311-316.
58. **Kreusch, A., A. Neubuser, E. Schiltz, J. Weckesser, and G. E. Schulz.** 1994. Structure of the membrane channel porin from Rhodopseudomonas blastica at 2.0 A resolution. Protein Sci **3:**58-63.
59. **Lau, S. Y., and H. I. Zgurskaya.** 2005. Cell division defects in Escherichia coli deficient in the multidrug efflux transporter AcrEF-TolC. J Bacteriol **187:**7815-25.
60. **Letain, T. E., and K. Postle.** 1997. TonB protein appears to transduce energy by shuttling between the cytoplasmic membrane and the outer membrane in Escherichia coli [published erratum appears in Mol Microbiol 1997 Aug;25(3):617]. Mol Microbiol **24:**271-83.
61. **Locher, K. P., B. Rees, R. Koebnik, A. Mitschler, L. Moulinier, J. P. Rosenbusch, and D. Moras.** 1998. Transmembrane signaling across the ligand-

gated FhuA receptor: crystal structures of free and ferrichrome-bound states reveal allosteric changes. Cell **95:**771-8.
62. **Lou, K. L., N. Saint, A. Prilipov, G. Rummel, S. A. Benson, J. P. Rosenbusch, and T. Schirmer.** 1996. Structural and functional characterization of OmpF porin mutants selected for larger pore size. I. Crystallographic analysis. J Biol Chem **271:**20669-75.
63. **Lowry, O. H., N. J. Rosebrough, A. L. Farr, and R. J. Randall.** 1951. Protein measurement with the Folin phenol reagent. J Biol Chem **193:**265-75.
64. **Luckey, M., and H. Nikaido.** 1980. Specificity of diffusion channels produced by lambda phage receptor protein of Escherichia coli. Proc Natl Acad Sci U S A **77:**167-71.
65. **Ma, L., W. Kaserer, R. Annamalai, D. C. Scott, B. Jin, X. Jiang, Q. Xiao, H. Maymani, L. M. Massis, L. C. Ferreira, S. M. Newton, and P. E. Klebba.** 2007. Evidence of ball-and-chain transport of ferric enterobactin through FepA. J Biol Chem. **282:**397-406. Epub 2006 Oct 20.
66. **Matsushiro, A.** 1963. Specialized transduction of tryptophan markers in Escherichia coli K12 by bacteriophage phi-80. Virology **19:**475-82.
67. **McCorquodale, D. J.** 1999. T5 Bacteriophage and Related Bacteriophages, vol. 2e. Academic Press, New York.
68. **McIntosh, M. A., and C. F. Earhart.** 1976. Effect of iron of the relative abundance of two large polypeptides of the Escherichia coli outer membrane. Biochem Biophys Res Commun **70:**315-22.
69. **Merianos, H. J., N. Cadieux, C. H. Lin, R. J. Kadner, and D. S. Cafiso.** 2000. Substrate-induced exposure of an energy-coupling motif of a membrane transporter. Nat Struct Biol **7:**205-9.
70. **Miller, J. H.** 1972. Experiments in Molecular Genetics, vol. Cold Spring Harbor Laboratory, Cold Spring Harbor, NY.
71. **Mondigler, M., T. Holz, and K. J. Heller.** 1996. Identification of the receptor-binding regions of pb5 proteins of bacteriophages T5 and BF23. Virology **219:**19-28.
72. **Nakamura, K., and S. Mizushima.** 1976. Effects of heating in dodecyl sulfate solution on the conformation and electrophoretic mobility of isolated major outer membrane proteins from Escherichia coli K-12. J Biochem (Tokyo) **80:**1411-22.
73. **Neidhardt, F. C., P. L. Bloch, and D. F. Smith.** 1974. Culture medium for enterobacteria. J Bacteriol **119:**736-47.
74. **Newton, S. M., J. S. Allen, Z. Cao, Z. Qi, X. Jiang, C. Sprencel, J. D. Igo, S. B. Foster, M. A. Payne, and P. E. Klebba.** 1997. Double mutagenesis of a positive charge cluster in the ligand-binding site of the ferric enterobactin receptor, FepA. Proc Natl Acad Sci U S A **94:**4560-5.
75. **Newton, S. M., J. D. Igo, D. C. Scott, and P. E. Klebba.** 1999. Effect of loop deletions on the binding and transport of ferric enterobactin by FepA. Mol Microbiol **32:**1153-1165.
76. **Nikaido, H.** 1992. Porins and specific channels of bacterial outer membranes. Mol Microbiol **6:**435-42.

77. **Nikaido, H., and T. Nakae.** 1979. The outer membrane of Gram-negative bacteria. Adv Microb Physiol **20:**163-250.
78. **Nikaido, H., and M. H. Saier, Jr.** 1992. Transport proteins in bacteria: common themes in their design. Science **258:**936-42.
79. **O'Brien, I. G., and F. Gibson.** 1970. The structure of enterochelin and related 2,3-dihydroxy-N-benzoylserine conjugates from Escherichia coli. Biochim Biophys Acta **215:**393-402.
80. **Ong, S. A., T. Peterson, and J. B. Neilands.** 1979. Agrobactin, a siderophore from Agrobacterium tumefaciens. J Biol Chem **254:**1860-5.
81. **Payne, M. A., J. D. Igo, Z. Cao, S. B. Foster, S. M. Newton, and P. E. Klebba.** 1997. Biphasic binding kinetics between FepA and its ligands. J Biol Chem **272:**21950-5.
82. **Peacock, S. R., A. M. Weljie, S. Peter Howard, F. D. Price, and H. J. Vogel.** 2005. The solution structure of the C-terminal domain of TonB and interaction studies with TonB box peptides. J Mol Biol **345:**1185-97. Epub 2004 Dec 15.
83. **Phan, P. G., N. Cadieux, and R. J. Kadner.** 1999. Presented at the 99th General Meeting of the American Society for Microbiology, Chicago, Illinois.
84. **Pinner, R. W., S. M. Teutsch, L. Simonsen, L. A. Klug, J. M. Graber, M. J. Clarke, and R. L. Berkelman.** 1996. Trends in infectious diseases mortality in the United States. Jama **275:**189-93.
85. **Plastow, G. S., and I. B. Holland.** 1979. Identification of an Escherichia coli inner membrane polypeptide specified by a lambda-tonB transducing. Biochem Biophys Res Commun **90:**1007-14.
86. **Pollack, J. R., and J. B. Neilands.** 1970. Enterobactin, an iron transport compound from Salmonella typhimurium. Biochem Biophys Res Commun **38:**989-92.
87. **Ponting, C. P., L. Aravind, J. Schultz, P. Bork, and E. V. Koonin.** 1999. Eukaryotic signalling domain homologues in archaea and bacteria. Ancient ancestry and horizontal gene transfer. J Mol Biol **289:**729-45.
88. **Postle, K.** 1993. TonB protein and energy transduction between membranes. J Bioenerg Biomembr **25:**591-601.
89. **Postle, K., and R. F. Good.** 1983. DNA sequence of the Escherichia coli tonB gene. Proc Natl Acad Sci U S A **80:**5235-9.
90. **Pugsley, A. P., and P. Reeves.** 1976. Characterization of group B colicin-resistant mutants of Escherichia coli K-12: colicin resistance and the role of enterochelin. J Bacteriol **127:**218-28.
91. **Pugsley, A. P., and P. Reeves.** 1976. Iron uptake in colicin B-resistant mutants of Escherichia coli K-12. J Bacteriol **126:**1052-62.
92. **Rabsch, W., L. Ma, G. Wiley, F. Z. Najar, W. Kaserer, D. W. Schuerch, J. E. Klebba, B. A. Roe, J. A. Laverde Gomez, M. Schallmey, S. M. Newton, and P. E. Klebba.** 2007. FepA- and TonB-dependent Bacteriophage H8: Receptor Binding and Genomic Sequence. J Bacteriol **25:**25.
93. **Randall-Hazelbauer, L., and M. Schwartz.** 1973. Isolation of the bacteriophage lambda receptor from Escherichia coli. J Bacteriol **116:**1436-46.

94. **Richmond, M. H., and N. A. Curtis.** 1974. The interplay of beta-lactamases and intrinsic factors in the resistance of gram-negative bacteria to penicillins and cephalosporins. Ann N Y Acad Sci **235:**553-68.
95. **Roof, S. K., J. D. Allard, K. P. Bertrand, and K. Postle.** 1991. Analysis of Escherichia coli TonB membrane topology by use of PhoA fusions. J Bacteriol **173:**5554-7.
96. **Roos, U., R. E. Harkness, and V. Braun.** 1989. Assembly of colicin genes from a few DNA fragments. Nucleotide sequence of colicin D. Mol Microbiol **3:**891-902.
97. **Rutz, J. M., J. Liu, J. A. Lyons, J. Goranson, S. K. Armstrong, M. A. McIntosh, J. B. Feix, and P. E. Klebba.** 1992. Formation of a gated channel by a ligand-specific transport protein in the bacterial outer membrane. Science **258:**471-5.
98. **Saint, N., K. L. Lou, C. Widmer, M. Luckey, T. Schirmer, and J. P. Rosenbusch.** 1996. Structural and functional characterization of OmpF porin mutants selected for larger pore size. II. Functional characterization. J Biol Chem **271:**20676-80.
99. **Santini, C. L., A. Bernadac, M. Zhang, A. Chanal, B. Ize, C. Blanco, and L. F. Wu.** 2001. Translocation of jellyfish green fluorescent protein via the Tat system of Escherichia coli and change of its periplasmic localization in response to osmotic up-shock. J Biol Chem **276:**8159-64.
100. **Sauter, A., S. P. Howard, and V. Braun.** 2003. In vivo evidence for TonB dimerization. J Bacteriol. **185:**5747-54.
101. **Schirmer, T.** 1998. General and specific porins from bacterial outer membranes. J Struct Biol **121:**101-9.
102. **Schirmer, T., T. A. Keller, Y. F. Wang, and J. P. Rosenbusch.** 1995. Structural basis for sugar translocation through maltoporin channels at 3.1 A resolution [see comments]. Science **267:**512-4.
103. **Schneider, H., H. Fsihi, B. Kottwitz, B. Mygind, and E. Bremer.** 1993. Identification of a segment of the Escherichia coli Tsx protein that functions as a bacteriophage receptor area. J Bacteriol **175:**2809-17.
104. **Schulz, G. E.** 1996. Porins: general to specific, native to engineered passive pores. Curr Opin Struct Biol **6:**485-90.
105. **Scott, D. C., Z. Cao, Z. Qi, M. Bauler, J. D. Igo, S. M. Newton, and P. E. Klebba.** 2001. Exchangeability of N termini in the ligand-gated porins of Escherichia coli. J Biol Chem **276:**13025-33.
106. **Scott, D. C., S. M. Newton, and P. E. Klebba.** 2002. Surface loop motion in FepA. J Bacteriol **184:**4906-11.
107. **Smit, J., Y. Kamio, and H. Nikaido.** 1975. Outer membrane of Salmonella typhimurium: chemical analysis and freeze- fracture studies with lipopolysaccharide mutants. J Bacteriol **124:**942-58.
108. **Stevenson, G., B. Neal, D. Liu, M. Hobbs, N. H. Packer, M. Batley, J. W. Redmond, L. Lindquist, and P. Reeves.** 1994. Structure of the O antigen of Escherichia coli K-12 and the sequence of its rfb gene cluster. J Bacteriol **176:**4144-56.

109. **Terskikh, A., A. Fradkov, G. Ermakova, A. Zaraisky, P. Tan, A. V. Kajava, X. Zhao, S. Lukyanov, M. Matz, S. Kim, I. Weissman, and P. Siebert.** 2000. "Fluorescent timer": protein that changes color with time. Science **290:**1585-8.
110. **Vakharia, H. L., and K. Postle.** 2002. FepA with globular domain deletions lacks activity. J Bacteriol **184:**5508-12.
111. **Van Amersfoort, E. S., T. J. Van Berkel, and J. Kuiper.** 2003. Receptors, mediators, and mechanisms involved in bacterial sepsis and septic shock. Clin Microbiol Rev **16:**379-414.
112. **Van Gelder, P., N. Saint, P. Phale, E. F. Eppens, A. Prilipov, R. van Boxtel, J. P. Rosenbusch, and J. Tommassen.** 1997. Voltage sensing in the PhoE and OmpF outer membrane porins of Escherichia coli: role of charged residues. J Mol Biol **269:**468-72.
113. **Wang, J., M. Hofnung, and A. Charbit.** 2000. The C-terminal portion of the tail fiber protein of bacteriophage lambda is responsible for binding to LamB, its receptor at the surface of Escherichia coli K-12. J Bacteriol **182:**508-12.
114. **Wang, J., Y. Jiang, M. Vincent, Y. Sun, H. Yu, Q. Bao, H. Kong, and S. Hu.** 2005. Complete genome sequence of bacteriophage T5. Virology **332:**45-65.
115. **Wayne, R., K. Frick, and J. B. Neilands.** 1976. Siderophore protection against colicins M, B, V, and Ia in Escherichia coli. J Bacteriol **126:**7-12.
116. **Weaver, C. A., and J. Konisky.** 1980. tonB-independent ferrichrome-mediated iron transport in Escherichia coli spheroplasts. J Bacteriol **143:**1513-8.
117. **Weiss, M. S., U. Abele, J. Weckesser, W. Welte, E. Schiltz, and G. E. Schulz.** 1991. Molecular architecture and electrostatic properties of a bacterial porin. Science **254:**1627-30.
118. **Weiss, M. S., and G. E. Schulz.** 1992. Structure of porin refined at 1.8 A resolution. J Mol Biol **227:**493-509.
119. **Weiss, M. S., T. Wacker, J. Weckesser, W. Welte, and G. E. Schulz.** 1990. The three-dimensional structure of porin from Rhodobacter capsulatus at 3 A resolution. FEBS Lett **267:**268-72.
120. **Young, G. M., and K. Postle.** 1994. Repression of tonB transcription during anaerobic growth requires Fur binding at the promoter and a second factor binding upstream. Mol Microbiol **11:**943-54.